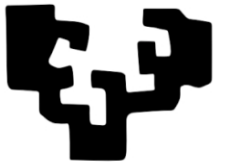

DOCTORAL THESIS

2016

Title: Biophysical properties of aqueous humour in ocular pathologies.

Author: Javier Cabrerizo[1,2,4]

Directors: Elena Vecino[3,4], Aritz Urcola[1,2,4]

1 Department of Ophthalmology, University Hospital of Alava, Spain

2 Green Eye Project, Research, Spain

3 Department of Cell Biology and Histology, University of the Basque Country, UPV/EHU, Spain

4 Experimental Ophthalmo-Biology Group, (GOBE), University of the Basque Country, (UPV/EHU), Spain

LIST OF ABBREVIATIONS

1-ether, 2-acylglycerophosphocholine	**MEMAPC**
Aqueous humour	**AH**
Ceramides	**Cer**
Cholesteryl ester/ cholesteryl esters	**ChoE**
Descemet membrane endothelial keratoplasty	**DMEK**
Diacylglycerophosphocholines	**DAPC**
Fuchs endothelial dystrophy	**FED**
Intraocular pressure	**IOP**
Non perforating deep sclerectomy	**NPDE**
Open angle glaucoma	**OAG**
Phosphatidylcholine/ Phosphatidylcholines	**PC**
Sphingomyelin/ Sphingomyelins	**SM**
Surface tension	**ST**
Ultra-performance lipidomic mass spectrometry	**UPLC-MS**

TABLE OF CONTENTS

1. INTRODUCTION

1.1 State of the art

1.1.1 Aqueous humor dynamics

1.1.2 Lipid metabolism

1.1.3 ST in biological fluids

1.2 Hypothesis

1.3 Objectives

2. OBJECTIVES

3. MATERIAL AND METHODS

3.1 Optical goniometry

3.2 Lipidomic profiling

3.3 Scanning electron microscopy

3.4 Sampling and storage

3.5 Statistical analyses

3.6 Ethical statement

4. RESULTS

4.1 Paper 1: “Changes in lipidomic profile of aqueous humor in Fuchs endothelial dystrophy” (submitted)

4.1.1 Abstract

4.1.2 Introduction

4.1.3 Material and methods

4.1.4 Results

4.1.5 Discussion

4.1.6 References

4.2 Paper 2: “Changes in surface tension of aqueous humor in anterior segment ocular pathologies” (submitted)

4.2.1 Abstract

4.2.2 Introduction

4.2.3 Material and methods

4.2.4 Results

4.2.5 Discussion

4.2.6 References

4.3 Paper 3:”Changes in lipidomic profile of aqueous humor in open angle glaucoma” (submitted)

4.3.1 Abstract

4.3.2 Introduction

4.3.3 Material and methods

4.3.4 Results

4.3.5 Discussion

4.3.6 References

5. GENERAL DISCUSSION

6. CONCLUSIONS

7. REFERENCES

8. ACKNOWLEDGMENTS

1. INTRODUCTION

1.1 STATE OF THE ART

1.1.1 AQUEOUS HUMOR DYNAMICS

Currently, aqueous humor (AH) dynamics are known to be involved in some of the leading causes of irreversible blindness in the world. Thus, the anatomical structures and the physiological processes involved in its regulation are a topic of deep study in the past years.

AH is synthesized by the ciliary processes, elongated bilayer epithelial structures highly vascularized with fenestrated capillaries. The outer pigmented and the inner non pigmented layers of epithelium are joined by tight junctions, which entail the blood–aqueous barrier. Active secretion accounts for the majority of AH production and involves the activity of the enzyme carbonic anhydrase II. Furthermore, in the ciliary processes, the hydrostatic pressure difference between capillary pressure and intraocular pressure (IOP) favors secretion, whereas the osmotic gradient between the two opposes to it, being a potential regulator for AH synthesis(1).

In relation to plasma, AH has an excess of hydrogen and chloride ions, an excess of ascorbate, and a deficit of bicarbonate. AH is essentially protein free (1/200–1/500 of the protein found in plasma), which allows for optical clarity and reflects the integrity of the blood–aqueous barrier of the normal eye. Albumin accounts for about half of the total protein. Other components include growth factors; several enzymes, such as carbonic anhydrase, lysozyme, diamine oxidase, plasminogen activator, dopamine β-hydroxylase,

and phospholipase A2; and prostaglandins, cyclic adenosine monophosphate (cAMP), catecholamines, steroid hormones, and hyaluronic acid. AH is produced at an average rate of 2.0–2.5 μL/min, and its composition alters as it flows anteriorly(1).

The corneoscleral limbus containing structures were designed to evacuate the AH from the anterior chamber of the eye into the general circulation. These structures can be found within an anatomically complex region between the scleral spur and the Schwalbe's line with its transition to the Descemet membrane. Drained by the collector channels that evacuate to the Schlemm's canal through the trabecular meshwork, this structure is divided in three regions of key physiological importance to the AH outflow and subsequently to the IOP: uveal, corneoscleral, and juxtacanalicular region. In non pathological conditions, it is a pressure-driven system capable to maintain a constant IOP through various adaptive mechanisms(2). The trabecular meshwork is self regulated by afferent and efferent innervation and may undergo a glomerule-like regulation where the IOP modifies its morphology and subsequently its outflow resistance(3). Furthermore, contraction of the ciliary muscle causes expansion of the Schlemm's canal, decreasing intracanal pressure and the increasing outflow gradient(4).

The Schlemm's canal is a circular circumference of 36 μm and 350-500 mm in diameter at its inner light. The inner surface is covered by endothelial cells that are interconnected by tight junctions, zonula occludens. In the inner wall of the channel along its winding path, cytoplasmic vesicles or vacuoles up to 14 microns(5) undergo a pinocitic-like transition through the channel forming with occasional openings to channel light 0.3-2.0 um(6),(7). It has been postulated that this might be a direct drainage from trabecular spaces into Schlemm's canal(8).

Certain changes in the peri- and intra-trabecular meshwork structures have been associated with variations in the IOP such as an increase in extracellular deposition of fibrillar material originating from the extracellular matrix(9),(10). The size and number of pinocytotic vacuoles increase with elevated IOP(9) and with IOP related changes in the diameter of the canal(11). These processes of vacuole formation and migration are the main mechanisms of AH drainage through the juxtacanalicular tissue and the endothelial monolayer of the Schlemm's canal. There is a controversy in relation to the presence of transcellular pores in the Schlemm's inner wall in relation with the IOP, while some reports, supported by electron microscopy findings, state that their increase in number correlates with IOP(12), and others conclude that their number is reduced in glaucomatous eyes(13).

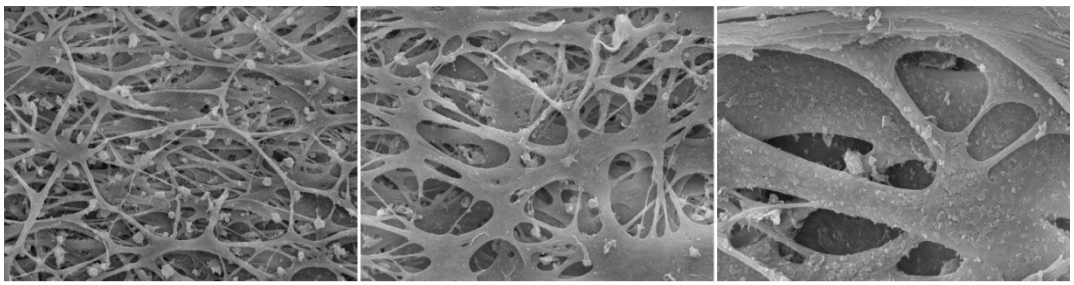

Figure 1: Electron microscopy images of the trabecular meshwork in increasing magnification.

The dynamic characteristics of the ocular outflow anatomical system and the close relationship between histological changes and IOP may suggest the modulating role of AH in this scenario. Accordingly, this work aims to address potential changes in AH composition and biophysical properties related to anterior segment pathologies.

1.1.2 LIPID METABOLISM

Lipids play a key role in organism development and take part in complex metabolic pathways. In serum, lipids are transported in lipoproteins, together with non esterified cholesterol and sphingolipids which are found in the lipoprotein membranes. Further relevant and apolar compounds, such as ChoE and glycerolipids are located in their nucleus. Any subtle change in the lipids found in serum could affect the physical and chemical properties of lipoproteins and alter their numerous functions(14).

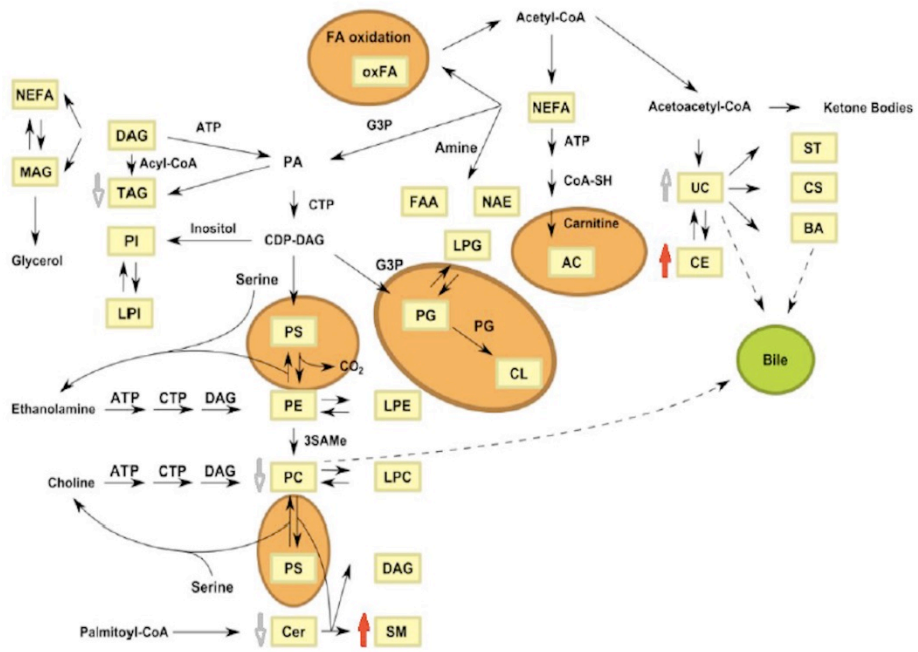

Figure 2: Simplified diagram of the most important lipid fluxes, describing the synthesis of the major lipids analyzed in the present Thesis. Non esterified fatty acids, oxidized fatty acids, primary fatty amides, N-Acyl ethanolamines, glycerol 3-phosphate, phosphatidic

acids, phosphatidylinositols, lysophosphatidylinositols, monoacylglycerides, diacylglycerides, triacylglycerides, acyl carnitines, unesterified cholesterol, cholesterol sulfate, ChoEs, phosphatidylserines, phosphatidylethanolamines, lysophosphatidylethanolamines, phosphatidylcholines, lysophosphatidylcholines, phosphatidylglycerols, lysophosphatidylglycerols, cardiolipins, ceramides, SMs, S-adenosylmethionine. Areas in orange represent processes carried out in the mitochondria.

The fatty acid group is the fundamental building block of complex lipids. Fatty acids may undergo β-, α-, and ω-oxidation. The major glycerophospholipids assembled in the endoplasmic reticulum are phosphatidylcholines, phosphatidylethanolamines, their lyso-forms, phosphatidylinositols, phosphatidylserines, and phosphatidic acids. In addition, the endoplasmic reticulum synthesizes ceramides, galactosylceramides, unesterified and esterified cholesterols. UC is the principal substrate for bile synthesis, which is also produced from bile acids and phosphatidylcholine. Both the endoplasmic reticulum and lipid droplets participate in steryl ester, di- and triacylglycerides synthesis. The Golgi lumen is the site of synthesis of sphingomyelins (SM), where the phosphatidylcholine is also generated. Approximately 45% of the phospholipids in mitochondria, mostly PE, PA, and cardiolipins are autonomously synthesized by the organelle.

The fatty acid product released from fatty acid synthase is palmitate (via the action of palmitoyl thioesterase), which is a 16:0 fatty acid. Elongation and unsaturation of fatty acids occur in both the mitochondria and endoplasmic reticulum (microsomal membranes). The predominant sites of these processes are the endoplasmic reticulum membranes. Elongation involves condensation of acyl-CoA groups with malonyl-CoA. The resultant product is two carbons longer (CO_2 is released from malonyl-CoA as in the FAS reaction) which undergoes reduction, dehydration, and reduction yielding a saturated fatty acid. The

reduction reactions of elongation require NADPH as cofactor just as for the similar reactions catalyzed by FAS. Mitochondrial elongation involves acetyl-CoA units and is a reversal of oxidation except that the final reduction utilizes NADPH instead of FADH2 as cofactor.

The desaturation of fatty acids occurs in the endoplasmic reticulum (ER) membranes as well. In mammalian cells fatty acid desaturation involves 3 broad specificity fatty acyl-CoA desaturases (non-heme iron containing enzymes). These enzymes introduce unsaturation at C5, Δ5-eicosatrienoyl-CoA desaturase, C6, Δ6-oleoyl(linolenoyl)-CoA desaturase and C9, Δ9-stearoyl-CoA desaturase. The latter desaturase is the rate-limiting enzyme catalyzing the synthesis of monounsaturated fatty acids, primarily oleate (18:1) and palmitoleate (16:1). These two monounsaturated fatty acids represent the majority of monounsaturated fatty acids present in membrane phospholipids, triglycerides, and ChoE. The ratio of saturated to monounsaturated fatty acids in membrane phospholipids is critical to normal cellular function and alterations in this ratio have been correlated with diabetes, obesity, cardiovascular disease, and cancer. Thus, the regulation of the expression and activity of CoA desaturase has important physiological significance.

These enzymes cannot introduce sites of unsaturation beyond C9 and, therefore, they cannot synthesize either linoleate (18:2Δ9,12) or linolenate (18:3Δ9,12,15). These fatty acids must be acquired from the diet and are, therefore, referred to as essential fatty acids. Linolenate is especially important for the synthesis of arachidonic acid. Arachindonate is a precursor for the eicosanoids (prostaglandins, thromboxanes, and leukotrienes). It is this role of fatty acids in eicosanoid synthesis that leads to poor growth, slowed wound healing, and dermatitis in persons on fat free diets. Also, linolenate acid is a constituent of epidermal cell sphingolipids that function as the skin water permeability barrier.

Lipid pathways have been shown to be altered in certain conditions related to inflammation and oxidative stress(19),(20),(21). Specific eicosanoids have been shown to be characteristically present in aged lens, serving as biomarkers for early cataract development(17). Some lipid species have also shown anti inflammatory properties, inhibiting the cyclooxigenase pathway. Some of those are currently been studied for their potential clinical use in ocular surface diseases(18).

Recent reports indicate that many lipid species serve as modulators of the apoptotic response to oxidative stress. Conversely, enhanced apoptotic signaling can significantly alter lipid metabolism in the liver, adipose tissue, skeletal muscle, and macrophage in the context of infection, diabetes, and atherosclerosis(22). Hence, some lipid metabolites have been recently postulated as useful biomarkers for oxidative stress(23). Changes in cell lipid synthesis would be expected in the endothelial cell metabolism in Fuchs endothelial dystrophy (FED), where DNA damage and oxidative stress chronically coexist(24),(25).

1.1.3 SURFACE TENSION IN BIOLOGICAL FLUIDS

The tension of the surface film of a liquid caused by the attraction of the particles in the surface layer by the bulk of the liquid is known as surface tension (ST). This force tends to minimize surface area of the fluid and defines its interfacial properties(26). The ST of organic fluids is highly dynamic and related to its composition. All biological liquids of the human organism contain surface active compounds, mainly proteins and lipids. These surfactants are characterized by a high adsorption activity at low bulk concentrations which significantly effects equilibrium interfacial properties and the kinetics of physicochemical processes taking place at interfaces (disperse systems of biological liquids, cell membranes).

Numerous reports show disease-linked variations of the lipidomic composition of certain glycerophospholipids in organic fluids(27). Increase of phospholipids in human fluids has been related with a decrease in the ST of potential clinical relevance(28).

Human biologic liquids contain various surfactants capable of adsorbing at liquid interfaces and changing the surface (interfacial) tension. Adsorption processes involve proteins, phospholipids, and low molecular weight surfactants, which play a significant role in vital functions of the human organism, in respiratory processes and vascular synthesis.

With protein adsorption, surface denaturation takes place, leading to the unfolding of protein molecules within the surface layer, at least at low surface pressures, defining surfactant property.

Studies in which the protein/surfactants adsorption layer parameters can be measured, in order to better understand the formation process and the properties of these interfacial layers, surface rheology has shown to provide important information about the structure of mixed protein/surfactant layers, as they are formed by biological liquids(29).

All biological liquids of the human organism contain surface active compounds, such as proteins, lipids, and molecules of other nature. These surfactants are characterized by a high adsorption activity at low bulk concentrations which significantly effects equilibrium interfacial properties and the kinetics of physicochemical processes taking place at interfaces (disperse systems of biological liquids, cell membranes). Furthermore, dynamic ST has shown to depend on sex and age and to vary during pregnancy(29).

The osmolarity of urine probably can affect significantly its dynamic ST. Depending on the

water/electrolyte balance of the organism, the osmotic concentration of urine changes. The portion of plasmatic secreted proteins in this case is negligible, and the excretion of osmotically active substances depends on the absolute and relative amounts of soluble electrolytes (sodium, potassium, ammonium). The misbalance in the composition of protein and fat in blood can lead to coagulation even in healthy persons. This, in turn, can affect ST parameters.

Equilibrium ST of serum and urine obtained from female are higher than male. This might be attributed to lower contents of some proteins, lipids and hydrocarbon in blood serum. In particular, female serum has lower physiological level of low density and very low density lipoproteins, and a number of enzymes(30).

Furthermore, sex related differences exist in the occurrence of protein molecules that contain amino-acids possessing hydrophilic radicals, fibronectin being a good example among others. Thus the concentration of fibronectin in serum is 35 to 40% lower than in plasma. The lower the amount of fibronectin in the blood, the higher is the level of circulating fibrinogen/fibrin complexes therein(31). The concentration of fibronectin is directly correlated with the concentration of cholesterol, triglycerides, and low density lipoproteins. It should be stressed that the content of fibronectin in blood serum for healthy males is much higher than for females(32).

It was shown that an inverse correlation exists between equilibrium ST of blood serum for healthy people, and the concentration of such surfactants as cholesterol, triglycerides and fibronectin.

Differences between equilibrium ST values for persons of different gender may not only be

due to proteins but can result from different levels of eicosanoids (prostanoids, fatty oxyacids, leukotrienes) and non-lipid (palmitic and hyaluronic acid) or non-protein nitrous components (urea, creatinine, uric acid). Therefore, for males the differences in content and structure of protein and lipid components of urine result in a more pronounced decrease of ST.

With the increase in age, a gradual growth of ST of blood and a gradual decrease of ST of urine take place with most pronounced changes occurring in very short time ranges.

An extremely important feature of mature placenta is the production of secretory proteins, which are used for the building of enzymes, globulins, and hormones which possess surface active properties. Therefore variations in the surfactant composition of blood and amniotic liquid should primarily affect the ST of these biological liquids.

The content of lipid fractions in maternal plasma is always higher than in the fetus. At the end of the gestation period the amount of free fatty acids and phospholipids, like lysophosphatidyl choline and SM sharply increase in placental tissue.
It is quite clear that variations in the protein and lipid composition in the gestating organism should affect the ST of biological liquids which is supported by experimental data. For example, at the end of the gestation period, a significant decrease in the ST of serum and amniotic liquid at long times are observed, and these values become close to one another as time passes.

Dynamic ST characteristics of biological liquids depend on sex and age and are known to vary in certain systemic pathologies. Our study aims to give an insight into their clinical relevance within some pathologies of the anterior segment of the eye.

1.2 HYPOTHESIS

Cataract, glaucoma and Fuchs endothelial dystrophy represent the common pathologies of the anterior segment of the eye. The potential need of a surgical procedure makes them appropriate conditions for aqueous humor sampling without adding comorbidity. Intraoperative extraction of 150 microliters of aqueous humor through a corneal paracentesis as the first step of an anterior segment surgery represents a reproducible, technically feasible and relatively safe method to obtain aqueous humor samples. This sample size represents a volume threshold, from which anterior chamber swallowing and significant hypotony may occur.

Due to the close anatomical and physiological relation between the aqueous humor and the anterior chamber structures, pathology driven differences in the aqueous humor metabolic profile are expected. The metabolical characteristics of these changes should give insight within the psychopathology of the underlying condition.

Quantitative and qualitative variations in aqueous humor metabolites may trigger changes in the fluids biophysical properties, such as surface tension. This may play a role in the aqueous humor outflow pathways as well as in their metabolical functions towards the corneal endothelium, the trabecular meshwork and the anterior lens.

The hypothesis of this Doctoral Thesis is the presence of disease driven lipidomic changes in aqueous humor that correlate with changes in the fluid's surface tension. These changes should evolve from the physiopathology of the underlying condition.

2. OBJECTIVES

To determine potential differences in surface tension of aqueous humor related to different anterior segment pathologies.

To determine potential differences in the lipidomic profile of aqueous humor related to different anterior segment pathologies.

To offer an insight into the potential relation between those changes in aqueous humor composition and biophysical properties and the physiopathological processes involved in those conditions.

3. MATERIAL AND METHODS

3.1 OPTICAL GONIOMETRY

The pendant drop is a drop optical goniometry suspended from a needle in a bulk liquid or gaseous phase. The shape of the drop results from the relationship between the surface tension (ST) or interfacial tension and gravity. In the pendant drop method, the ST or interfacial tension is calculated from the shadow image of a pendant drop using drop shape analysis.

An increased pressure is produced inside the drop as a result of the interfacial tension between inner and outer phase. The correlation between the pressure difference Δp, the radius of curvature of the surface r1 and r2 and the interfacial tension is described by the Young-Laplace equation:

$$\Delta p = \sigma \, (1/r^1 + 1/r^2)$$

Young-Laplace equation reflects the commonly observed interfacial phenomena of the existence of curvature due to the presence of interfacial tension in isotropic materials. A consequence of the formed curvature is the increase of pressure on the concave side of the interface. The equation relates the pressure difference between these two phases to the mean curvature(33).

In the pendant drop method the drop is deformed under the effect of gravity, as a hydrostatic pressure which affects the main radius of curvature r1 and r2 is produced inside the drop due to the weight. As the hydrostatic pressure is dependent on height, the curvature of the drop interface also changes in the vertical direction. This results in the

characteristic “pear shape” of a pendant drop.

The degree of deviation from the spherical shape is given by the ratio between the weight of the drop and its ST. If the density difference between the phases is known, the ST can be calculated from the shape of the drop. The shape cannot be scaled at will; in fact the actual dimensions of the drop are used in the calculation.

When making a measurement, the scale of the video image is measured first in order to give access to the actual drop dimensions. The shape of the drop is then determined from the video image of the dosed drop using greyscale analysis. A shape parameter designated by B is then varied in a numerical method until the calculated drop shape corresponds with the actual shape. The interfacial tension is calculated from the density difference Δρ and the modified B parameter.

Figure 2: Video-based optical contact angle measuring system OCA 15EC displaying the contact angle measuring technique and drop shape analysis.

3.2 LIPIDOMIC PROFILING

A successful metabolic profiling experiment relies on the ability to determine changes in the metabolite concentrations of an organism's biofluid or tissue. Ultra-performance liquid chromatography tandem mass-spectrometry (UPLC-MS) is well suited to such analyses due to its high sensitivity, large coverage over different classes of metabolites, high throughput capacity, and wide dynamic range. In this study, a lipidomic UPLC-MS based platform was used to analyze endogenous metabolites for inclusion in subsequent statistical analysis procedures used to study metabolic differences between the groups of samples of interest(34),(35).

Metabolite extraction was accomplished by fractionating the aqueous humor (AH) samples into pools of species with similar physicochemical properties, using appropriate combinations of organic solvents. The following methods were used according to the targeted metabolite's chemical class(36): glycerolipids, ChoEs, sphingolipids, and glycerophospholipids profiling.

AH extracts were mixed with sodium chloride (50 mM) and chloroform / methanol (2:1) in 1.5 ml microtubes at room temperature. The extraction solvent was spiked with metabolites not detected in unspiked human serum extracts. After brief vortex mixing, the samples were incubated for 1 hour at -20°C. After centrifugation at 16,000 x g for 15 minutes, the organic phase was collected and the solvent removed. The dried extracts were then reconstituted in acetronitrile / isopropanol (50:50), centrifuged (16,000 x g for 5 minutes), and transferred to vials for UPLC-MS analysis.

Additionally, two different types of quality control (QC) samples were used to assess the data quality(37). The QC samples are reference serum samples, which are evenly distributed over the batches and extracted and analysed at the same time as the individual samples. Firstly, a QC Calibration sample was used to correct the different response factors between and within batches. Secondly, a QC Validation sample was used to assess how well data pre-processing procedure improved the data quality. For each of the three analytical platforms, randomized duplicate sample injections were performed, with each of the QC calibration and validation extracts uniformly interspersed throughout the entire batch run.

A test mixture of standard compounds was analyzed before and after the entire set of randomized, duplicated sample injections in order to examine the retention time stability (generally < 6 s variation, injection-to-injection), mass accuracy (generally < 3 ppm for *m/z* 400-1000, and < 1.2 mDa for *m/z* 50-400) and sensitivity of the system. For each injection batch, the overall quality of the analysis procedure was monitored using five repeat extracts of the QC Validation sample.

All data were processed using the TargetLynx application manager for MassLynx 4.1 software (Waters Corp., Milford, USA). A set of predefined retention time, mass-to-charge ratio pairs, *Rt-m/z*, corresponding to metabolites included in the analysis are fed into the program. Associated extracted ion chromatograms (mass tolerance window = 0.05 Da) are then peak-detected and noise-reduced in both the liquid chromatography and mass spectrometry domains such that only true metabolite related features are processed by the software. A list of chromatographic peak areas is then generated for each sample injection.

For identified metabolites, representative mass spectrometry detection response curves

were generated using an internal standard for each chemical class included in the analysis. By assuming similar detector response levels for all metabolites belonging to a given chemical class, this allowed a linear detection range to be defined for each variable. Maximum values were defined as those at which the detector response became non-linear with respect to the concentration of the representative internal standard. Variables were not considered for further analysis where more than 30% of data points were found outside their corresponding linear detection range. For example, variables that used to be excluded from the serum analysis at this stage were the most abundant species detected in that kind of biofluids, e.g. ChoE(18:2) [blood concentration_2 mM], PC(16:0/0:0) [blood concentration_0.1 mM].

Normalization factors were calculated for each metabolite by dividing their intensities in each sample by the recorded intensity of an appropriate internal standard in that same sample(28). The most appropriate internal standard for each variable was defined as that which resulted in a minimum relative standard deviation after correction, as calculated from the quality control calibration samples over all the analysis batches. In general, as one would have expected, best internal standard trends followed chemical structural similarities between spiked compounds and endogenous variables.

Linear regression (internal standard corrected response as a function of sample injection order) was used to estimate in the quality control calibration samples any intra-batch drift not corrected for by internal standard correction. For all variables, internal standard corrected response in each batch was divided by its corresponding intra-batch drift trend, such that normalised abundance values of the study samples were expressed with respect to the batch averaged quality control calibration serum samples (arbitrarily set to 1).

Following normalization, the concordance between duplicate sample injection response

values was assessed. Where coefficients of variation > 30% were found, corresponding sample injection data were returned for manual inspection of the automated integration performed by the TargetLynx software, and modifications performed where appropriate. Any remaining zero values in the sample injection variable were replaced with missing values before averaging to form the final dataset that was used for study sample statistical analyses.

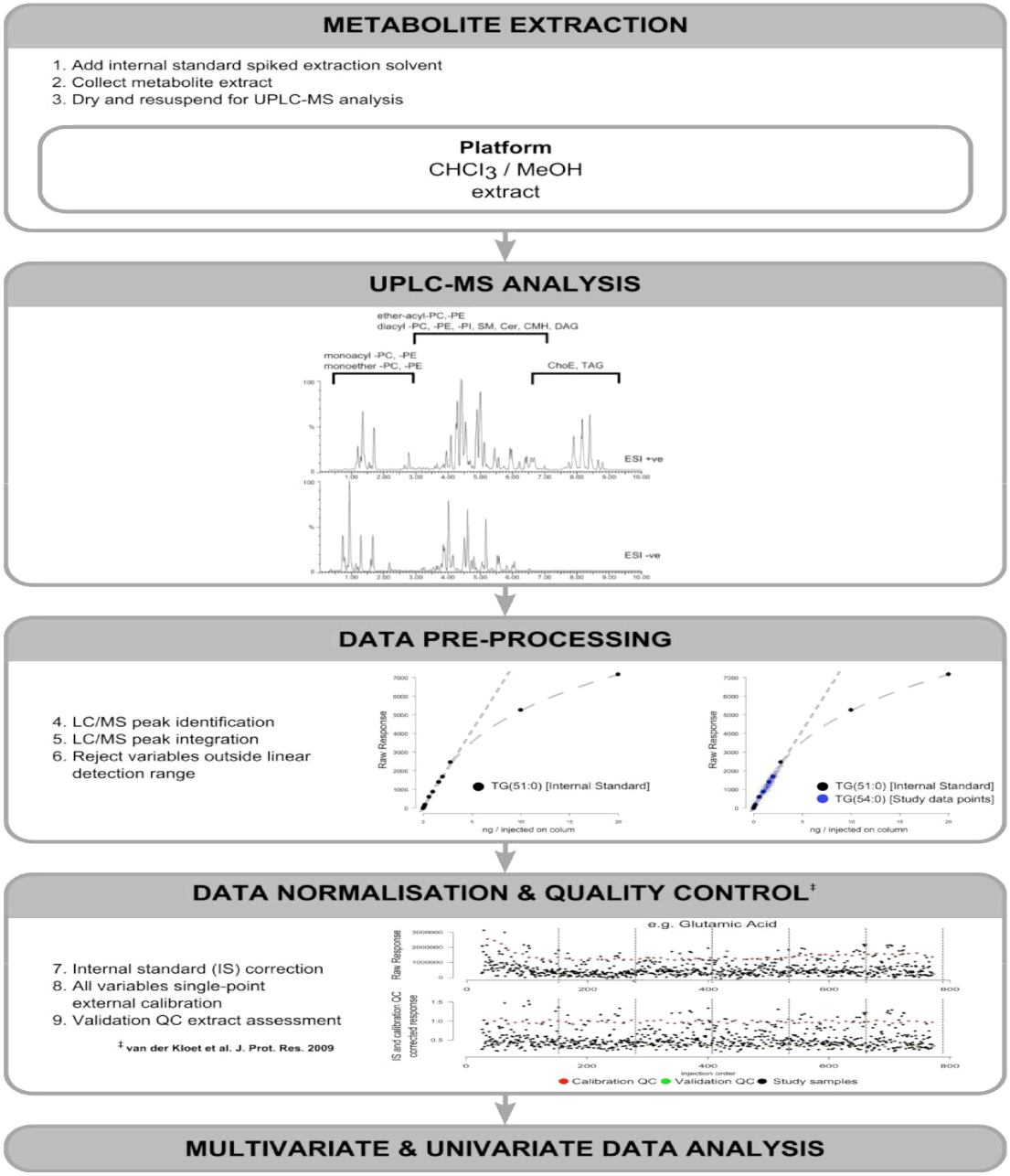

Figure 3: Lipidomic profiling workflow through the different stages of the process.

3.3 SCANNING ELECTRON MICROSCOPY

One human cornea with 2 mm of scleral rim was prepared for SEM after Descemet membrane endothelial keratoplasty (DMEK) graft preparation. A 1 × 10mm sample of tissue was obtained from the iris root. The fixative was 2% glutaraldehyde in 80 mM sodium cacodylate buffer (pH 7.2–7.4, 320–340 mOsm/kg). The sample was processed with gold-coated magnetic particles for solid-phase immunoassays and examined by SEM (JEOL JSM-7000F, JEOL, Peabody, USA) after critical point of drying was achieved. 12 Regions in the middle of the sample were observed at final magnifications of ×200 and ×5000.

3.4 SAMPLING AND STORAGE

AH was obtained during the first step of a surgical procedure, refractive lensectomy in controls and DMEK in FED patients. After topical 1% povidone iodine instillation, around 150 microliters of AH were directly aspirated through a unique corneal side port using a 27-gauge blunt cannula. No noteworthy adverse events were noticed during the aspiration process. A moderate shallowing of the anterior chamber was occasionally perceived. AH was directly introduced in a 0.5 ml tube (Eppendorf AG, Hamburg, Germany) after aspiration and stored at -80°C at the tissue bank for up to 9 months (range: 1-9). Prior to the analyses, samples were left at 24°C for three hours to gradually adjust to room temperature.

3.5 STATISTICAL ANALYSES

Statistical analyses was performed with IBM SPSS Statistics, Version 20.0, (IBM, USA)

and R (Development Core Team (2008). R Foundation for Statistical Computing, Vienna, Austria. After normality assessment, multivariate and univariate analysis were performed. Principal Component Analysis and Partial Least Squares Discriminant Analysis were used to reduce the data matrix to a series of principal components which aim to explain independently the maximum amount of variance possible. These MVA analyses were applied by exporting the normalized data to the SIMCA-P+ software package (version 14.0 Umetrics, Sweden). Subsequent analyses were performed after centering the variables to zero and scaled to unit variance. All the univariate calculations were performed using R. Univariate statistical significance was estimated using unpaired Student's t test (or Welch´s t test where unequal variances were found). A p-value < 0.05 was considered significant. Non parametric tests (Mann Whitney U, Spearman and Kruskal- Wallis) were used in the statistical analyses of ST data with IBM SPSS.

3.6 ETHICAL STATEMENT

This doctoral thesis has the approval of the competent scientific regulatory authority, Comite Ético de Investigación Clínica de Euskadi (CEIC-E). Following the guidelines of the ethical committee, all patients received information about the study design and purpose, and signed an informed consent prior to their enrollment. The research reported in this thesis adhered to the tenets of the Declaration of Helsinki.

4. RESULTS

Feb 01 2016 06:21:46:506PM

Dear Mr. Cabrerizo:

Your submission entitled "Changes in lipidomic profile of aqueous humor in Fuchs endothelial dystrophy." has been assigned the following manuscript number: CORNEA-D-16-00101.

You will be able to check on the progress of your paper by logging on to Editorial Manager as an author.

http://cornea.edmgr.com/

Your username is: javisea

Your password is: available at this link

http://cornea.edmgr.com/Default.aspx?pg=accountFinder.aspx&firstname=Javier&lastname=Cabrerizo&email_address=javi.cabrerizo@gmail.com

Thank you for submitting your work to Cornea. The journal Cornea is sponsored by The Cornea Society. You can learn more about the Cornea Society and apply for membership at www.corneasociety.org.

Kind Regards,

Leslie Burke

Managing Editor

4.1 PAPER 1

Changes in lipidomic profile of aqueous humour in Fuchs endothelial dystrophy.

Authors:

Authors: Javier Cabrerizo[1,3,4], J. Aritz Urcola[2,3,4], Elena Vecino[4], Gerrit Melles[5,6].

Affiliations:

1 Department of Ophthalmology. Rigshospitalet/Glostrup. University of Copenhagen, Denmark.

2 Department of Ophthalmology. University Hospital of Alava. Spain.

3 Green Eye Project. Research, Spain.

4 Experimental Ophthalmo-Biology Group, (GOBE). University of the Basque Country, (UPV/EHU). Spain.

5 Netherlands Institute for Innovative Ocular Surgery, (NIIOS). The Netherlands.

6 Melles Cornea Clinic Rotterdam. The Netherlands.

4.1.1 ABSTRACT

Purpose:

To identify and determine differences in lipid profiles of aqueous humor (AH) in patients with Fuchs endothelial dystrophy (FED).

Material and methods:

Lipidomic profile of 10 AH samples of FED patients and 10 control samples were analyzed. Patients with previous history of anterior segment surgery, anterior segment pathology or intra-ocular injections were excluded. Topical ocular medications within the last 6 months

were reported. AH was obtained during the first step of Descemet membrane endothelial keratoplasty (DMEK) in FED patients and during refractive lensectomy in the control group. Lipidomic ultra performance liquid chromatography mass spectrometry (UPLC-MS) was used to perform an optimal profiling of glycerolipids, sterol lipids, sphingolipids, and glycerophospholipids. Metabolite extraction was accomplished by fractionating the samples into pools of species with similar physicochemical properties.

Results:

The levels of 32 out of 110 lipids change in the AH of FED eyes when compared to control samples. The concentration of most DAPC and MEMAPC increase in the AH of FED eyes when compared to healthy controls. In addition, 9 SMs (SM) and to 2 long-chain highly unsaturated choleteryl esters (ChoE) present higher levels in FED samples when compared to controls.

Discussion:

The lipid composition of AH in FED patients shows differences when compared with AH of healthy subjects. Those changes may be related to pathological changes in the lipid metabolism of the corneal endothelial cells in FED.

4.1.2 INTRODUCTION

FED is a degenerative corneal condition characterized by deposits of collagen in Descemet membrane (DM), subsequent changes in cell morphology, apoptosis(29),(30),(31), and endothelial cell loss. The characteristic clinical features typically appear between the 4^{th} and 5^{th} decade of life and vary from macroscopic guttae producing light scattering and decrease in visual quality, to chronic, full thickness corneal

edema in the later stages(32).

Currently, the disease is considered to be a multifactorial condition, in which genetic and environmental factors contribute.

Genetics behind FED have been studied and autosomal dominant mutations (L450W and Q455K) in gene COL8A2, encoding the a2 chain of type VIII collagen, have been linked to early onset of the disease in human(33),(34) and in animal model(35). Other gene mutations have been proven to cause specific metabolic changes connected with the physiology of FED, like decrease transmembrane water permeability(36), intracellular protein retention(37), and protein aggregation in DM(38).

UV light-induced oxidative stress(39) remains the main environmental factor for the clinical onset of the disease. UV light causes reactive nitrogen species and reactive oxygen species accumulation(40), triggering metabolic pathways(41),(42), which may lead, in a context of genetic predisposition, to the clinical onset of FED(43).

Recent studies point to the endothelial cell metabolism as a key to understand the physiopathology of the disease. Findings report an increase in intracellular unfolded protein response(44),(16), expression of oxidative stress markers(31), DNA fragmentation(45),(46), down-regulation of protective p53- and nuclear factor (erythroid-derived 2)-like 2 (NFE2L2) -related(47) anti-oxidative stress pathways(31),(48)and subsequent cell apoptosis(46). Although those mechanisms seem to be triggered by changes in cell shape due to aberrant extracellular matrix depositions, oxidative stress has also proven to cause FED-like morphological changes in endothelial cells in vitro(31). This bidirectional relation between oxidative stress and altered cell metabolism, leading to DNA fragmentation, cytoplasmic shrinkage, nuclear collapse and apoptosis, has been reported

to constitute a crucial key in the physiological background of FED. However, the extent of the metabolic changes in FED endothelial cells is still unclear. Following this line of work, our study aims to report potential changes in the lipidomic profile of AH in FED.

Lipids play a key role in organism development, signaling and metabolism. They are synthesized in the endoplasmic reticulum, the Golgi lumen, mainly sphingomyelins (SM), and in the mitochondria (45% of the phospholipids)(49).

Lipid pathways have been shown to be altered in certain conditions related to inflammation and oxidative stress(11),(12),(13) serving as modulators of the apoptotic response in those cases.

Conversely, enhanced apoptotic signaling can significantly alter lipid metabolism in the liver, adipose tissue, skeletal muscle, and macrophage in the context of infection, diabetes, and atherosclerosis(14). Hence, some lipid metabolites have been recently postulated as useful biomarkers for oxidative stress(15). Changes in AH lipidomic profile have been found in open angle glaucoma (OAG)(50). OAG and FED may have singular overlapping etiologies involving apoptosis(51) and oxidative stress(52). Consequently, changes in cell lipid synthesis could be expected in the endothelial cell metabolism in FED, where DNA damage and increased oxidative stress chronically coexist(16),(17).

Lipidomic research has been greatly facilitated by recent advances in lipidomic ultra performance liquid chromatography mass spectrometry (UPLC-MS)(53). UPLC-MS involves lipid extraction, lipid identification and data analysis supporting applications from qualitative and quantitative assessment of multiple lipid species, enabling optimal profiling of glycerolipids, sterol lipids, sphingolipids, and glycerophospholipids(27).

4.1.3 MATERIAL AND METHODS

Demographics:

Lipidomic profile of 20 AH samples, 10 controls, and 10 FED were analyzed. Patients with signs of lens sclerosis at slit lamp examination or a previous history of anterior segment surgery or chronic pathology were excluded from the study. Any topical ocular medications within the last 6 months before the taking of samples were reported.

The subjects were divided in two groups according to their diagnosis. Gender distribution of the two groups was: controls, 6 males and 4 females and FED, 8 males and 2 females. Age average at the moment of surgery was 55.9 years (range: 41-67) and 70.0 years (range: 59-83) in control and FED respectively. In the FED group 8 were pseudophakic and 2 phakic.

Diagnosis of FED was performed through clinical slit lamp examination, specular microscopy and corneal pachymetry. Clinical severity has been graded at the slit lamp by assessing the confluence and area of guttae, and the presence of posterior or full thickness corneal edema(54). All the patients presented a FED stage II with confluent guttae and minimal to mild posterior edema(55).

Ethical statement:

The study has the approval of the competent scientific regulatory authority, Comite Ético de Investigación Clínica de Euskadi (CEIC-E). Following the guidelines of the ethical committee, all patients received information about the study design and purpose, and signed an informed consent prior to their enrollment. The research reported in this study adhered to the tenets of the Declaration of Helsinki.

Sampling and storage:

AH was obtained during the first step of a surgical procedure, refractive lensectomy in controls and DMEK in FED patients. After topical 1% povidone-iodine instillation, around 150 microliters of AH were directly aspirated through a unique corneal side port using a 27-gauge blunt cannula. No noteworthy adverse events were noticed during the aspiration process. A moderate shallowing of the anterior chamber was occasionally perceived. AH was directly introduced in a 0.5 ml tube (Eppendorf AG, Hamburg, Germany) after aspiration and stored at -80°C at the tissue bank for up to 9 months (range: 1-9). Prior to the analyses, samples were left at 24°C for three hours to gradually adjust to room temperature.

Venue:

Control samples were obtained at Begitek Clínica Oftalmológica **(**Plaza Teresa de Calcuta, 7, 20012 Donostia, Guipúzcoa, Spain). FED samples were obtained at Netherlands Institute of Innovative Ocular Surgery (Laan op Zuid 88 3071 AA Rotterdam, The Netherlands). Metabolomic analyses were performed by OWL Metabolomics (Parque Tecnológico de Bizkaia 502, Derio, Spain).

Lipidomic profiling:

A UHPLC coupled to time of flight mass spectrometry based platform was used to perform an optimal profiling of glycerolipids, sterol lipids, sphingolipids, and glycerophospholipids(27).

Aforementioned UPLC-MS was used to perform lipidomic analyses. Metabolite extraction was accomplished by fractionating the samples into pools of species with similar physicochemical properties, using appropriate combinations of organic solvents.

Data pre-processing generated a list of chromatographic peak areas for the metabolites detected in each sample injection. Data normalization was performed following the previously reported procedures(28). After data correction with quality controls, internal standards, and trend amendment a limit of detection was established as three times the background noise level (blanks). Metabolites with more than 5 sample values under the limit of detection were excluded from the analysis.

A normalization procedure was applied after data correction with quality controls, internal standards, and trend amendment by dividing every metabolite species relative concentration by its corresponding “total ion” parameter. This parameter is the result of adding up all the signal intensities (all areas corresponding to ion feature metabolite peaks) integrated in the study within each individual sample.

Metabolite extraction:

Metabolic extraction was accomplished by fractionating the AH samples into pools of species with similar physicochemical properties as previously described(56),(27). AH extracts were mixed with sodium chloride (50 mM) and chloroform / methanol (2:1) in 1.5 ml micro tubes at room temperature. The extraction solvent was spiked with metabolites not detected in unspiked human AH extracts. After brief vortex mixing, the samples were incubated for 1 hour at -20°C. After centrifugation at 16,000 x g for 15 minutes, the organic phase was collected and the solvent removed. The dried extracts were then reconstituted in acetronitrile / isopropanol (1:1), centrifuged (16,000 x g for 5 minutes), and transferred to vials for UHPLC-ToF-MS analysis.

Additionally, a pooled sample was included in the analysis and considered as quality control sample. These quality control samples were evenly distributed over the batch and

extracted and analyzed at the same time as the individual samples. They were used to assess the data quality of the study.

UHPLC-ToF-MS analysis:

Chromatography was performed on a 1 mm i.d. × 100 mm ACQUITY 1.7 µm C8 BEH column (Waters Corp., Milford, USA) using an ACQUITY UPLC system (Waters Corp., Milford, USA). Chromatographic separation and mass spectrometric detection conditions employed were previously described by Barr et al(56).

Data pre-processing:

All data were pre-processed using the TargetLynx application manager for MassLynx4.1software (Waters Corp., Milford, USA). Data pre-processing generated a list of chromatographic peak areas for the metabolites detected in each sample injection. A normalization procedure was applied after data correction with quality controls, internal standards, and trend amendment by dividing every metabolite species relative concentration by its corresponding “total ion” parameter. This parameter is the result of adding up all the signal intensities (all areas corresponding to ion feature metabolite peaks) integrated in the study within each individual sample. A limit of detection limit of detection was established as three times the background noise level. Metabolites with more than 5 sample values under the limit of detection were excluded from the analysis.

The detected lipidomic features were included in the subsequent univariate and multivariate data analysis. Both univariate and multivariate approaches are complementary and their results do not necessarily coincide. The advantages of using both approaches in data mining have been recently reviewed(57).

Multivariate data analysis:

Principal Component Analysis and Partial Least Squares Discriminant Analysis were used to reduce the data matrix to a series of principal components which aim to explain independently the maximum amount of variance possible. These MVA analyses were applied by exporting the normalized data to the SIMCA-P+ software package (version 14.0 Umetrics, Sweden). Subsequent analyses were performed after centering the variables to zero and scaled to unit variance.

Univariate data analysis:

All the univariate calculations were performed using R v2.13.0 (R Development Core Team, 2010; http://cran.r-project.org) with MASS, xlxs, robustbase and pwr packages. Univariate statistical significance was estimated using unpaired Student's t test (or Welch´s t test where unequal variances were found). A p-value < 0.05 was considered significant.

Metabolite classification:

The metabolites were identified before the analysis, as described previously(27),(56). The metabolite classification used in this study follows the comprehensive classification system proposed by the International Lipid Classification and Nomenclature Committee (ILCNC)(58),(59).

4.1.3 RESULTS

Multivariate Analysis (MVA):

The obtained Principal Component Analysis (PCA)(60) scores plot shows clear clustering between FED and control samples in the first component (t1), which explains 27% of the variation of the data (Fig. 1). The PCA does not show any potential outlier. Applying Chauvenet's criterion no lipid species within the sample qualified for data rejection.

Cumulative R^2 is 0.51 and Q^2 values are 0.16, respectively, indicating that the PCA model has a notable degree of fit and predictive ability for the studied sample.

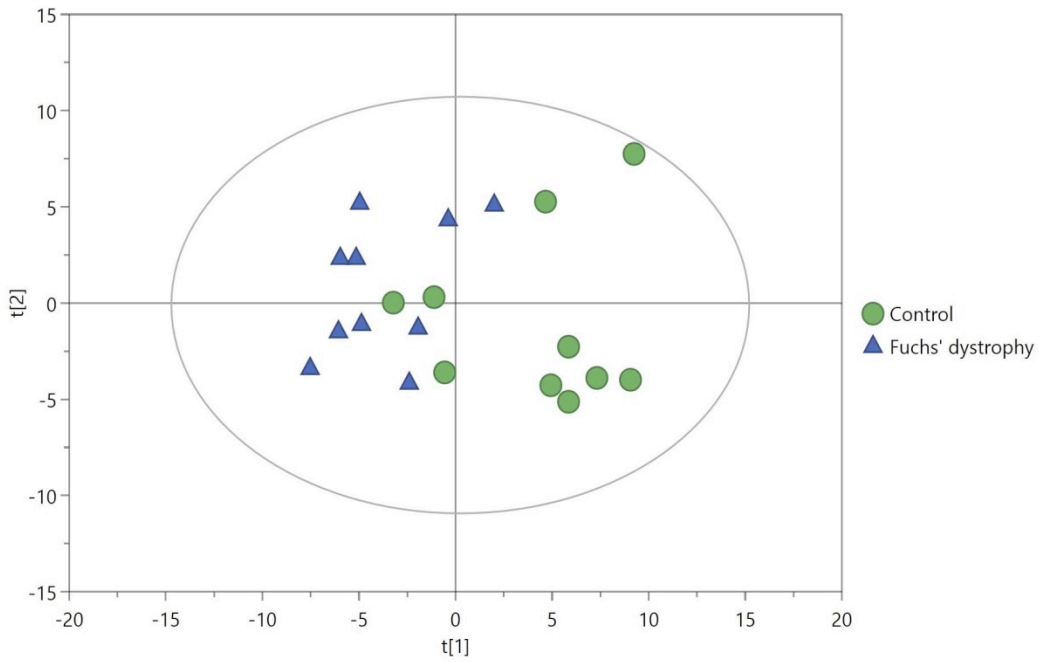

Figure 1: Principal component analyse plot shows the conversions of the studied variables (concentration of different lipid species) into linear uncorrelated variables. The first principal component (t1) accounts for the largest possible variability of the data of FED (n=10) and control samples (n=10).

Lipids responsible for the patterns seen among the groups of samples can be observed in the lower chart (Fig. 2). The highest differences are due to the elevated SM and ChoE levels in FED samples when compared to controls. The supervised analysis (PLS-DA) sample distribution dovetails with the unsupervised PCA findings.

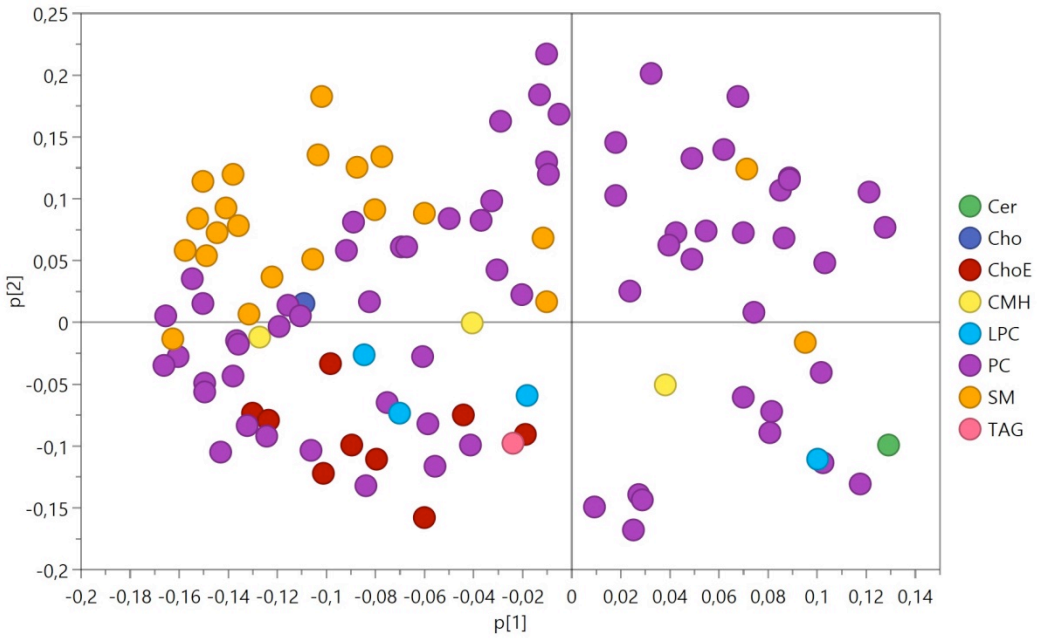

Figure 2. Loadings biplot of FED (n=10) and control samples (n=10) showing the data of every lipid species in relation with the principal components analysis. Lipid species: ceramides (Cer), cholesterol(Cho); ChoEs (ChoE); monohexosylceramides (CMH), Lysophosphatidylcholines (LPC), phosphatidylcholines (PC), SMs (SM), Triacylglycerols (TAG). The diagram shows the importance of variables ChoE and SM in the differences between both groups.

Multivariate analyses after logarithmic or square-root transformations were also applied, seeking to correct aspects that hinder the biological interpretation of data sets by emphasizing the biological information and thus, improving their physiological interpretability(61). Nevertheless, no additional models were found.

Univariate Analysis (UVA):

The concentration of 32 out of 110 lipids changes statistically significantly ($p<0.05$) in FED samples when compared to controls (Fig. 3). The majority of these species (19) belong to the chemical groups of Diacylglycerophosphocholines (DAPC) and 1-ether, 2-acylglycerophosphocholine (MEMAPC), while SM and ChoE also present various significant lipid species altered in FED (Table 1).

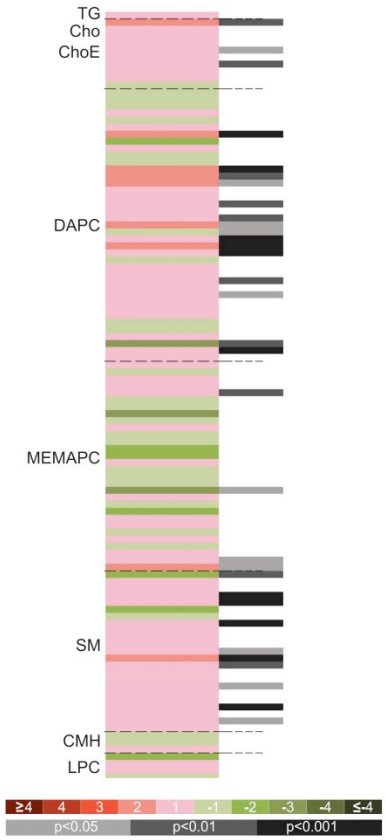

Figure 3: Heatmap of the lipidomic features obtained from the fold-changes and significances derived from the comparison of FED patients versus controls. Color codes for

fold-changes and Student´s t test P-values are indicated in the figure legend. Band thickness refers to the concentration of different species.

Table 1: Lipid species ordered according to their P-values in the comparison of FED and control AH.

The levels of most DAPC and MEMAPC increase in FED samples except for PC(18:1/22:0) + PC(22:0/18:1) and PC(22:4e/16:0) + PC(18:1e/20:3), which decrease about 85%. In addition, PC(18:0/18:1) has been found to decrease only 16%. The greatest increases observed in this chemical group are displayed by PC(16:1/18:2), which is 3.8-fold higher in FED samples when compared to controls.

Up to 9 SM increase significantly in FED, reaching in SM(d18:1/21:0) + SM(d17:1/22:0) + SM(d16:1/23:0) + SM(d19:1/20:0) an increase of 2.3-fold when compared to healthy samples.

Up to 2 long-chain highly unsaturated ChoE; ChoE(20:3), and ChoE(18:2) present higher concentration in FED, showing an increase of about 73% in average. In addition, the individual species of Cer(d18:1/16:0) decreases 73% and unesterified cholesterol increases more than 2-fold in FED samples when compared to controls (Fig. 4).

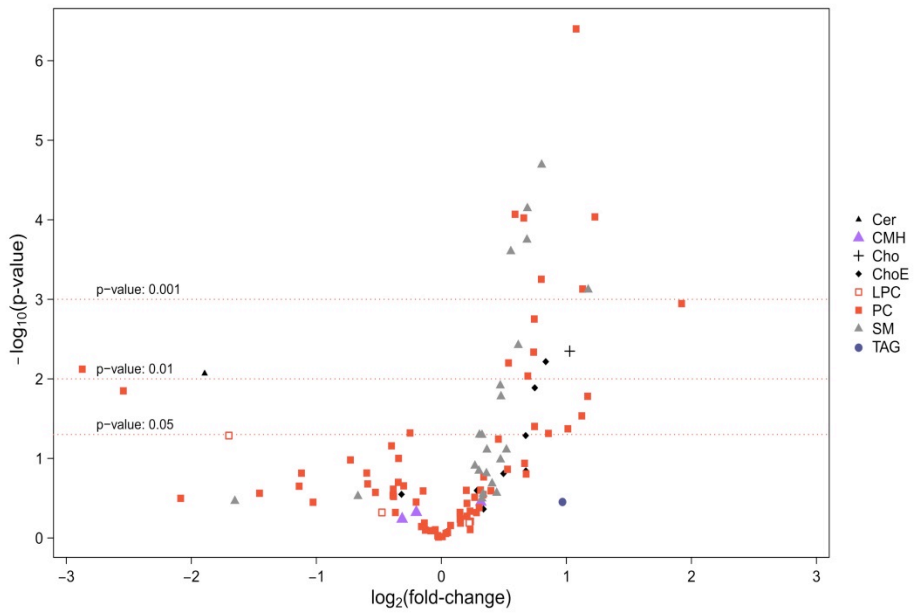

Figure 4: Effect versus significance Volcano Plot [log10(p-value) vs. log2(fold-change)] for the comparison of FED samples versus controls. The plot combines statistical significance (y-axis) with the magnitude of the fold change (x-axis). The higher a lipid specie is represented in the diagram the closer it is to statistically significant levels. Complementarily, the more peripheral a specie is represented in the diagram the greater is the concentration fold change compared to controls.

The average lipid concentrations of the following chemical groups increase in FED samples: ChoE (52%) and SM (27%).

There is an increase of 31% in the ratio SM+DG/Cer+PC in FED, which reflects an up regulation of the synthesis of SM and diacylglycerol from Cer and PC by the enzyme SM synthase (SMS).

4.1.4 DISCUSSION

The physiological changes leading to the clinical features of FED have been a subject of study during past years. Accumulating evidence suggests the role of oxidative stress and genetic predisposition in triggering metabolic-related changes within the endothelial cell(12),(3). When UV-related oxidative stress exceeds the antioxidant-driven response threshold, reactive oxygen species accumulates(43), activating intracellular metabolical Src tyrosine kinase-mediated pathways(44), resulting in apoptosis and secondary worsening of previous oxidative misbalance(45). Genetics seem to have a two level effect in FED; identified mutations in COL8A2(5),(6) are responsible for abnormal collagen deposition in early onset of the disease, and down-regulation of p-53(20) and NFE2L2(21) response have been found in the late FED onset. However, the metabolical link between

etiology and the long time known macroscopic(46) and morphologic changes of corneal endothelium, involving nuclei redistribution around guttae(47), vacuolization(48) and peripheral cytoplasmic thinning(47), remains poorly understood.

This study has unravelled individual and distinctive lipidomic features of AH in patients with FED compared with controls. Regarding lipid chemical groups, divergences lay in the elevated SM and ChoE levels in FED reflecting the rise in the synthesis of SM and DAPC. Our findings link with previously reported AH proteomic profile in FED(49), suggesting that metabolic alterations of endoplasmic reticulum related lipid and protein pathways may take place within the pathophysiological process of the disease. This could represent an additional strand in the oxidative stress-morphological changes tradeoff explaining FED.

Cell type-specific lipid profiles have been shown to influence differential cell vulnerabilities toward chronic oxidative stress(50). ChoE and cholesterol have shown cytoprotective properties of potential clinical relevance(51). Correspondingly, oxidative stress has been reported to affect lipid biosynthesis and fatty acid oxidation cardiovascular and psychiatric disorders(52) and fatty acid oxidation seems to play a role in the physiological response to oxidative stress(53). Correlating to those findings, over-expression of cholesterol acyltransferase and subsequent increase in ChoE have been reported under oxidative stress(54) and ChoE has shown to be specially susceptible to oxidation in cultured cells under metabolic-induced oxidative stress(55). Furthermore, SM synthase-related protein is a suppressor of ceramide induced mitochondrial apoptosis(56). Thus, ceramide channels seem to participate in the protein release from mitochondria during the induction phase of apoptosis(57). Adding evidence presents the rise in SM as a potential part of the endothelial cell response to oxidative stress in FED.

Unfolded proteins response is a well-orchestrated ER response to intracellular oxidative stress and inflammation(58), proven to be enhanced in FED(16). unfolded protein response and oxidative induced ER stress have shown to have important connections to lipid metabolism(59). Thus, major lipid perturbations are found alongside unfolded protein response signaling activation(58), and changes in membrane phospholipid composition are likely to influence activation of unfolded protein response and inflammation pathways(58). Complementarily, unfolded protein response activation may result in dysregulation of lipid synthesis(60).

In addition, several reports suggest that protein folding secondary to insufficient unfolded protein response results in generation of reactive oxygen species as a byproduct of protein oxidation in the ER(61),(62), increasing intracellular oxidative stress. Complementarily, reactive oxygen species can activate unfolded protein response by changing the redox state in the reticulum lumen and reactive oxygen species production is increased during endoplasmic reticulum stress(63),(64). Morphological changes in ER have been found under electron microscopy in several conditions connected with oxidative stress(65). These findings may advocate for a bidirectional cause-effect scenario in the etiology of FED and strengthen the key role of unfolded protein response in the pathogenesis of the condition (Fig. 5).

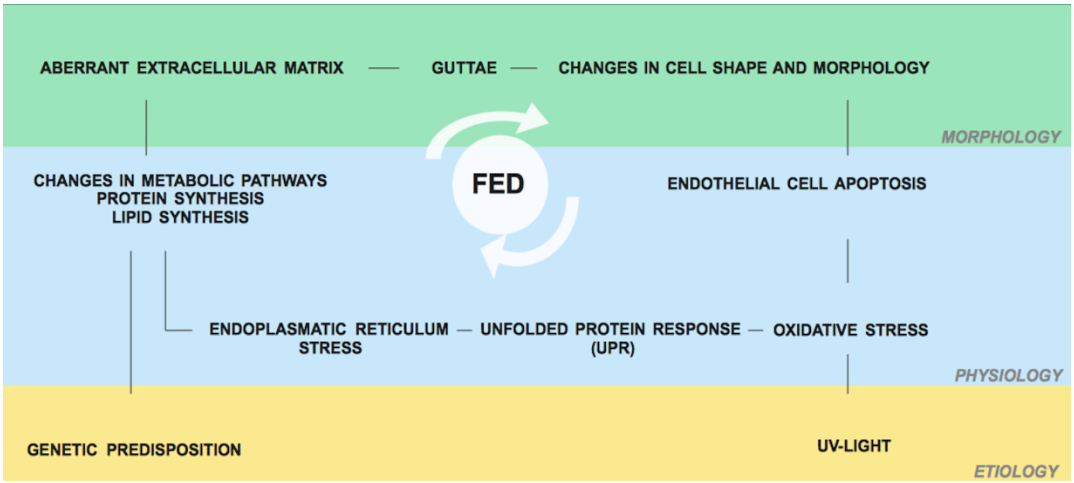

Figure 5: Diagram of FED pathogenesis, evolving its multifactorial etiology, self-perpetuating physiopathological processes and clinically significant morphological changes.

AH is a fast changing, highly dynamic medium and these characteristics constitute the main limitation of our study. Despite topical treatment monitoring, strong inclusion criteria and standardized sample extraction and storage conditions, findings could be attributed to lens capsule permeability or changes in AH production.

The anterior lens capsule is selectively permeable, acting as a barrier for most bacterial and viral infections(66), but enabling solute and Ca2+- and pH-regulated water(67) exchange between the cortex and the AH. Lens anterior permeability is reported to be restricted to small and mid-size molecules, with a cut off molecular weight of 166 ± 82 kDa(68), three to six folds smaller than lipid species studied in this work (SM around 350 kDa, PC around 800 kDa).

Controls, who underwent a refractive lensectomy, were myopic, showing statistically

significant differences in axial length compared with FED patients. Levels of vascular endothelial growth factor, pigment epithelium-derived factor(69) and matrix metalloproteinase 2(70) may increase in AH in highly myopic eyes. However, some of those changes may be associated with matrix metalloproteinase gene polymorphisms(71) and no evidence of lipid-related alterations in AH of myopic patients has been reported.

AH is a complex, highly regulated mechanism, with some unknown aspects still to be elucidated. However, no differences in known AH modulators like day-night fluctuation(72), oral medication(73) or metabolic conditions(74) were identified in both groups. However, FED patients underwent a yag-laser iridotomy 1 to 3 weeks prior to surgery and treatment with topical fluormetholone was established for one week after the procedure. Steroids are well known regulators of water and sodium transport in epithelial tissue and can cause a clinically significant rise of IOP(75). Despite its mild potency and the short time of treatment, fluormetholone induced minor effects on AH composition at the moment of surgery can not be discarded.

In addition, age distribution could arguably play a role in AH composition(76). FED patients were on average 10 years older in this study, however multivariate analysis did not show age-related difference in lipid levels, dovetailing with previously reported AH proteome analysis in FED, where proteomic differences were independent of age distribution(49).

In summary, our study demonstrates changes in the lipidomic profile of AH in FED, mainly related to the increase of SM and ChoE levels and the potential up-regulation of SMS activity. Recognizing the limitations of AH samples to indirectly determine endothelial cell lipid metabolism, our results point to the presence of intracellular lipid-related metabolic changes that could be active players in the pathophysiology of the disease. Those changes may evolve in future biomarkers for disease severity and characterization, potentially enabling preclinical diagnosis and/or a more case specific clinical approach.

A more detailed identification of the interconnection between these processes and a better understanding of the biophysical parameters that govern the modulation of the endothelial morphological changes, remain future challenges in FED research.

3.1.5 REFERENCES

1. Borderie VM, Baudrimont M, Vallée A, Ereau TL, Gray F, Laroche L. Corneal endothelial cell apoptosis in patients with Fuchs' dystrophy. Invest Ophthalmol Vis Sci. 2000 Aug;41(9):2501–5.

2. Czarny P, Kasprzak E, Wielgorski M, Udziela M, Markiewicz B, Blasiak J, et al. DNA damage and repair in Fuchs endothelial corneal dystrophy. Mol Biol Rep. 2013 Apr;40(4):2977–83.

3. Jurkunas UV, Bitar MS, Funaki T, Azizi B. Evidence of Oxidative Stress in the Pathogenesis of Fuchs Endothelial Corneal Dystrophy. Am J Pathol. 2010 Nov;177(5):2278–89.

4. Zhang J, Patel DV. The pathophysiology of Fuchs' endothelial dystrophy--a review of molecular and cellular insights. Exp Eye Res. 2015 Jan;130:97–105.

5. Gottsch JD, Zhang C, Sundin OH, Bell WR, Stark WJ, Green WR. Fuchs corneal dystrophy: aberrant collagen distribution in an L450W mutant of the COL8A2 gene. Invest Ophthalmol Vis Sci. 2005 Dec;46(12):4504–11.

6. Biswas S, Munier FL, Yardley J, Hart-Holden N, Perveen R, Cousin P, et al. Missense mutations in COL8A2, the gene encoding the alpha2 chain of type VIII collagen, cause two forms of corneal endothelial dystrophy. Hum Mol Genet. 2001 Oct 1;10(21):2415–23.

7. Jun AS, Meng H, Ramanan N, Matthaei M, Chakravarti S, Bonshek R, et al. An alpha 2 collagen VIII transgenic knock-in mouse model of Fuchs endothelial corneal dystrophy shows early endothelial cell unfolded protein response and apoptosis.

Hum Mol Genet. 2012 Jan 15;21(2):384–93.

8. Vilas GL, Loganathan SK, Liu J, Riau AK, Young JD, Mehta JS, et al. Transmembrane water-flux through SLC4A11: a route defective in genetic corneal diseases. Hum Mol Genet. 2013 Nov 15;22(22):4579–90.

9. Vilas GL, Loganathan SK, Quon A, Sundaresan P, Vithana EN, Casey J. Oligomerization of SLC4A11 protein and the severity of FECD and CHED2 corneal dystrophies caused by SLC4A11 mutations. Hum Mutat. 2012 Feb;33(2):419–28.

10. Lopez IA, Rosenblatt MI, Kim C, Galbraith GC, Jones SM, Kao L, et al. Slc4a11 gene disruption in mice: cellular targets of sensorineuronal abnormalities. J Biol Chem. 2009 Sep 25;284(39):26882–96.

11. Karamichos D, Hutcheon AEK, Rich CB, Trinkaus-Randall V, Asara JM, Zieske JD. In vitro model suggests oxidative stress involved in keratoconus disease. Sci Rep [Internet]. 2014 Apr 9 [cited 2015 Aug 5];4. Available from: http://www.nature.com/doifinder/10.1038/srep04608

12. Buddi R, Lin B, Atilano SR, Zorapapel NC, Kenney MC, Brown DJ. Evidence of oxidative stress in human corneal diseases. J Histochem Cytochem Off J Histochem Soc. 2002 Mar;50(3):341–51.

13. Greinert R, Volkmer B, Henning S, Breitbart EW, Greulich KO, Cardoso MC, et al. UVA-induced DNA double-strand breaks result from the repair of clustered oxidative DNA damages. Nucleic Acids Res. 2012 Nov 1;40(20):10263–73.

14. Cai CX, Birk DE, Linsenmayer TF. Nuclear Ferritin Protects DNA From UV Damage in Corneal Epithelial Cells. Mol Biol Cell. 1998 May 1;9(5):1037–51.

15. Zhang J, Patel DV. The pathophysiology of Fuchs' endothelial dystrophy--a review of molecular and cellular insights. Exp Eye Res. 2015 Jan;130:97–105.

16. Engler C, Kelliher C, Spitze AR, Speck CL, Eberhart CG, Jun AS. Unfolded protein response in fuchs endothelial corneal dystrophy: a unifying pathogenic pathway? Am J Ophthalmol. 2010 Feb;149(2):194–202.e2.

17. Wojcik K, Kaminska A, Blasiak J, Szaflik J, Szaflik J. Oxidative Stress in the Pathogenesis of Keratoconus and Fuchs Endothelial Corneal Dystrophy. Int J Mol Sci. 2013 Sep 23;14(9):19294–308.

18. Szentmáry N, Szende B, Süveges I. Epithelial cell, keratocyte, and endothelial cell apoptosis in Fuchs' dystrophy and in pseudophakic bullous keratopathy. Eur J Ophthalmol. 2005 Feb;15(1):17–22.

19. Li QJ, Ashraf MF, Shen DF, Green WR, Stark WJ, Chan CC, et al. The role of apoptosis in the pathogenesis of Fuchs endothelial dystrophy of the cornea. Arch Ophthalmol Chic Ill 1960. 2001 Nov;119(11):1597–604.

20. Azizi B, Ziaei A, Fuchsluger T, Schmedt T, Chen Y, Jurkunas UV. p53-regulated increase in oxidative-stress--induced apoptosis in Fuchs endothelial corneal dystrophy: a native tissue model. Invest Ophthalmol Vis Sci. 2011;52(13):9291–7.

21. Ziaei A, Schmedt T, Chen Y, Jurkunas UV. Sulforaphane decreases endothelial cell apoptosis in fuchs endothelial corneal dystrophy: a novel treatment. Invest Ophthalmol Vis Sci. 2013 Oct;54(10):6724–34.

22. Nelson DL, Cox MM, Lehninger AL. Lehninger principles of biochemistry. 6., internat. ed. New York: Freeman; 2013.

23. Kunchithapautham K, Atkinson C, Rohrer B. Smoke exposure causes endoplasmic reticulum stress and lipid accumulation in retinal pigment epithelium through oxidative stress and complement activation. J Biol Chem. 2014 May 23;289(21):14534–46.

24. Turkdogan KA, Akpinar O, Karabacak M, Akpinar H, Turkdogan FT, Karahan O. Association between oxidative stress index and serum lipid levels in healthy young adults. JPMA J Pak Med Assoc. 2014 Apr;64(4):379–81.

25. Mukhopadhyay R. Mouse models of atherosclerosis: explaining critical roles of lipid metabolism and inflammation. J Appl Genet. 2013 May;54(2):185–92.

26. van Diepen JA, Berbée JFP, Havekes LM, Rensen PCN. Interactions between inflammation and lipid metabolism: relevance for efficacy of anti-inflammatory drugs in the treatment of atherosclerosis. Atherosclerosis. 2013 Jun;228(2):306–15.

27. Niki E. Lipid peroxidation products as oxidative stress biomarkers. BioFactors Oxf Engl. 2008;34(2):171–80.

28. Burgess LG, Uppal K, Walker DI, Roberson RM, Tran V, Parks MB, et al. Metabolome-Wide Association Study of Primary Open Angle Glaucoma. Invest Ophthalmol Vis Sci. 2015 Jul 1;56(8):5020–8.

29. Guo L, Moss SE, Alexander RA, Ali RR, Fitzke FW, Cordeiro MF. Retinal ganglion cell apoptosis in glaucoma is related to intraocular pressure and IOP-induced effects on extracellular matrix. Invest Ophthalmol Vis Sci. 2005 Jan;46(1):175–82.

30. Ferreira SM, Lerner SF, Brunzini R, Evelson PA, Llesuy SF. Oxidative stress markers in aqueous humor of glaucoma patients. Am J Ophthalmol. 2004

Jan;137(1):62–9.

31. Kim EC, Meng H, Jun AS. N-Acetylcysteine increases corneal endothelial cell survival in a mouse model of Fuchs endothelial corneal dystrophy. Exp Eye Res. 2014 Oct;127:20–5.

32. Nygren H, Seppänen-Laakso T, Castillo S, Hyötyläinen T, Orešič M. Liquid chromatography-mass spectrometry (LC-MS)-based lipidomics for studies of body fluids and tissues. Methods Mol Biol Clifton NJ. 2011;708:247–57.

33. Barr J, Vázquez-Chantada M, Alonso C, Pérez-Cormenzana M, Mayo R, Galán A, et al. Liquid Chromatography−Mass Spectrometry-Based Parallel Metabolic Profiling of Human and Mouse Model Serum Reveals Putative Biomarkers Associated with the Progression of Nonalcoholic Fatty Liver Disease. J Proteome Res. 2010 Sep 3;9(9):4501–12.

34. Louttit MD, Kopplin LJ, Igo RP, Fondran JR, Tagliaferri A, Bardenstein D, et al. A multicenter study to map genes for Fuchs endothelial corneal dystrophy: baseline characteristics and heritability. Cornea. 2012 Jan;31(1):26–35.

35. Adamis AP, Filatov V, Tripathi BJ, Tripathi RC. Fuchs' endothelial dystrophy of the cornea. Surv Ophthalmol. 1993 Oct;38(2):149–68.

36. van der Kloet FM, Bobeldijk I, Verheij ER, Jellema RH. Analytical error reduction using single point calibration for accurate and precise metabolomic phenotyping. J Proteome Res. 2009 Nov;8(11):5132–41.

37. Barr J, Caballería J, Martínez-Arranz I, Domínguez-Díez A, Alonso C, Muntané J, et al. Obesity-Dependent Metabolic Signatures Associated with Nonalcoholic Fatty

Liver Disease Progression. J Proteome Res. 2012 Apr 6;11(4):2521–32.

38. Martínez-Arranz I, Mayo R, Pérez-Cormenzana M, Mincholé I, Salazar L, Alonso C, et al. Data in support of enhancing metabolomics research through data mining. Data Brief. 2015 Jun;3:155–64.

39. Fahy E. A comprehensive classification system for lipids. J Lipid Res. 2005 Feb 16;46(5):839–62.

40. Fahy E, Subramaniam S, Murphy RC, Nishijima M, Raetz CRH, Shimizu T, et al. Update of the LIPID MAPS comprehensive classification system for lipids. J Lipid Res. 2008 Dec 19;50(Supplement):S9–14.

41. Jolliffe IT. Principal component analysis [Internet]. New York: Springer; 2002 [cited 2015 Jul 23]. Available from: http://site.ebrary.com/id/10047693

42. van den Berg RA, Hoefsloot HCJ, Westerhuis JA, Smilde AK, van der Werf MJ. Centering, scaling, and transformations: improving the biological information content of metabolomics data. BMC Genomics. 2006;7:142.

43. Heck DE, Vetrano AM, Mariano TM, Laskin JD. UVB light stimulates production of reactive oxygen species: unexpected role for catalase. J Biol Chem. 2003 Jun 20;278(25):22432–6.

44. Giannoni E, Buricchi F, Raugei G, Ramponi G, Chiarugi P. Intracellular reactive oxygen species activate Src tyrosine kinase during cell adhesion and anchorage-dependent cell growth. Mol Cell Biol. 2005 Aug;25(15):6391–403.

45. Espinosa-Diez C, Miguel V, Mennerich D, Kietzmann T, Sánchez-Pérez P, Cadenas

S, et al. Antioxidant responses and cellular adjustments to oxidative stress. Redox Biol. 2015 Dec;6:183–97.

46. Fuchs E. Dystrophia epithelialis cornea. Albrecht Von Graefes Arch Klin Ophthalmol. 1910;76(478–508).

47. Bergmanson JP, Sheldon TM, Goosey JD. Fuchs' endothelial dystrophy: a fresh look at an aging disease. Ophthalmic Physiol Opt J Br Coll Ophthalmic Opt Optom. 1999 May;19(3):210–22.

48. Kayes J, Holmberg A. The Fine Structure of the Cornea in Fuchs' Endothelial Dystrophy. Invest Ophthalmol Vis Sci. 1964 Feb;3:47–67.

49. Richardson MR, Segu ZM, Price MO, Lai X, Witzmann FA, Mechref Y, et al. Alterations in the aqueous humor proteome in patients with Fuchs endothelial corneal dystrophy. Mol Vis. 2010;16:2376–83.

50. Clement AB, Gamerdinger M, Tamboli IY, Lütjohann D, Walter J, Greeve I, et al. Adaptation of neuronal cells to chronic oxidative stress is associated with altered cholesterol and sphingolipid homeostasis and lysosomal function. J Neurochem. 2009 Nov;111(3):669–82.

51. Zager RA, Kalhorn TF. Changes in free and esterified cholesterol: hallmarks of acute renal tubular injury and acquired cytoresistance. Am J Pathol. 2000 Sep;157(3):1007–16.

52. Assies J, Mocking RJT, Lok A, Ruhé HG, Pouwer F, Schene AH. Effects of oxidative stress on fatty acid- and one-carbon-metabolism in psychiatric and cardiovascular disease comorbidity. Acta Psychiatr Scand. 2014 Sep;130(3):163–80.

53. McFadden JW, Aja S, Li Q, Bandaru VVR, Kim E-K, Haughey NJ, et al. Increasing fatty acid oxidation remodels the hypothalamic neurometabolome to mitigate stress and inflammation. PloS One. 2014;9(12):e115642.

54. Kim J-H, Ee S-M, Jittiwat J, Ong E-S, Farooqui AA, Jenner AM, et al. Increased expression of acyl-coenzyme A: cholesterol acyltransferase-1 and elevated cholesteryl esters in the hippocampus after excitotoxic injury. Neuroscience. 2011 Jun 30;185:125–34.

55. Saito Y, Yoshida Y, Niki E. Cholesterol is more susceptible to oxidation than linoleates in cultured cells under oxidative stress induced by selenium deficiency and free radicals. FEBS Lett. 2007 Sep 4;581(22):4349–54.

56. Tafesse FG, Vacaru AM, Bosma EF, Hermansson M, Jain A, Hilderink A, et al. Sphingomyelin synthase-related protein SMSr is a suppressor of ceramide-induced mitochondrial apoptosis. J Cell Sci. 2014 Jan 15;127(Pt 2):445–54.

57. Siskind LJ. Mitochondrial Ceramide and the Induction of Apoptosis. J Bioenerg Biomembr. 2005 Jun;37(3):143–53.

58. Volmer R, Ron D. Lipid-dependent regulation of the unfolded protein response. Curr Opin Cell Biol. 2015 Apr;33:67–73.

59. Yano M, Yamamoto T, Nishimura N, Gotoh T, Watanabe K, Ikeda K, et al. Increased Oxidative Stress Impairs Adipose Tissue Function in Sphingomyelin Synthase 1 Null Mice. Siskind LJ, editor. PLoS ONE. 2013 Apr 12;8(4):e61380.

60. Basseri S, Austin RC. Endoplasmic Reticulum Stress and Lipid Metabolism: Mechanisms and Therapeutic Potential. Biochem Res Int. 2012;2012:1–13.

61. Malhotra JD, Kaufman RJ. Endoplasmic reticulum stress and oxidative stress: a vicious cycle or a double-edged sword? Antioxid Redox Signal. 2007 Dec;9(12):2277–93.

62. Gregersen N, Bross P. Protein misfolding and cellular stress: an overview. Methods Mol Biol Clifton NJ. 2010;648:3–23.

63. Santos CXC, Tanaka LY, Wosniak J, Laurindo FRM. Mechanisms and implications of reactive oxygen species generation during the unfolded protein response: roles of endoplasmic reticulum oxidoreductases, mitochondrial electron transport, and NADPH oxidase. Antioxid Redox Signal. 2009 Oct;11(10):2409–27.

64. Li G, Scull C, Ozcan L, Tabas I. NADPH oxidase links endoplasmic reticulum stress, oxidative stress, and PKR activation to induce apoptosis. J Cell Biol. 2010 Dec 13;191(6):1113–25.

65. Chiang P-C, Chien C-L, Pan S-L, Chen W-P, Teng C-M, Shen Y-C, et al. Induction of endoplasmic reticulum stress and apoptosis by a marine prostanoid in human hepatocellular carcinoma. J Hepatol. 2005 Oct;43(4):679–86.

66. Danysh BP, Duncan MK. The lens capsule. Exp Eye Res. 2009 Feb;88(2):151–64.

67. Varadaraj K, Kumari S, Shiels A, Mathias RT. Regulation of Aquaporin Water Permeability in the Lens. Investig Opthalmology Vis Sci. 2005 Apr 1;46(4):1393.

68. Kastner C, Löbler M, Sternberg K, Reske T, Stachs O, Guthoff R, et al. Permeability of the anterior lens capsule for large molecules and small drugs. Curr Eye Res. 2013 Oct;38(10):1057–63.

69. Shin YJ, Nam WH, Park SE, Kim JH, Kim HK. Aqueous humor concentrations of vascular endothelial growth factor and pigment epithelium-derived factor in high myopic patients. Mol Vis. 2012;18:2265–70.

70. Jia Y, Hu D-N, Zhu D, Zhang L, Gu P, Fan X, et al. MMP-2, MMP-3, TIMP-1, TIMP-2, and TIMP-3 protein levels in human aqueous humor: relationship with axial length. Invest Ophthalmol Vis Sci. 2014 Jun;55(6):3922–8.

71. Wojciechowski R, Bailey-Wilson JE, Stambolian D. Association of Matrix Metalloproteinase Gene Polymorphisms with Refractive Error in Amish and Ashkenazi Families. Investig Opthalmology Vis Sci. 2010 Oct 1;51(10):4989.

72. Göbel K, Rüfer F, Erb C. [Physiology of aqueous humor formation, diurnal fluctuation of intraocular pressure and its significance for glaucoma]. Klin Monatsblätter Für Augenheilkd. 2011 Feb;228(2):104–8.

73. Shahidullah M, Wilson WS, Yap M, To C. Effects of ion transport and channel-blocking drugs on aqueous humor formation in isolated bovine eye. Invest Ophthalmol Vis Sci. 2003 Mar;44(3):1185–91.

74. Kiel JW, Hollingsworth M, Rao R, Chen M, Reitsamer HA. Ciliary blood flow and aqueous humor production. Prog Retin Eye Res. 2011 Jan;30(1):1–17.

75. Rauz S, Cheung CMG, Wood PJ, Coca-Prados M, Walker EA, Murray PI, et al. Inhibition of 11 -hydroxysteroid dehydrogenase type 1 lowers intraocular pressure in patients with ocular hypertension. QJM. 2003 Jul 1;96(7):481–90.

76. Goel M. Aqueous Humor Dynamics: A Review~!2010-03-03~!2010-06-17~!2010-09-02~! Open Ophthalmol J. 2010 Sep 3;4(1):52–9.

Biophysical properties of aqueous humour in ocular pathologies

Ref. MS No. EXER16-102

Title: Changes in surface tension of aqueous humor in anterior segment ocular pathologies.

Authors: Javier Cabrerizo, M.D.; J Aritz Urcola, PhD; Elena Vecino, Professor

Article Type: Research article

Dear Mr. Cabrerizo,

Your submission referenced above has been assigned the following manuscript number: EXER16-102.

You will be able to check on the progress of your paper by logging on to Elsevier Editorial System as an author.

The URL is http://ees.elsevier.com/yexer/.

Your username is: javi.cabrerizo@gmail.com

Thank you for submitting your work to this journal.

Yours sincerely,

Experimental Eye Research

4.2 PAPER 2

Changes in surface tension of aqueous humour in anterior segment ocular pathologies.

Authors: Javier Cabrerizo[1,3,5], J. Aritz Urcola[2,3], Gerrit Melles[5,6], Elena Vecino[4].

Affiliations:

1 Department of Ophthalmology. Rigshospitalet/Glostrup. University of Copenhagen, Denmark.

2 Department of Ophthalmology. University Hospital of Alava. Spain.

3 Green Eye Project. Research. Spain.

4 Experimental Ophthalmo-Biology Group, (GOBE). University of the Basque Country, (UPV/EHU). Spain.

5 Netherlands Institute for Innovative Ocular Surgery, (NIIOS). The Netherlands.

6 Melles Cornea Clinic Rotterdam. The Netherlands.

4.2.1 ABSTRACT

Purpose:

To identify and determine differences in surface tension (ST) of aqueous humor (AH) in patients with cataract, glaucoma and Fuchs endothelial dystrophy (FED).

Material and methods:

202 samples of AH were analyzed (control n=22, cataract n=56, glaucoma n=81, and n=FED 43). Patients with previous history of anterior segment surgery, anterior segment pathology or intraocular injections were excluded from the study.

Topical ocular medications within the last 6 months were reported. Different types of glaucoma were identified, cataracts were graded using total phaco time data during surgery and clinical severity of FED was graded by clinical features at slit lamp examination. Around 150 microliters AH were obtained during the first step of a surgical procedure, lensectomy, phacoemulsification, nonperforating deep sclerectomy (NPDE), and Descemet membrane endothelial keratoplasty (DMEK). A pendant drop based optical goniometer, OCA-15 (Dataphysics, Filderstadt, Germany) was used to measure ST. SPSS21 (IBM, Armonk, NY, USA) was used for the statistical analysis of the data.

Results:

Mean ST was 65.74±3.76, 63.59±5.50, 64.35±6.99, and 60,89±3.73 in control, cataract, glaucoma and FED patients respectively. Statistically significant differences between FED and control group were found (P=0.00). Lens condition, cataract maturity, age, and gender did not show influence in ST.

Discussion:

ST of AH is significantly decreased in FED patients independently from age and lens condition. Those findings may aid to the understanding of the physiopathology of the disease.

4.2.2 INTRODUCTION

ST is the elastic tendency of fluids caused by intermolecular attraction forces in the surface layer, which makes them acquire the least surface area possible(1). ST defines the interfacial properties of a fluid(2). ST of organic fluids is highly dynamic and closely related to the concentration and the type of surface active compounds. These surfactants, mainly

proteins and lipids, are characterized by a high surface protein adsorption activity at low bulk concentrations, drastically affecting fluid interfacial properties. As ST is highly sensitive to even small changes in the type and/or concentration of surfactant constituents, it bears diagnostic potential to detect changes in the lipid and protein profile of body fluids, and their changes in pathological conditions(3).

Many surfactants play a significant role in vital functions of the human organism. Surfactant dependent increased in ST induces narrowing of alveolar capillaries and oxygen desaturation, being of crucial clinical relevance in neonatology(4). Increasing evidence suggest the influence of ST in embryological organ development of the vascular system, remodeling vascular patterns and controlling cell to cell adhesion(5). There are known physiological differences in ST of human fluids related to age, gender and pregnancy, linked with physiological variations of protein concentration in serum and urine(6). Thus, an inverse correlation exists between ST of serum and concentration of surfactants in healthy subjects. Dovetailing with this, increase of phospholipids in human fluids has been related with a decrease in its ST, showing potential influence in ST regulated physiological processes.

In addition, numerous reports show disease-linked variations in levels of specific surface active molecules in organic fluids(7). Although in many cases those changes are known to have great influence in the onset of the condition and result from disease progression, in others, its potential etiological relevance remains unknown(8).

AH production is a complex, highly regulated mechanism, with some unknown aspects still to be elucidated. Production and composition of AH is altered under several circumstances, circadian day-night fluctuations(9), systemic conditions(10),(11), topical medication(12) and ocular diseases(13).

Proteomic and lipidomic studies of AH suggest an increase in proteins and lipid compounds in some anterior segment pathologies(14),(15). Accordingly, resulting changes in AH interfacial properties with potential clinical significance may be expected. Following this line of work, our study aims to address changes in ST of AH in three common anterior segment pathologies: cataract, glaucoma and FED.

4.2.3 MATERIAL AND METHODS

Demographics:

Table 1: Demographic data displaying age, gender and lens condition within each of the 4 groups.

202 samples of AH were analyzed (Table 1). Patients with previous history of anterior segment surgery, anterior segment pathology or intraocular injections were not included in the study. Any topical ocular medications within the last 6 months were reported.

AH in 22 controls was obtained at the first step of an elective lensectomy or Implantable Collamer Lens (ICL) implant. All cataract surgeries were performed by the same surgeon. In 44 of them severity was graded by the following phacoemulsification parameters: total phaco time, longitudinal phaco time, torsional phaco time, and cumulative dissipated energy. Data were generated by the phacoemulsification device (Infinity, Alcon, Fort Worth, Texas, United States). Different types of glaucoma were identified and classified in 8 groups as follows: open angle (n=55), narrow angle (n=7), pseudoexfoliative (n=8), pigmentary (n=2), neovascular (n=1), steroid induced (n=1), uveitic (n=6), and myopic (n=1). Diagnosis of FED was performed through clinical slit lamp examination, specular microscopy, and corneal pachymetry. Clinical severity has been graded at the slit lamp by assessing the confluence and area of guttae, and the presence of posterior or full thickness corneal edema(16).

Ethical statement:

The research was approved by the competent institutional human experimentation committee, Comite Ético de Investigación Clínica de Euskadi (CEIC-E). Following the guidelines of the committee, informed consent was obtained from the subjects after explanation of the nature and possible consequences of the study, prior to their enrolment. The research reported in this study adhered to the tenets of the Declaration of Helsinki.

Sampling:

AH was obtained during the first step of a surgical procedure, refractive lensectomy, phacoemulsification, NPDE, and DMEK, in controls, cataract, glaucoma, and FED patients respectively. After topical 1% povidone-iodine instillation, around 150 microliters of AH were directly aspirated through a unique corneal side port using a 27-gauge blunt cannula. No noteworthy adverse events were noticed during the aspiration process. A moderate

shallowing of the anterior chamber was occasionally perceived. AH was directly introduced in a 0.5 ml tube (Eppendorf AG, Hamburg, Germany) after aspiration and stored at -80°C at the tissue bank for up to 9 months (range: 1-9). Prior to the analyses, samples were left at 24°C for three hours to gradually adjust to room temperature.

Venue:

Control samples were obtained at Begitek Clínica Oftalmológica **(**Plaza Teresa de Calcuta, 7, 20012 Donostia, Guipúzcoa, Spain). Cataract and glaucoma cases were obtained at Araba University Hospital (C/ Jose Atxotegi, s/n, 01009 Vitoria-Gasteiz, Álava, Spain). FED samples were obtained at Netherlands Institute of Innovative Ocular Surgery (Laan op Zuid 88 3071 AA Rotterdam, The Netherlands). ST analysis was performed at the Laboratory of Experimental Ophthalmology at the University Hospital of Alava.

Sample manipulation and storage:

After extraction, samples were stored frozen at -80°C at the research tissue bank for up to 9 months (range 1-9). Prior to the start of the analyses, samples were left at 24°C for three hours to gradually adjust to room temperature.

ST analyses:

A pendant drop method based optical goniometer, OCA-15 (Dataphysics, Filderstadt, Germany) was used to measure ST. The technique involves the acquisition of a silhouette of an axisymmetric fluid droplet, and iterative fitting of the Young-Laplace equation that balances gravitational deformation of the drop with the restorative interfacial tension. The unit consists of a computerized optical video camera and a high precision syringe holder. The AH is aspirated by an 18 gauge metal cannula connected to a 200 microliter metal precision syringe (Hamilton, Reno, Nevada, USA) and is placed vertical in the syringe

holder. A software controlled system activates a motor which presses the piston of the syringe at constant speed. When the fluid reaches the tip of the cannula, a drop starts to form. The high quality optical camera takes a snapshot of the drop at the critical hydrostatic energy point (Fig. 1). This point is characterized by a visible “neck” in the transition between the fluid and the tip of the cannula. The radius of curvature at the apex of the drop (R) is calculated. Using the Bashford-Adams method, the ST is inferred by applying the Young-Laplace equation to the outline of the drop. ST results are given in accordance to the International System of Units in Newton per meter (N/m).

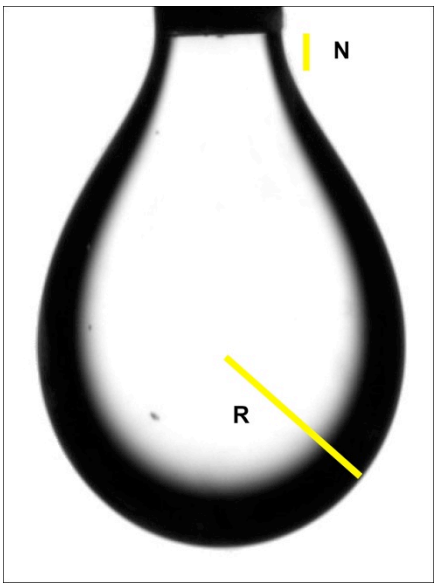

Figure 1: Snapshot of a pendant drop at the moment of ST calculation. The neck area (N), with a constant diameter, defines the critical hydrostatic energy point. Radius of curvature at the apex of the drop (R) is calculated by the software.

Density, altitude and temperature are recognized as crucial parameters to alter ST of a fluid. We used bovine AH density (1.007g/cm^3) as the closest estimation available in literature(17). Room temperature was monitored throughout the whole process and was

kept stable at 24°C. 9 samples (3 control group, 1 cataract group, 5 FED group) were dismissed due to insufficient sample volume and are not included in the demographics of the study(18),(19),(20).

Data processing:

The data were processed using the device specific software. 40 measurements were taken of every optimal drop image. Only results within a range of 0.2 were considered valid. Higher deviations were considered perturbations on accuracy due to vibrations and measurements were repeated(21). This threshold was set due to prior 20 repeated measurements with ultra pure water type1 (Mili-Q, Millipore Corporation, Darmstadt, Germany). The standard deviation (SD) of the 20 measurements was 0.045. For the ST data, maximal accepted standard error was set at 1.2. Results variability and instrument related measurement bias were studied in a series of 20 repeated measurements with ultra pure water type1 (Mili-Q, Millipore Corporation, Darmstadt, Germany) with very low SD (0.045). SPSS21 (IBM, Armonk, NY, USA) was used for the statistical analysis of the data.

4.2.4 RESULTS

Demographics:

Table 1: Demographic data displaying age, gender and lens condition within each of the 4 groups.

ST between groups (Table 2):

Table 2: Descriptive analysis of ST data.

Man-Witney U test was applied to address differences in ST between controls and each group. Statistically significant differences between FED and control group were found (p=0.000). No statistically significant differences between cataracts and controls and glaucoma and controls were found (Fig. 2A-B)

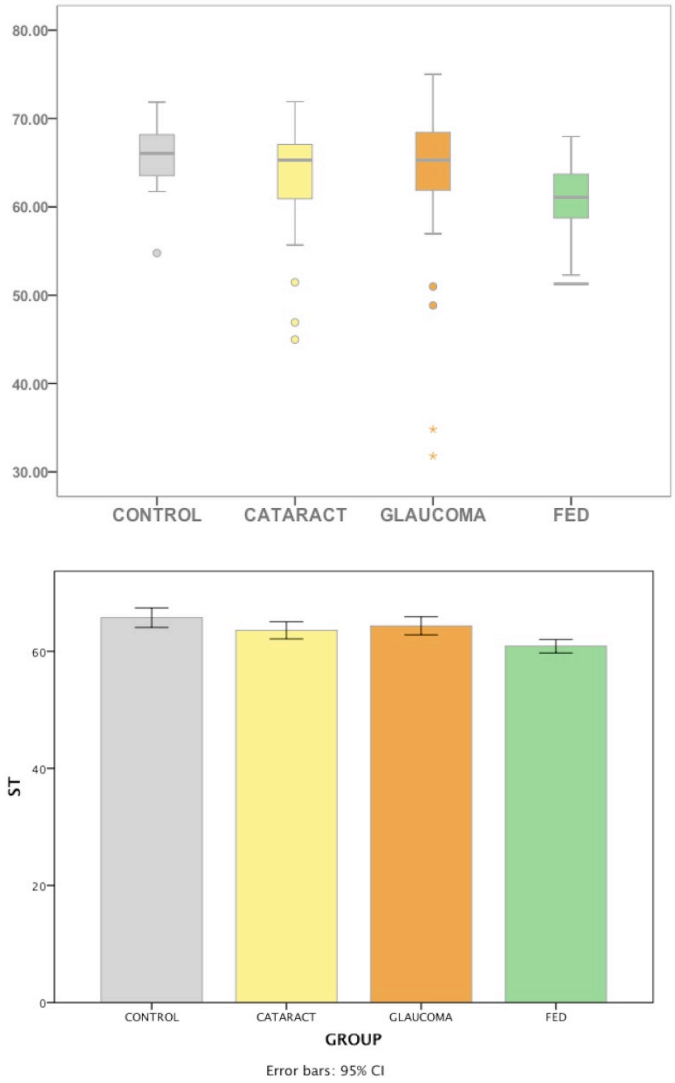

Figure 2A-B: Box-Plot diagram representing ST data for the four groups. ST, y-axis, is measured in N/m.

Age / gender distribution:

Spearman's rank test did not find correlation between age and St and gender and ST.

Lens condition and cataract maturity:

We addressed the potential influence of the lens condition (phakic/pseudophakic/aphakic) in ST. No differences in ST between phakic and pseudophakic patients within FED and glaucoma groups were found (P=0.430 and P=0.702) respectively (Fig. 3).

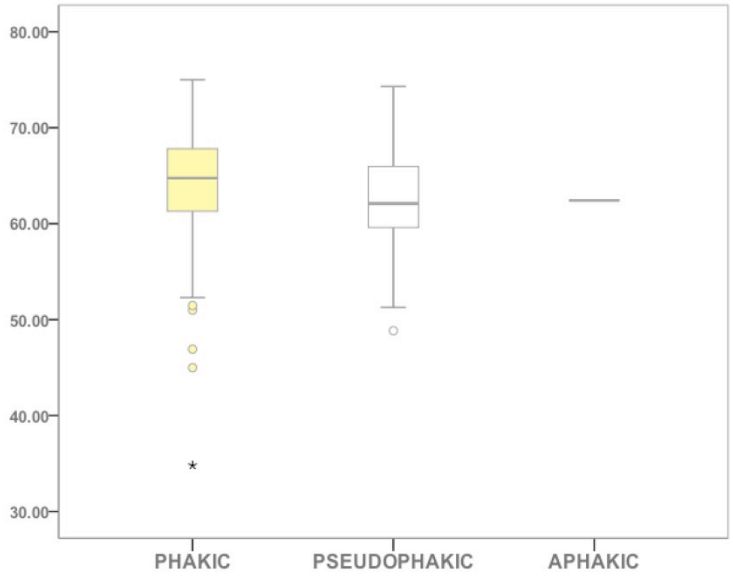

Figure 3: Box-Plot diagram representing ST data for different lens conditions.

To study the hypothetical role of cataract maturity in ST we graded cataract cases using the intraoperative phaco parameters. All the surgeries were performed by the same, experienced surgeon. Surgery conditions were similar throughout all the cases. No correlation between total phaco time, torsional phaco time, longitudinal phaco time and cumulative dissipated energy and ST was found (Fig. 4).

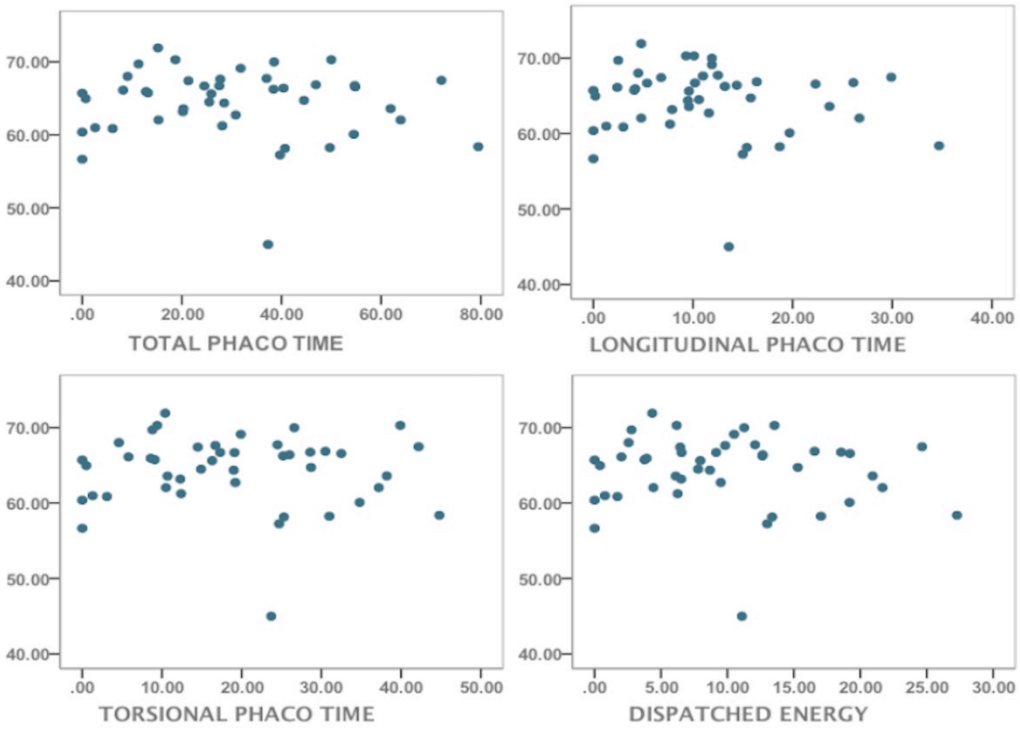

Figure 4: Scatter plots showing the phaco parameters in 44 cataract cases. Data are shown in seconds and ST (y-axis) in N/m.

8 different types of glaucoma (Table 3) were identified. Kruskal-Wallis one-way analysis of variance was used to address differences between groups. No statistical significant differences in ST data were found between groups (Fig. 5).

Table 3: ST statistical analyses between the different glaucoma groups.

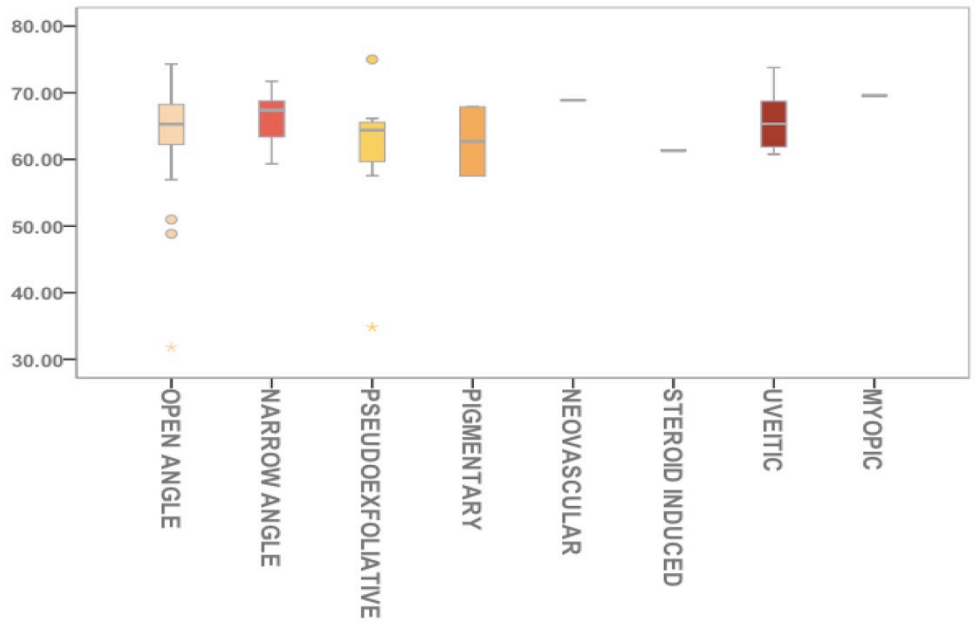

Figure 5: Box-Plot diagram representing ST data for different types of glaucoma.

The effect of topical medication was also studied. Anti-glaucomatous topical medication within the last 6 months before surgery was reported. Patients were divided in 4 groups by the number of medications that they were instilling. No difference was made between one

component medication or fixed-combinations. The number of topical medications did not show to affect ST data. In addition, no further relations between anti-glaucomatous type and ST were found (Fig. 6).

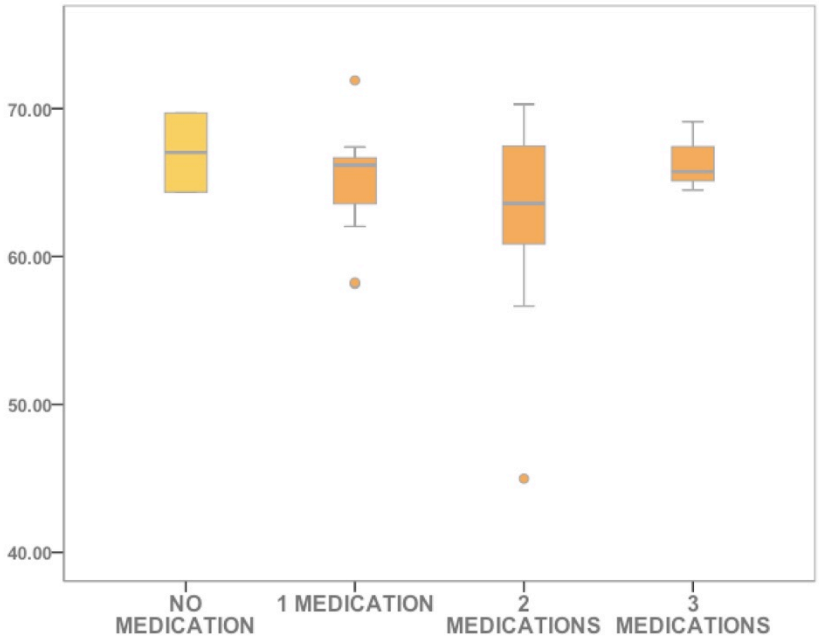

Figure 6: Box-Plot diagram representing ST data for glaucoma cases with different number of medication.

Statistically significant differences in ST data were found between FED and controls (P=0.000) (Fig. 7). Kruskal-Wallis rank test was used to address the effect accounted for FED in ST. FED shown to have 31.4% (R^2=0.314) influence in the data of ST. Those differences were independent of the lens condition within FED group (P=0.436) (Table 4).

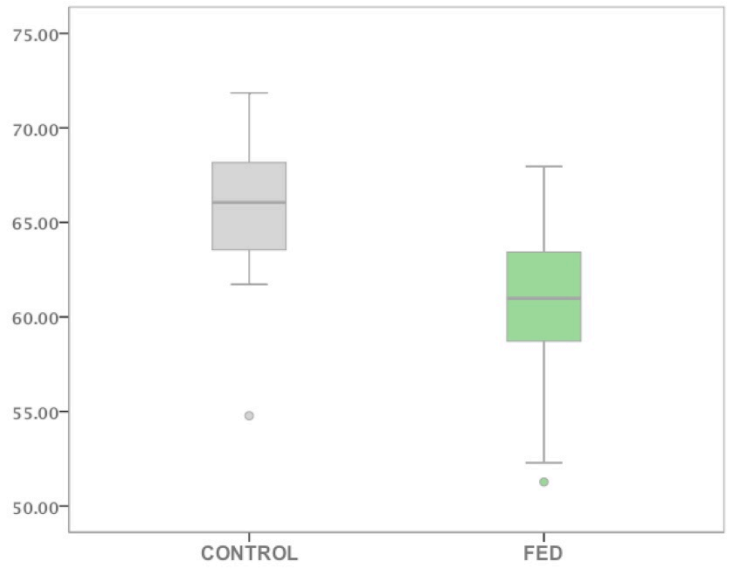

Figure 7: Box-Plot diagram of ST data for controls and FED.

Table 4: ST statistical analyses between control and FED and between phakic and pseudophakic FED cases.

4.2.5 DISCUSSION

This study unravelled differences in ST between FED AH samples and controls. We did not find differences between age distribution, gender or lens status. These findings suggest disease related variations in concentration of organic surfactants with a potential

role in the physiology of the disease.

AH composition in ocular pathologies has been a matter of study in recent years. Differences in AH composition have been associated to common pathologies. Specific changes in lipid peroxidation markers of AH have been found to be a good predictor of cataract maturity(22) and an up-regulated expression of inflammatory proteins has been found in AH of highly myopic patients with cataract. Furthermore, increasing lens capsule permeability in cataract(23) could also affect AH composition. However, lens anterior permeability is reported to be restricted to small and mid-size molecules, with a cut off molecular weight of 166 ± 82 kDa(24), significantly smaller than most organic surfactants.. Accordingly, ST did not show to be a good predictor of cataract maturity in our study.

The physiopathology of glaucoma is strongly related to fluid interphase properties at the Schlemm's canal and the juxtacanalicular portion of the trabecular meshwork(25). The main bulk of the outflow resistance takes place at the juxtacanalicular portion(26), where also close metabolic relations between epithelial cell and AH take place potentially altering AH composition(27),(28). In addition, the last part of the transport of AH to the Schlemm's canal is a pinocitosis-like process, where giant vacuoles play a role(29). ST of the fluid influences vacuole forming and stability and may have potential influence in the final part of AH outflow.

Recent studies point to the endothelial cell metabolism as a key to understand the physiopathology of the FED. Findings report an increase in intracellular unfolded protein response(30),(31), expression of oxidative stress markers(32), DNA fragmentation(33),(34), down-regulation of protective anti-oxidative stress pathways(32), and subsequent cell apoptosis(34). Recent works demonstrated changes in the lipidomic

profile of AH in FED(15), mainly related to the increase of lipid compounds, like sphingomyelin (SM) and cholesteryl esters (ChoE), with proven surfactant activity(35). In addition, AH of FED patients shows changes in the proteomic profile and increase in overall protein levels(36). Those findings dovetail with our current results, suggesting a relation between the increase of lipids levels and the decrease in ST in AH of patients with FED.

AH is a fast changing, highly dynamic medium and these characteristics constitute the most relevant limitation of our study. Special attention was paid to surgery protocol, topical treatment monitoring, standardization of sample extraction, and storage conditions to minimize spurious data variability. Regulation of the production of AH is highly complex and many of its mechanisms are still only partially known. Thus, this was recognized as one of the potential limitations of our work. We traced for AH production modulators throughout the whole sample processing and no differences regarding day-night fluctuations(9), oral medication(37) or metabolic conditions(38) were identified. In addition, age distribution could arguably play a role in ST. FED patients are in average around 10 years older than controls and AH composition may change with age(10). However, multivariate analysis did not show age-related differences in ST.

Patients with FED were under topical fluormetholone 0.1% during 1-2 weeks following laser iridotomy to avoid postoperative air-induced angle closure. Topical steroids alter trabecular meshwork cell morphology by increasing nuclear transport of the human glucocorticoid receptor GRbeta(39) and increase expression and secondary accumulation, of extracellular matrix protein fibronectin, polymerized glycosaminoglycans, and elastin(40). Although reports suggest minor influence of fluormetholone in AH production(41) and most patients ended the treatment days to weeks prior to surgery,

potential influence in ST can not be completely discarded.

Our results contrast with previous reports assessing ST differences in AH of patients with glaucoma where significant differences between both groups were found(18). Sample size and wider inclusion criteria, including patients that underwent combined glaucoma and cataract surgery, may help to explain those inconsistencies. Due to the challenging aspects of the experimental conditions when using optical goniometry on biological fluids, a deeper standardization of the measuring procedure should be pursued by future works in order to successfully adapt the field of optical goniometry to clinical research.

4.2.6 REFERENCES

1. White HE. Modern college physics. London; New York: Van Nostrand; 1972.

2. Malijevský A, Jackson G. A perspective on the interfacial properties of nanoscopic liquid drops. J Phys Condens Matter Inst Phys J. 2012 Nov 21;24(46):464121.

3. Kazakov VN. Dynamic surface tensiometry in medicine [Internet]. Amsterdam; New York: Elsevier; 2000 [cited 2015 Jul 27]. Available from: http://site.ebrary.com/id/10190301

4. Ikegami M, Weaver TE, Grant SN, Whitsett JA. Pulmonary surfactant surface tension influences alveolar capillary shape and oxygenation. Am J Respir Cell Mol Biol. 2009 Oct;41(4):433–9.

5. Czirok A, Little CD. Pattern formation during vasculogenesis. Birth Defects Res Part C Embryo Today Rev. 2012 Jun;96(2):153–62.

6. Kazakov VN, Vozianov AF, Sinyachenko OV, Trukhin DV, Kovalchuk VI, Pison U. Studies on the application of dynamic surface tensiometry of serum and cerebrospinal liquid for diagnostics and monitoring of treatment in patients who have rheumatic, neurological or oncological diseases. Adv Colloid Interface Sci. 2000 May 24;86(1-2):1–38.

7. Faria R, Santana MM, Aveleira CA, Simões C, Maciel E, Melo T, et al. Alterations in phospholipidomic profile in the brain of mouse model of depression induced by chronic unpredictable stress. Neuroscience. 2014 Jul 25;273:1–11.

8. Kawai M, Kirkness JP, Yamamura S, Imaizumi K, Yoshimine H, Oi K, et al. Increased phosphatidylcholine concentration in saliva reduces surface tension and improves

airway patency in obstructive sleep apnoea. J Oral Rehabil. 2013 Aug;n/a – n/a.

9. Göbel K, Rüfer F, Erb C. [Physiology of aqueous humor formation, diurnal fluctuation of intraocular pressure and its significance for glaucoma]. Klin Monatsblätter Für Augenheilkd. 2011 Feb;228(2):104–8.

10. Goel M. Aqueous Humor Dynamics: A Review~!2010-03-03~!2010-06-17~!2010-09-02~! Open Ophthalmol J. 2010 Sep 3;4(1):52–9.

11. Chudgar SM, Deng P, Maddala R, Epstein DL, Rao PV. Regulation of connective tissue growth factor expression in the aqueous humor outflow pathway. Mol Vis. 2006;12:1117–26.

12. Uda T, Suzuki T, Mitani A, Tasaka Y, Kawasaki S, Mito T, et al. Ocular penetration and efficacy of levofloxacin using different drug-delivery techniques for the prevention of endophthalmitis in rabbit eyes with posterior capsule rupture. J Ocul Pharmacol Ther Off J Assoc Ocul Pharmacol Ther. 2014 May;30(4):333–9.

13. Cvenkel B, Kopitar AN, Ihan A. Inflammatory Molecules in Aqueous Humour and on Ocular Surface and Glaucoma Surgery Outcome. Mediators Inflamm. 2010;2010:1–7.

14. Tezel G. A decade of proteomics studies of glaucomatous neurodegeneration. PROTEOMICS - Clin Appl. 2014 Apr;8(3-4):154–67.

15. Cabrerizo J, Urcola JH, Saracibar G, Vecino. Changes in lipidomic profile of aqueous humor in Fuchs endothelial corneal dystrophy. In Denver, CO; 2015.

16. Louttit MD, Kopplin LJ, Igo RP, Fondran JR, Tagliaferri A, Bardenstein D, et al. A

multicenter study to map genes for Fuchs endothelial corneal dystrophy: baseline characteristics and heritability. Cornea. 2012 Jan;31(1):26–35.

17. Su X, Vesco C, Fleming J, Choh V. Density of ocular components of the bovine eye. Optom Vis Sci Off Publ Am Acad Optom. 2009 Oct;86(10):1187–95.

18. Ross A, Blake RC, Ayyala RS. Surface tension of aqueous humor. J Glaucoma. 2010 Sep;19(7):456–9.

19. Berry JD, Neeson MJ, Dagastine RR, Chan DYC, Tabor RF. Measurement of surface and interfacial tension using pendant drop tensiometry. J Colloid Interface Sci. 2015 Sep 15;454:226–37.

20. Chang Y-Y, Wu M-Y, Hung Y-L, Lin S-Y. Accurate surface tension measurement of glass melts by the pendant drop method. Rev Sci Instrum. 2011 May;82(5):055107.

21. Saad SMI, Neumann AW. Laplacian drop shapes and effect of random perturbations on accuracy of surface tension measurement for different drop constellations. Adv Colloid Interface Sci. 2014 Nov 13;

22. Miric DJ, Kisic BM, Zoric LD, Miric BM, Mirkovic M, Mitic R. Influence of cataract maturity on aqueous humor lipid peroxidation markers and antioxidant enzymes. Eye. 2014 Jan;28(1):72–7.

23. Kastner C, Löbler M, Reske T, Sternberg K, Guthoff R, Schmitz K-P. Determination of human anterior lens capsule permeability for fluorescent model substances and after-cataract preventive drugs. Biomed Eng Biomed Tech [Internet]. 2012 Jan 27 [cited 2015 Aug 3];57(SI-1 Track-D). Available from: http://www.degruyter.com/view/j/bmte.2012.57.issue-s1-D/bmt-2012-4340/bmt-2012-

4340.xml

24. Kastner C, Löbler M, Sternberg K, Reske T, Stachs O, Guthoff R, et al. Permeability of the anterior lens capsule for large molecules and small drugs. Curr Eye Res. 2013 Oct;38(10):1057–63.

25. Vranka JA, Kelley MJ, Acott TS, Keller KE. Extracellular matrix in the trabecular meshwork: intraocular pressure regulation and dysregulation in glaucoma. Exp Eye Res. 2015 Apr;133:112–25.

26. Braunger BM, Fuchshofer R, Tamm ER. The aqueous humor outflow pathways in glaucoma: A unifying concept of disease mechanisms and causative treatment. Eur J Pharm Biopharm Off J Arbeitsgemeinschaft Pharm Verfahrenstechnik EV. 2015 May 7;

27. Knepper PA, Goossens W, Hvizd M, Palmberg PF. Glycosaminoglycans of the human trabecular meshwork in primary open-angle glaucoma. Invest Ophthalmol Vis Sci. 1996 Jun;37(7):1360–7.

28. Kuleshova ON, Zaidman AM, Korel' AV. Glycosaminoglycans of the trabecular meshwork of the eye in primary juvenile glaucoma. Bull Exp Biol Med. 2007 Mar;143(3):381–4.

29. Parc CE, Johnson DH, Brilakis HS. Giant vacuoles are found preferentially near collector channels. Invest Ophthalmol Vis Sci. 2000 Sep;41(10):2984–90.

30. Engler C, Kelliher C, Spitze AR, Speck CL, Eberhart CG, Jun AS. Unfolded protein response in fuchs endothelial corneal dystrophy: a unifying pathogenic pathway? Am J Ophthalmol. 2010 Feb;149(2):194–202.e2.

31. Wojcik K, Kaminska A, Blasiak J, Szaflik J, Szaflik J. Oxidative Stress in the Pathogenesis of Keratoconus and Fuchs Endothelial Corneal Dystrophy. Int J Mol Sci. 2013 Sep 23;14(9):19294–308.

32. Jurkunas UV, Bitar MS, Funaki T, Azizi B. Evidence of Oxidative Stress in the Pathogenesis of Fuchs Endothelial Corneal Dystrophy. Am J Pathol. 2010 Nov;177(5):2278–89.

33. Szentmáry N, Szende B, Süveges I. Epithelial cell, keratocyte, and endothelial cell apoptosis in Fuchs' dystrophy and in pseudophakic bullous keratopathy. Eur J Ophthalmol. 2005 Feb;15(1):17–22.

34. Li QJ, Ashraf MF, Shen DF, Green WR, Stark WJ, Chan CC, et al. The role of apoptosis in the pathogenesis of Fuchs endothelial dystrophy of the cornea. Arch Ophthalmol Chic Ill 1960. 2001 Nov;119(11):1597–604.

35. Smaby JM, Baumann WJ, Brockman HL. Lipid structure and the behavior of cholesteryl esters in monolayer and bulk phases. J Lipid Res. 1979 Aug;20(6):784–8.

36. Richardson MR, Segu ZM, Price MO, Lai X, Witzmann FA, Mechref Y, et al. Alterations in the aqueous humor proteome in patients with Fuchs endothelial corneal dystrophy. Mol Vis. 2010;16:2376–83.

37. Shahidullah M, Wilson WS, Yap M, To C. Effects of ion transport and channel-blocking drugs on aqueous humor formation in isolated bovine eye. Invest Ophthalmol Vis Sci. 2003 Mar;44(3):1185–91.

38. Kiel JW, Hollingsworth M, Rao R, Chen M, Reitsamer HA. Ciliary blood flow and aqueous humor production. Prog Retin Eye Res. 2011 Jan;30(1):1–17.

39. Wordinger RJ, Clark AF. Effects of glucocorticoids on the trabecular meshwork: towards a better understanding of glaucoma. Prog Retin Eye Res. 1999 Sep;18(5):629–67.

40. Steely HT, Browder SL, Julian MB, Miggans ST, Wilson KL, Clark AF. The effects of dexamethasone on fibronectin expression in cultured human trabecular meshwork cells. Invest Ophthalmol Vis Sci. 1992 Jun;33(7):2242–50.

41. Akingbehin AO. Comparative study of the intraocular pressure effects of fluorometholone 0.1% versus dexamethasone 0.1%. Br J Ophthalmol. 1983 Oct;67(10):661–3.

Biophysical properties of aqueous humour in ocular pathologies

Feb 12, 2016 JOG-D-16-0072

Dear Mr. Cabrerizo,

Your submission entitled "Changes in lipidomic profile of aqueous humor in open angle glaucoma." has been assigned the following manuscript number: JOG-D-16-0072.

You will be able to check on the progress of your paper by logging on to Editorial Manager as an author.

http://jog.edmgr.com/

Your username is: javisea
Your password is: available at this link
http://jog.edmgr.com/Default.aspx?pg=accountFinder.aspx&firstname=Javier&lastname=Cabrerizo&email_address=javi.cabrerizo@gmail.com

Thank you for submitting your work to Journal of Glaucoma.

Kind Regards,

Samantha Z Porter,
Editorial Assistant

4.3 PAPER 3:

Changes in lipidomic profile of aqueous humour in open angle glaucoma.

Authors:

Javier Cabrerizo[1,2,3], J. Aritz Urcola[1,2,3], Elena Vecino[3].

Affiliations:

1 Department of Ophthalmology, University Hospital of Alava, Spain

2 Green Eye Foundation, Research, Spain

3 Experimental Ophthalmo-Biology Group, GOBE, University of the Basque Country, UPV/EHU, Spain

4.3.1 ABSTRACT

Purpose:

To identify and determine differences in lipid profiles of aqueous humor (AH) in patients with open angle glaucoma (OAG).

Material and methods:

Lipidomic profile of 10 samples of AH of patients with OAG and 10 controls were analyzed. Patients with previous history of anterior segment surgery, anterior segment pathology or intra-ocular injections were dismissed. Topical ocular medications within the last 6 months were reported. AH was obtained during the first step of non-perforating deep sclerectomy (NPDS) in OAG patients and during refractive lensectomy in controls. Lipidomic ultra performance liquid chromatography mass spectrometry (UPLC-MS) was used to perform an optimal profiling of glycerolipids, sterol lipids, sphingolipids, and glycerophospholipids.

Metabolite extraction was accomplished by fractionating the samples into pools of species with similar physicochemical properties.

Results:

The levels of 37 out of 110 lipids change in OAG when compared to controls samples. The concentration of most diacylglycerophosphocholines (DAPC) and 1-ether, 2-acylglycerophosphocholine (MEMAPC) increases in OAG when compared to healthy controls. In addition, 14 sphingomyelin (SM) increase significantly, up to 2.75-fold, in OAG. 5 cholesteryl ester (ChoE) present also higher levels in OAG when compared to controls.

Discussion:

The lipid composition of AH in OAG patients shows differences when compared with healthy subjects. Those changes may be relevant to pathological changes involving the lipid metabolism in OAG.

4.3.2 INTRODUCTION

OAG is a degenerative neuropathy causing optic nerve ganglion cell loss(122),(123) and subsequent decrease in visual function(124). Its etiology evolves a vast array of mechanisms, including genetic predisposition(125), anterior segment morphology(93),(126), AH outflow regulation(127), and neuronal death(128). Disparate physiopathological changes take place in several anatomical locations, from the trabecular meshwork(113),(95) to the optic disc pre laminar region, coexisting to a different extent, in different types and stages of the disease.

Currently, OAG is considered to be a multifactorial condition in which rise of IOP is a

major, and a relatively modifiable, risk factor(129). As of today, rise of IOP has become the therapeutical target in glaucoma treatment. However, the metabolical cause and consequence scenario around the rise of IOP, involving outflow resistance and AH composition, is a current topic of interest and remains partially unknown.

Recent reports suggest the importance of molecular interactions between AH and the later segment of the trabecular meshwork in IOP regulation(130). In OAG, the most frequent form of glaucoma, increasing evidence links the increase in TGF-β mediated outflow resistance in OAG characteristic morphological changes of juxtacanalicular cells, specially in the inner wall(131), site of highest outflow resistance(132). The rho-associated kinase signaling pathway controls cellular adhesion by actin cytoskeleton-modulating signals(133). Pathway inhibition results in tight junction disruption and increased Schlemm's canal permeability(134),(130) and increase in optic nerve perfusion(135). Furthermore, K-115 mediated rho-associated kinase inhibition may influence intracellular oxidative stress, decreasing lipid oxidation and reactive oxygen species reactive oxygen species production(136). Accordingly, up-regulation of oxidative stress markers has been found in AH of OAG(137). Those findings point to the rho kinase pathway as a promising double effect therapeutic option, protecting neural cell death and decreasing intraocular pressure (IOP) (138),(136).

AH composition changes in OAG, specially regarding inflammatory molecules(139), extracellular and structural metabolites like glucosaminoglycans(140) and proteins(141). Those changes may affect the tight AH/trabecular meshwork (TM) metabolic relation, changing cell morphology and potentially increasing outflow resistance. In addition, those AH metabolic changes may reflect pathological pathways with future potential interest in glaucoma therapy. Following this line of work, our study aims, for the first time in literature,

to report changes in the lipidomic profile of AH in AOG, seeking potential biomarkers for the physiopathology of the disease.

Lipids play a key role in organism development, signaling and metabolism. They are synthesized in the endoplasmic reticulum, the Golgi lumen, mainly sphingomyelins (SM), and in the mitochondria (45% of the phospholipids)(49). Lipid pathways have been shown to be altered in certain conditions related to inflammation and oxidative stress(11),(12),(13) and some species serve as modulators of the apoptotic response in those cases. Conversely, enhanced apoptotic signaling can significantly alter lipid metabolism in the liver, adipose tissue, skeletal muscle, and macrophage in the context of infection, diabetes, and atherosclerosis(14). Hence, some lipid metabolites have been recently postulated as useful biomarkers for oxidative stress(15),(142). Changes in cell lipid synthesis could be expected in OAG where local(52) and systemic(143) oxidative stress and apoptosis(144),(145) chronically coexist.

Lipidomic research has been greatly facilitated by recent advances in lipidomic ultra performance liquid chromatography mass spectrometry (UPLC-MS)(53). UPLC-MS involves lipid extraction, lipid identification, and data analysis supporting applications from qualitative and quantitative assessment of multiple lipid species, enabling optimal profiling of glycerolipids, sterol lipids, sphingolipids, and glycerophospholipids(27)

4.3.3 MATERIAL AND METHODS

Demographics:

Lipidomic profile of 20 samples, 10 controls and 10 OAG were analyzed. Patients with signs of lens sclerosis at slit lamp examination or previous history of anterior segment

surgery or chronic pathology were excluded from the study. Any topical ocular medications within the last 6 months before sample extraction were reported.

The subjects were divided in two groups according to their diagnosis. Gender distribution of the two groups was: controls, 6 males and 4 females and OAG, 4 males and 6 females. Age average at the moment of surgery was 55.9 years (range: 41-67) and 68.8 (range: 57-82) in control and OAG respectively. In the OAG group 9 were phakic and 1 pseudophakic.

Classification of OAG was performed according to the European Glaucoma Society Guidelines(146) through slit lamp examination, visual fields (Humphrey Field Analyzer – HFA II-i Series, Zeiss, Oberkochen), corneal pachymetry and retinal nerve fiber layer thickness by OCT (Cirrus HD-OCT, Zeiss, Oberkochen). All 10 OAG cases were classified as progressing OAG prior to the enrollment in the study.

Ethical statement:

The study has the approval of the competent scientific regulatory authority, Comité Ético de Investigación Clínica de Euskadi (CEIC-E). Following the guidelines of the ethical committee, all patients received information about the study design and purpose, and signed an informed consent prior to their enrollment. The research reported in this study adhered to the tenets of the Declaration of Helsinki.

Sampling and storage:

AH was obtained during the first step of a surgical procedure, refractive lensectomy in controls and non-perforating deep sclerectomy (NPDE) in OAG patients. After topical 1% povidone-iodine instillation, around 150 microliters of AH were directly aspirated through a unique corneal side port using a 27-gauge blunt cannula. No noteworthy adverse events

were noticed during the aspiration process. A moderate shallowing of the anterior chamber was occasionally perceived. AH was directly introduced in a 0.5 ml tube (Eppendorf AG, Hamburg, Germany) after aspiration and stored at -80°C at the tissue bank for up to 9 months (range: 1-9). Prior to the analyses, samples were left at 24°C for three hours to gradually adjust to room temperature.

Venue:

Control samples were obtained at Begitek Clínica Oftalmológica **(**Plaza Teresa de Calcuta, 7, 20012 Donostia, Guipúzcoa, Spain). OAG samples were obtained at University Hospital of Alava (Jose Atxotegui s/n, 01009 Vitoria-Gasteiz, Spain). Metabolomic analyses were performed by OWL Metabolomics (Parque Tecnológico de Bizkaia 502, Derio, Spain).

Lipidomic profiling:

A lipidomic ultra high performance liquid chromatography coupled to time of flight mass spectrometry (UHPLC-ToF-MS) based platform was used to perform an optimal profiling of glycerolipids, sterol lipids, sphingolipids and glycerophospholipids(27).

Aforementioned UPLC-MS was used to perform lipidomic analyses. Metabolite extraction was accomplished by fractionating the samples into pools of species with similar physicochemical properties, using appropriate combinations of organic solvents.

Data pre-processing generated a list of chromatographic peak areas for the metabolites detected in each sample injection. Data normalization was performed following the previously reported procedures(28). After data correction with quality controls, internal standards, and trend amendment a limit of detection was established as three times the background noise level (blanks). Metabolites with more than 5 sample values under the

were excluded from the analysis.

A normalization procedure was applied after data correction with quality controls, internal standards, and trend amendment by dividing every metabolite species relative concentration by its corresponding “total ion” parameter. This parameter is the result of adding up all the signal intensities (all areas corresponding to ion feature metabolite peaks) integrated in the study within each individual sample.

Metabolite extraction:

Metabolic extraction was accomplished by fractionating the AH samples into pools of species with similar physicochemical properties as previously described(56),(27). AH extracts were mixed with sodium chloride (50 mM) and chloroform / methanol (2:1) in 1.5 ml micro tubes at room temperature. The extraction solvent was spiked with metabolites not detected in unspiked human AH extracts. After brief vortex mixing, the samples were incubated for 1 hour at -20°C. After centrifugation at 16,000 x g for 15 minutes, the organic phase was collected and the solvent removed. The dried extracts were then reconstituted in acetronitrile / isopropanol (1:1), centrifuged (16,000 x g for 5 minutes), and transferred to vials for UHPLC-ToF-MS analysis.

Additionally, a pooled sample was included in the analysis and considered as quality control sample. These samples were evenly distributed over the batch and extracted and analyzed at the same time as the individual samples. They were used to assess the data quality of the study.

UHPLC-ToF-MS analysis:

Chromatography was performed on a 1 mm i.d. × 100 mm ACQUITY 1.7 µm C8 BEH column (Waters Corp., Milford, USA) using an ACQUITY UPLC system (Waters Corp.,

Milford, USA). Chromatographic separation and mass spectrometric detection conditions employed were previously described by Barr et al(56).

Data pre-processing:

All data were pre-processed using the TargetLynx application manager for MassLynx4.1software (Waters Corp. Milford, USA). Data pre-processing generated a list of chromatographic peak areas for the metabolites detected in each sample injection. A normalization procedure was applied after data correction with quality controls, internal standards, and trend amendment by dividing every metabolite species relative concentration by its corresponding "total ion" parameter. This parameter is the result of adding up all the signal intensities (all areas corresponding to ion feature metabolite peaks) integrated in the study within each individual sample. A limit of detection was established as three times the background noise level. Metabolites with more than 5 sample values under the limit of detection were excluded from the analysis.

The detected lipidomic features were included in the subsequent univariate and multivariate data analysis. Both univariate and multivariate approaches are complementary and their results do not necessarily coincide. The advantages of using both approaches in data mining have been recently reviewed(57).

Multivariate data analysis:

Principal Component Analysis and Partial Least Squares Discriminant Analysis (PLS-DA) were used to reduce the data matrix to a series of principal components which aim to explain independently the maximum amount of variance possible. These MVA analyses were applied by exporting the normalized data to the SIMCA-P+ software package (version 14.0 Umetrics, Sweden). Subsequent analyses were performed after centering the

variables to zero and scaled to unit variance.

Univariate data analysis:

All the univariate calculations were performed using R v2.13.0 (R Development Core Team, 2010; http://cran.r-project.org) with MASS, xlxs, robustbase and pwr packages. Univariate statistical significance was estimated using unpaired Student's t test (or Welch´s t test where unequal variances were found). A p-value < 0.05 was considered significant.

Metabolite classification:

The metabolites were identified before the analysis, as described previously(27),(56). The metabolite classification used in this study follows the comprehensive classification system proposed by the International Lipid Classification and Nomenclature Committee (ILCNC)(58),(59).

4.3.4 RESULTS

Multivariate Analysis:

The obtained Principal Component Analysis (60) scores plot shows clear clustering between OAG and control samples in the first component (t1), which explains 29% of the variation of the data (Fig. 1). The PCA does not show any potential outlier. Applying Chauvenet's criterion no lipid species within the sample qualified for data rejection. Cumulative R^2 is 0.29 and Q^2 values are 0.17, respectively, indicating that the PCA model has notable degree of fit and predictive ability for the studied sample.

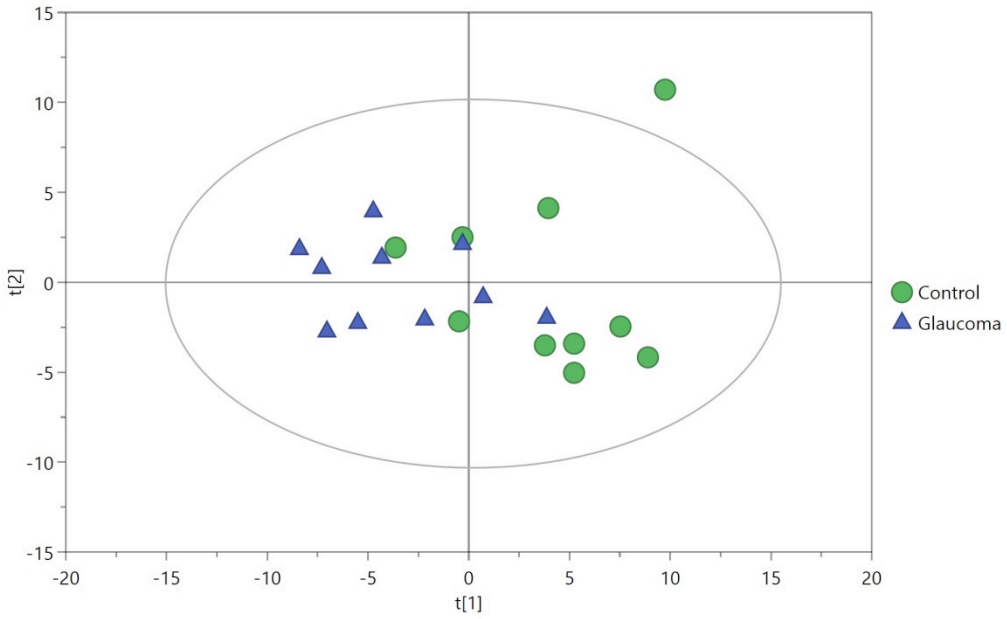

Figure 1: Principal component analyses scores of OAG (n=10) and control samples (n=10).

Lipids responsible for the patterns seen among the groups of samples can be observed in the lower chart (Fig. 2). The highest differences are due to the elevated SMs and ChoEs levels in OAG samples when compared to controls. The supervised analysis (PLS-DA) sample distribution dovetails with the unsupervised PCA findings.

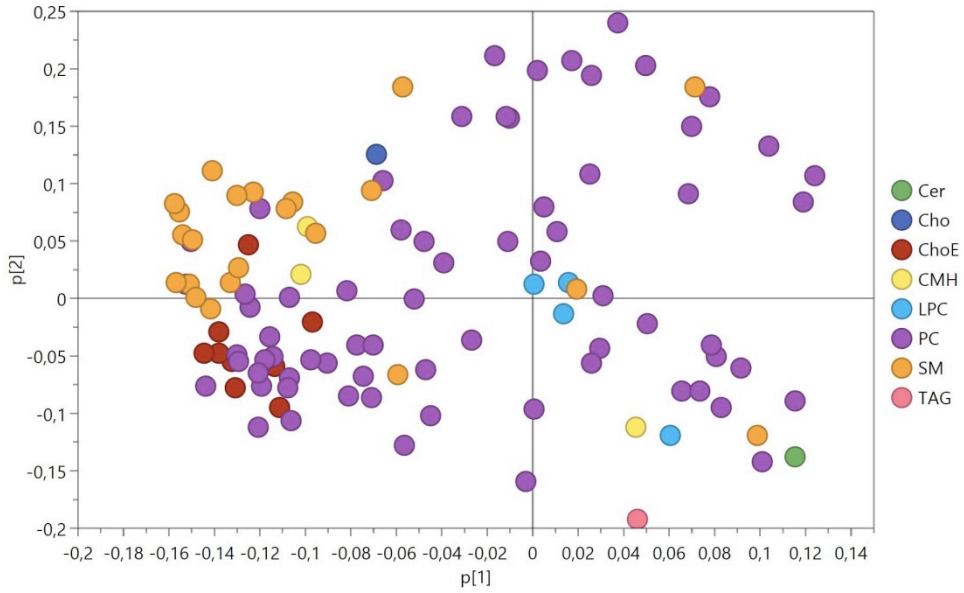

Figure 2: Loadings biplot of FED (n=10) and control samples (n=10) showing the data of every lipid species in relation with the principal components analysis. Lipid species: ceramides (Cer), cholesterol(Cho); ChoEs (ChoE); monohexosylceramides (CMH), Lysophosphatidylcholines (LPC), phosphatidylcholines (PC), SMs (SM), Triacylglycerols (TAG). The diagram shows the importance of variables ChoE and SM in the differences between both groups.

Multivariate analyses after logarithmic or square-root transformations were also applied, seeking to correct aspects that hinder the biological interpretation of data sets by emphasizing the biological information and thus, improving their physiological interpretability(61). Nevertheless, no additional models were found.

Univariate Analysis:

The concentration of 37 out of 110 lipids changes statistically significantly ($p<0.05$) in OAG samples when compared to controls (Fig. 3). The majority of these species (19) belong to

the chemical groups of diacylglycerophosphocholines (DAPC) and 1-ether, 2-acylglycerophosphocholine (MEMAPC), while SM and ChoE also present various significant lipid species altered in OAG (Table 1).

Figure 3 Heatmap of the lipidomic features obtained from the fold-changes and significances derived from the comparison of OAG patients versus controls. Color codes for fold-changes and Student´s t test P-values are indicated in the figure legend. Band thickness refers to the concentration of different species.

Table 1: Lipid species ordered according to their P-values in the comparison of OAG and control AH. Receiver operating characteristic (ROC) analyses results are shown in the last column.

The levels of most of DAPC and MEMAPC increase in AH of OAG compared to controls. The greatest increases observed in PC(P-16:0/20:4) and PC(O-22:0/20:4) which are ~2.6-fold higher in OAG (Fig. 3).

In addition, up to 14 SM increase significantly in OAG, reaching SM(d18:2/20:0) a 2.75-fold increase. Up to 5 ChoE present higher levels in OAG when compared to controls. 2 Long-chain and highly unsaturated ChoE, ChoE(20:3) and ChoE(20:4) display the greatest change, 2.44-fold. The metabolites that present the highest significances are SM, such as SM(d18:2/16:0) and SM(d18:1/18:0) (Fig. 4).

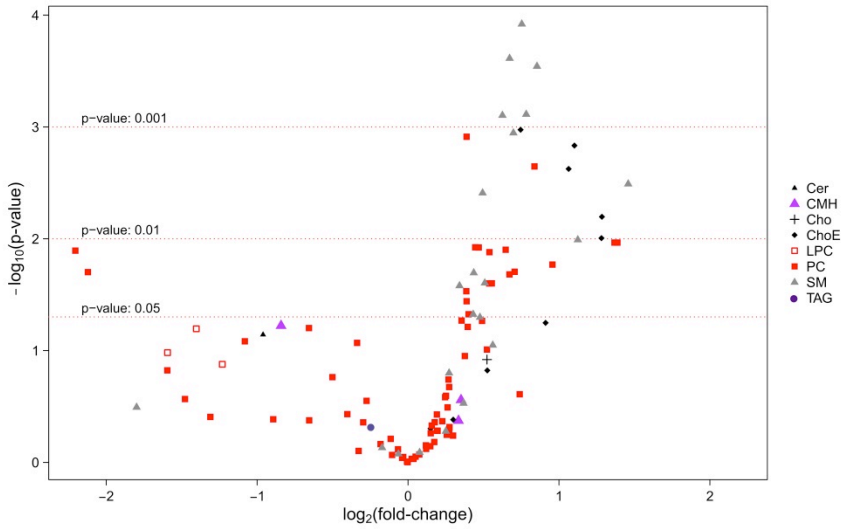

Figure 4. Effect versus significance Volcano Plot [log10(p-value) vs. log2(fold-change)] for the comparison of OAG samples versus controls. The plot combines statistical significance (y-axis) with the magnitude of the changefold change (x-axis). The higher a lipid specie is represented in the diagram the closer it is to statistically significant levels. Complementarily, the more peripheral a specie is represented in the diagram the greater is the concentration fold change compared to controls.

As observed in the multivariate analysis, the average lipid concentrations of the following chemical groups increase in AH of OAG when compared to controls: ChoE (97%) and SM (36%).

Regarding enzyme activity, there is an increase of 38% in the ratio SM+DG/Cer+PC, which reflects the potentially increased synthesis of SM and diacylglycerols from ceramides and PC by the enzyme SM synthase. In addition, the ratio Cer/SM reaction, indicator of the acid SM synthase activity, decreases 71%.

4.3.5 DISCUSSION

This study has unravelled individual and distinctive lipidomic features of AH in patients with OAG compared with controls. Divergences in SM and ChoE levels may reflect the potential rise in the synthesis of SM and DAG from Cr and PC by SMS. In addition, the ratio Cer/SM reaction, indicator of the acid SMS activity, decreases. Similar pattern in lipidomic profile has also been associated to metabolical conditions. According to previous findings about biophysical properties of AH, concentrations in metabolites change in a sodium hyaluronate injection glaucoma model(45).

Increased SMS activity in serum has been described to enhance the susceptibility of low density lipoproteins to secretory SMS, which leads to ceramides generation and the formation of aggregated LDL exhibiting a high atherogenic potential(46). The functional state of the SM cycle may also modulate the trabecular meshwork resistance/AH outflow ratio(47) and plays an important role in the radical lipid oxidation under intracellular oxidative stress. Furthermore, specific sphingolipid and Cer species have been found to be uniquely present in rodent OAG model(48). Higher levels of Apo AI, ApoCIII, ApoE, TTR, and α2M, serum biomarkers for Alzheimer disease, have been confirmed in OAG AH when compared to cataracts, irrespectively of age and gender(49) and some reports suggest compromised lysosomal system autophagy in the glaucomatous outflow pathway(50).

Meta-analyses based evidence links pathogenicity of OAG with inflammation(51),(52) and oxidative stress. A significant increase in superoxide dismutase and glutathione peroxidase activities was found in AH of OAG patients as compared to cataracts, evolving up regulation of physiological response to oxidative stress in OAG. In addition, levels of oxidative stress response vitamins C and E were also significantly lower(53). In addition, higher concentration of free radicals like superoxide, target of SOD mediated response,

were found in AH of patients with OAG when compared to cataract(54). Those findings suggest a combined mechanism, where a misbalance between a decreased anti-oxidative capacity and an increased ROS-mediated oxidative stress may be responsible for AH reflected metabolic changes.

Besides this, other mechanisms related to OAG have been associated with activation of apoptotic gene pathways. Rise of IOP causes mechanical citoplasmatic changes derived from the tissue stretching, and subsequent citoplasmatic elongation releasing intracellular signals that may trigger apoptosis(55). These findings connect the bidirectional cause-effect relation between apoptosis and OAG, being the rise of IOP the result of oxidative misbalance, and also the cause of apoptosis through mechanical stress.

Unfolded protein response is a well-orchestrated endoplasmic reticulum response to intracellular oxidative stress and inflammation(56), proven to be enhanced in OAG(57),(58). Together with oxidative induced endoplasmic reticulum stress, they have shown to have important connections to lipid metabolism(59). Thus, major lipid perturbations are found alongside unfolded protein response signaling activation(56) and changes in membrane phospholipid composition are likely to influence its activation(56). Complementarily, unfolded protein response activation may result in disregulation of lipid synthesis(60) and generation of reactive oxygen species as a byproduct of protein oxidation in the endoplasmic reticulum(61),(62), increasing intracellular oxidative stress. Reactive oxygen species can activate unfolded protein response by changing the redox state in the reticulum lumen and reactive oxygen species production is increased during ER stress(63),(64). Thus, recent studies suggest a compromised unfolded protein response in OAG as a potential contributor in the pathogenesis of the disease(58). Those findings may advocate for a bidirectional cause-effect scenario in the etiology of OAG and strengthen the key role of unfolded protein response in the pathophysiology of the

condition.

AH is a fast changing, highly dynamic medium and these characteristics constitute the main limitation of our study. Despite monitoring of glaucoma drops, strong inclusion criteria and standardized sample extraction and storage conditions, findings could be attributed to lens capsule permeability or changes in AH production, the latter specially being a major etiological cause in some types of glaucoma(65). Furthermore, no differences in known AH modulators like day-night fluctuation(66), oral medication(67) or metabolic conditions(5) were identified.

Anterior lens capsule is selectively permeable, acting as a barrier for most bacterial and viral infections(68). Lens anterior permeability is reported to be restricted to small and mid-size molecules, with a cut off molecular weight of 166 ± 82 kDa(69), three to six folds smaller than the lipid species studied in this work(SM around 350 kDa, PC around 800 kDa).

Controls, who underwent a refractive lensectomy, were hyperopic, showing statistically significant differences in axial length compared with OAG patients. Although levels of vascular endothelial growth factor, pigment epithelium-derived factor (PEDF)(70) and matrix metalloproteinase 2 (MMP-2)(71) may increase with axial length, no evidence of lipid-related alterations in AH of hyperopic patients has been reported. Although age distribution could arguably play a role in AH composition(10), other reports have not report metabolic differences in AH related to age(72).

In summary, our study demonstrates changes in the lipidomic profile of AH in OAG, mainly related to the increase in ChoE and decrease of SMS activity and resultant increase in SM. Results point to the presence of intracellular oxidative stress-related metabolic changes that play a role in the metabolic relation between AH and the juxtacanalicular segment of the trabecular meshwork, and subsequently may affect IOP regulation. Deeper

identification of the nature and extent between evident metabolic AH changes and physiopathological mechanisms behind the rise of IOP, remain future challenges.

4.3.6 REFERENCES

1. Na JH, Lee K, Lee JR, Baek S, Yoo SJ, Kook MS. Detection of macular ganglion cell loss in preperimetric glaucoma patients with localized retinal nerve fibre defects by spectral-domain optical coherence tomography. Clin Experiment Ophthalmol. 2013 Dec;41(9):870–80.

2. Fortune B, Cull G, Reynaud J, Wang L, Burgoyne CF. Relating Retinal Ganglion Cell Function and Retinal Nerve Fiber Layer (RNFL) Retardance to Progressive Loss of RNFL Thickness and Optic Nerve Axons in Experimental Glaucoma. Invest Ophthalmol Vis Sci. 2015 Jun;56(6):3936–44.

3. Medeiros FA, Gracitelli CPB, Boer ER, Weinreb RN, Zangwill LM, Rosen PN. Longitudinal changes in quality of life and rates of progressive visual field loss in glaucoma patients. Ophthalmology. 2015 Feb;122(2):293–301.

4. Wang R, Wiggs JL. Common and rare genetic risk factors for glaucoma. Cold Spring Harb Perspect Med. 2014 Dec;4(12):a017244.

5. Kiel JW, Hollingsworth M, Rao R, Chen M, Reitsamer HA. Ciliary blood flow and aqueous humor production. Prog Retin Eye Res. 2011 Jan;30(1):1–17.

6. Wang SY, Melles R, Lin SC. The impact of central corneal thickness on the risk for glaucoma in a large multiethnic population. J Glaucoma. 2014 Dec;23(9):606–12.

7. Rao PV. Bioactive lysophospholipids: role in regulation of aqueous humor outflow and intraocular pressure in the context of pathobiology and therapy of glaucoma. J Ocul Pharmacol Ther Off J Assoc Ocul Pharmacol Ther. 2014 Apr;30(2-3):181–90.

8. Van de Velde S, De Groef L, Stalmans I, Moons L, Van Hove I. Towards axonal regeneration and neuroprotection in glaucoma: Rho kinase inhibitors as promising therapeutics. Prog Neurobiol. 2015 Aug;131:105–19.

9. Vranka JA, Kelley MJ, Acott TS, Keller KE. Extracellular matrix in the trabecular meshwork: intraocular pressure regulation and dysregulation in glaucoma. Exp Eye Res. 2015 Apr;133:112–25.

10. Goel M. Aqueous Humor Dynamics: A Review~!2010-03-03~!2010-06-17~!2010-09-02~! Open Ophthalmol J. 2010 Sep 3;4(1):52–9.

11. Anderson AJ, Stainer MJ. A control experiment for studies that show improved visual sensitivity with intraocular pressure lowering in glaucoma. Ophthalmology. 2014 Oct;121(10):2028–32.

12. Inoue T, Tanihara H. Rho-associated kinase inhibitors: a novel glaucoma therapy. Prog Retin Eye Res. 2013 Nov;37:1–12.

13. Pattabiraman PP, Maddala R, Rao PV. Regulation of Plasticity and Fibrogenic Activity of Trabecular Meshwork Cells by Rho GTPase Signaling: TM CELL FIBROGENIC ACTIVITY. J Cell Physiol. 2014 Jul;229(7):927–42.

14. Johnson M. “What controls aqueous humour outflow resistance?” Exp Eye Res. 2006 Apr;82(4):545–57.

15. Bhadriraju K, Yang M, Alom Ruiz S, Pirone D, Tan J, Chen CS. Activation of ROCK by RhoA is regulated by cell adhesion, shape, and cytoskeletal tension. Exp Cell Res. 2007 Oct;313(16):3616–23.

16. Rao VP, Epstein DL. Rho GTPase/Rho kinase inhibition as a novel target for the treatment of glaucoma. BioDrugs Clin Immunother Biopharm Gene Ther. 2007;21(3):167–77.

17. Tokushige H, Inatani M, Nemoto S, Sakaki H, Katayama K, Uehata M, et al. Effects of topical administration of y-39983, a selective rho-associated protein kinase inhibitor, on ocular tissues in rabbits and monkeys. Invest Ophthalmol Vis Sci. 2007 Jul;48(7):3216–22.

18. Yamamoto K, Maruyama K, Himori N, Omodaka K, Yokoyama Y, Shiga Y, et al. The novel Rho kinase (ROCK) inhibitor K-115: a new candidate drug for neuroprotective treatment in glaucoma. Invest Ophthalmol Vis Sci. 2014 Nov;55(11):7126–36.

19. Goyal A, Srivastava A, Sihota R, Kaur J. Evaluation of oxidative stress markers in aqueous humor of primary open angle glaucoma and primary angle closure glaucoma patients. Curr Eye Res. 2014 Aug;39(8):823–9.

20. Isobe T, Mizuno K, Kaneko Y, Ohta M, Koide T, Tanabe S. Effects of K-115, a rho-kinase inhibitor, on aqueous humor dynamics in rabbits. Curr Eye Res. 2014 Aug;39(8):813–22.

21. Gabelt BT, Kaufman PL. Changes in aqueous humor dynamics with age and glaucoma. Prog Retin Eye Res. 2005 Sep;24(5):612–37.

22. Baba H. Probability of the presence of glycosaminoglycans in aqueous humor. Graefes Arch Clin Exp Ophthalmol Albrecht Von Graefes Arch Für Klin Exp Ophthalmol. 1983;220(3):117–21.

23. Izzotti A, Longobardi M, Cartiglia C, Saccà SC. Proteome alterations in primary open

angle glaucoma aqueous humor. J Proteome Res. 2010 Sep 3;9(9):4831–8.

24. Nelson DL, Cox MM, Lehninger AL. Lehninger principles of biochemistry. 6., internat. ed. New York: Freeman; 2013.

25. Kunchithapautham K, Atkinson C, Rohrer B. Smoke exposure causes endoplasmic reticulum stress and lipid accumulation in retinal pigment epithelium through oxidative stress and complement activation. J Biol Chem. 2014 May 23;289(21):14534–46.

26. Turkdogan KA, Akpinar O, Karabacak M, Akpinar H, Turkdogan FT, Karahan O. Association between oxidative stress index and serum lipid levels in healthy young adults. JPMA J Pak Med Assoc. 2014 Apr;64(4):379–81.

27. Mukhopadhyay R. Mouse models of atherosclerosis: explaining critical roles of lipid metabolism and inflammation. J Appl Genet. 2013 May;54(2):185–92.

28. van Diepen JA, Berbée JFP, Havekes LM, Rensen PCN. Interactions between inflammation and lipid metabolism: relevance for efficacy of anti-inflammatory drugs in the treatment of atherosclerosis. Atherosclerosis. 2013 Jun;228(2):306–15.

29. Niki E. Lipid peroxidation products as oxidative stress biomarkers. BioFactors Oxf Engl. 2008;34(2):171–80.

30. Yoshida Y, Umeno A, Shichiri M. Lipid peroxidation biomarkers for evaluating oxidative stress and assessing antioxidant capacity in vivo. J Clin Biochem Nutr. 2013;52(1):9–16.

31. Ferreira SM, Lerner SF, Brunzini R, Evelson PA, Llesuy SF. Oxidative stress

markers in aqueous humor of glaucoma patients. Am J Ophthalmol. 2004 Jan;137(1):62–9.

32. Tanito M, Kaidzu S, Takai Y, Ohira A. Status of Systemic Oxidative Stresses in Patients with Primary Open-Angle Glaucoma and Pseudoexfoliation Syndrome. Jandeleit-Dahm K, editor. PLoS ONE. 2012 Nov 26;7(11):e49680.

33. Himori N, Yamamoto K, Maruyama K, Ryu M, Taguchi K, Yamamoto M, et al. Critical role of Nrf2 in oxidative stress-induced retinal ganglion cell death. J Neurochem. 2013 Dec;127(5):669–80.

34. Quigley HA, Nickells RW, Kerrigan LA, Pease ME, Thibault DJ, Zack DJ. Retinal ganglion cell death in experimental glaucoma and after axotomy occurs by apoptosis. Invest Ophthalmol Vis Sci. 1995 Apr;36(5):774–86.

35. Nygren H, Seppänen-Laakso T, Castillo S, Hyötyläinen T, Orešič M. Liquid chromatography-mass spectrometry (LC-MS)-based lipidomics for studies of body fluids and tissues. Methods Mol Biol Clifton NJ. 2011;708:247–57.

36. Barr J, Vázquez-Chantada M, Alonso C, Pérez-Cormenzana M, Mayo R, Galán A, et al. Liquid Chromatography−Mass Spectrometry-Based Parallel Metabolic Profiling of Human and Mouse Model Serum Reveals Putative Biomarkers Associated with the Progression of Nonalcoholic Fatty Liver Disease. J Proteome Res. 2010 Sep 3;9(9):4501–12.

37. European Glaucoma Society, editor. Terminology and guidelines for glaucoma. 3rd. ed. Savona: Ed. Dogma; 2008. 183 p.

38. van der Kloet FM, Bobeldijk I, Verheij ER, Jellema RH. Analytical error reduction

using single point calibration for accurate and precise metabolomic phenotyping. J Proteome Res. 2009 Nov;8(11):5132–41.

39. Barr J, Caballería J, Martínez-Arranz I, Domínguez-Díez A, Alonso C, Muntané J, et al. Obesity-Dependent Metabolic Signatures Associated with Nonalcoholic Fatty Liver Disease Progression. J Proteome Res. 2012 Apr 6;11(4):2521–32.

40. Martínez-Arranz I, Mayo R, Pérez-Cormenzana M, Mincholé I, Salazar L, Alonso C, et al. Data in support of enhancing metabolomics research through data mining. Data Brief. 2015 Jun;3:155–64.

41. Fahy E. A comprehensive classification system for lipids. J Lipid Res. 2005 Feb 16;46(5):839–62.

42. Fahy E, Subramaniam S, Murphy RC, Nishijima M, Raetz CRH, Shimizu T, et al. Update of the LIPID MAPS comprehensive classification system for lipids. J Lipid Res. 2008 Dec 19;50(Supplement):S9–14.

43. Jolliffe IT. Principal component analysis [Internet]. New York: Springer; 2002 [cited 2015 Jul 23]. Available from: http://site.ebrary.com/id/10047693

44. van den Berg RA, Hoefsloot HCJ, Westerhuis JA, Smilde AK, van der Werf MJ. Centering, scaling, and transformations: improving the biological information content of metabolomics data. BMC Genomics. 2006;7:142.

45. Urcola JH, Hernández M, Vecino E. Three experimental glaucoma models in rats: comparison of the effects of intraocular pressure elevation on retinal ganglion cell size and death. Exp Eye Res. 2006 Aug;83(2):429–37.

46. Schissel SL, Jiang X, Tweedie-Hardman J, Jeong T, Camejo EH, Najib J, et al. Secretory sphingomyelinase, a product of the acid sphingomyelinase gene, can hydrolyze atherogenic lipoproteins at neutral pH. Implications for atherosclerotic lesion development. J Biol Chem. 1998 Jan 30;273(5):2738–46.

47. Aljohani AJ, Munguba GC, Guerra Y, Lee RK, Bhattacharya SK. Sphingolipids and ceramides in human aqueous humor. Mol Vis. 2013;19:1966–84.

48. Edwards G, Aribindi K, Guerra Y, Bhattacharya SK. Sphingolipids and ceramides of mouse aqueous humor: Comparative profiles from normotensive and hypertensive DBA/2J mice. Biochimie. 2014 Oct;105:99–109.

49. Inoue T, Kawaji T, Tanihara H. Elevated levels of multiple biomarkers of Alzheimer's disease in the aqueous humor of eyes with open-angle glaucoma. Invest Ophthalmol Vis Sci. 2013 Aug;54(8):5353–8.

50. Liton PB. The autophagic lysosomal system in outflow pathway physiology and pathophysiology. Exp Eye Res [Internet]. 2015 Jul [cited 2015 Sep 16]; Available from: http://linkinghub.elsevier.com/retrieve/pii/S0014483515002390

51. Nga ADC, Yap S-L, Samsudin A, Abdul-Rahman PS, Hashim OH, Mimiwati Z. Matrix metalloproteinases and tissue inhibitors of metalloproteinases in the aqueous humour of patients with primary angle closure glaucoma - a quantitative study. BMC Ophthalmol. 2014;14:33.

52. Agarwal P, Daher AM, Agarwal R. Aqueous humor TGF-β2 levels in patients with open-angle glaucoma: A meta-analysis. Mol Vis. 2015;21:612–20.

53. Goyal A, Srivastava A, Sihota R, Kaur J. Evaluation of oxidative stress markers in

aqueous humor of primary open angle glaucoma and primary angle closure glaucoma patients. Curr Eye Res. 2014 Aug;39(8):823–9.

54. Oshida E, Arai K, Sakai M, Chikuda M. [Study of free radicals in aqueous humor in glaucoma and cataracts: differences in presence or absence of diabetes mellitus and neovascular glaucoma]. Nippon Ganka Gakkai Zasshi. 2014 Sep;118(9):759–67.

55. Luna C, Qiu J, Epstein D, Gonzalez P. Role of miR-146a in the Regulation of Gene Expression Changes Induced by Mechanical Stress in Trabecular Meshwork Cells. In 2014.

56. Volmer R, Ron D. Lipid-dependent regulation of the unfolded protein response. Curr Opin Cell Biol. 2015 Apr;33:67–73.

57. Anholt RRH, Carbone MA. A molecular mechanism for glaucoma: endoplasmic reticulum stress and the unfolded protein response. Trends Mol Med. 2013 Oct;19(10):586–93.

58. Carbone MA, Chen Y, Hughes GA, Weinreb RN, Zabriskie NA, Zhang K, et al. Genes of the unfolded protein response pathway harbor risk alleles for primary open angle glaucoma. PloS One. 2011;6(5):e20649.

59. Yano M, Yamamoto T, Nishimura N, Gotoh T, Watanabe K, Ikeda K, et al. Increased Oxidative Stress Impairs Adipose Tissue Function in Sphingomyelin Synthase 1 Null Mice. Siskind LJ, editor. PLoS ONE. 2013 Apr 12;8(4):e61380.

60. Basseri S, Austin RC. Endoplasmic Reticulum Stress and Lipid Metabolism: Mechanisms and Therapeutic Potential. Biochem Res Int. 2012;2012:1–13.

61. Malhotra JD, Kaufman RJ. Endoplasmic reticulum stress and oxidative stress: a vicious cycle or a double-edged sword? Antioxid Redox Signal. 2007 Dec;9(12):2277–93.

62. Gregersen N, Bross P. Protein misfolding and cellular stress: an overview. Methods Mol Biol Clifton NJ. 2010;648:3–23.

63. Santos CXC, Tanaka LY, Wosniak J, Laurindo FRM. Mechanisms and implications of reactive oxygen species generation during the unfolded protein response: roles of endoplasmic reticulum oxidoreductases, mitochondrial electron transport, and NADPH oxidase. Antioxid Redox Signal. 2009 Oct;11(10):2409–27.

64. Li G, Scull C, Ozcan L, Tabas I. NADPH oxidase links endoplasmic reticulum stress, oxidative stress, and PKR activation to induce apoptosis. J Cell Biol. 2010 Dec 13;191(6):1113–25.

65. Janssen SF, Gorgels TG, van der Spek PJ, Jansonius NM, Bergen AA. In silico analysis of the molecular machinery underlying aqueous humor production: potential implications for glaucoma. J Clin Bioinforma. 2013;3(1):21.

66. Göbel K, Rüfer F, Erb C. [Physiology of aqueous humor formation, diurnal fluctuation of intraocular pressure and its significance for glaucoma]. Klin Monatsblätter Für Augenheilkd. 2011 Feb;228(2):104–8.

67. Shahidullah M, Wilson WS, Yap M, To C. Effects of ion transport and channel-blocking drugs on aqueous humor formation in isolated bovine eye. Invest Ophthalmol Vis Sci. 2003 Mar;44(3):1185–91.

68. Danysh BP, Duncan MK. The lens capsule. Exp Eye Res. 2009 Feb;88(2):151–64.

69. Kastner C, Löbler M, Sternberg K, Reske T, Stachs O, Guthoff R, et al. Permeability of the anterior lens capsule for large molecules and small drugs. Curr Eye Res. 2013 Oct;38(10):1057–63.

70. Shin YJ, Nam WH, Park SE, Kim JH, Kim HK. Aqueous humor concentrations of vascular endothelial growth factor and pigment epithelium-derived factor in high myopic patients. Mol Vis. 2012;18:2265–70.

71. Jia Y, Hu D-N, Zhu D, Zhang L, Gu P, Fan X, et al. MMP-2, MMP-3, TIMP-1, TIMP-2, and TIMP-3 protein levels in human aqueous humor: relationship with axial length. Invest Ophthalmol Vis Sci. 2014 Jun;55(6):3922–8.

72. Chowdhury UR, Madden BJ, Charlesworth MC, Fautsch MP. Proteome Analysis of Human Aqueous Humor. Investig Opthalmology Vis Sci. 2010 Oct 1;51(10):4921.

5. GENERAL DISCUSSION

The clinical value of surface tension (ST) has been traditionally studied within the boundaries of biophysics related conditions, mainly within fields such as neonatology, respiratory care and haematology(38), where gas-fluid interphase and fluidic properties are of key clinical relevance. However, the role of ST as a result of pathological changes or as a contributor to certain metabolic related ocular pathologies has remained unknown.

The biophysical properties of organic fluids are extremely sensible to external conditions, making the extraction of an accurate and reliable measurement a scientific challenge within the experimental laboratory setting. ST is a highly dynamic and alterable parameter. It varies significantly with small changes in the environment such as pressure, temperature or humidity(39). In addition, the sensibility of the currently available measuring devices to vibration, air currents and setting conditions makes the reliability and external validity of the ST data a challenge. During our study, calibration and standardization, aiming to minimize setting dependent bias, was of mayor concern and it was closely monitored as previously explained in this work.

Measurement timing has shown to be a crucial concept to obtain reliable and reproducible data. As soon as the pendant drop forms and the area of the gas-fluid interphase spikes, significant evaporation occurs. The loss of water increases the concentration of solutes within the drop, and changes in ST appear within seconds. This points out the importance of standardizing the sequence of events during the measuring process and highlights the critical effect of small changes in fluid composition in ST.

ST shows to have high sensitivity for small changes in physiological fluids composition, but

it is unable by itself to unravel and specify the metabolical origin behind those changes. Metabolomic, mainly proteomic and lipidomic, analyses are able to quantify differences in metabolite concentrations, providing a deeper insight into the clinically relevant causes behind ST changes by explaining the cause-effect relation between ST and fluid composition.

Leaving aside important previously disclosed external factors, the ST of a fluid results from the concentration of its components and their biophysical interactions, in which concepts as threshold concentration and saturation of surfactants play a role. The fine and complex way in which molecules structured together within a fluid depends not only on the ST of each of the solutes, but mostly on the electro-physical characteristics of each of them at that specific concentration and within a specific fluid composition(40). This explains how minor concentration changes of a solute in a fluid can entail major changes in ST(41).

Most lipids are surfactants, with significant ST related properties which depend on its molecular composition, size and chemical binding properties. In high concentrated lipid solutions, long lipids, over 8 carbons, build intermolecular electrophysical non covalent attraction forces that shape and determine the fluid's biophysical properties, such as viscosity and ST.

Phospholipids, phosphocolines and other membrane related ceramides, that have been found to undergo changes in some ocular pathologies, have shown to regulate membrane adhesions, cell transport and cellular transmembrane metabolic pathways(42),(43). They are also powerful organic surfactants due to their hydrophilic and hydrophobic ambivalence which enables hydrogen bonds at water surfaces and subsequent polymolecular micelle formation.

Molecular morphological changes, like peroxidation, also contribute to explain the complex biophysical behavior that defines the ST of a fluid. Peroxidation takes place under an oxidative stress environment when an unsaturated lipid species becomes a lipid peroxide by losing a hydrogen atom and binding with an oxygen molecule. During this process lipid peroxyl radicals are formed as intermediate metabolites contributing to a positive feedback of the underlying oxidative stress.

During cataract formation, metabolic changes occur within the lens capsule, including changes in the lens lipidomic profile(44). The implication of those changes in the aqueous humor (AH) composition is subordinated to the anterior lens permeability. During lens sclerosis intra capsular lactate/glucose ratio decreases suggesting a decrease in the pathway of glycilitic production of ATP(45). These findings, mainly studied in rodent model, dovetail with an increase in ribose-5-phosphate and suggest a restrained membrane metabolism during cataract formation.

The secondary loss of transparence during cataract formation comes from the aggregation of alpha, beta and gamma crystallines induced by redox changes within the lens metabolism(46). Those changes have been linked with an UV-related increase of aldol reductase activity and subsequent accumulation of sorbitol.

Furthermore, lens cells have been proven to synthesize, degrade, and remodel lipids. Endogenous lipid synthesis, together with AH uptake of cholesterol and certain fatty acids, enables the formation of SM, cholesterol and long-chain saturated fatty acids membranes. This cell membrane composition hinders lipid protein interactions in the lens, aiming to stabilize over time the lens structure, preserving its optical properties. In addition, certain pathways of lipid metabolism seem to have regulatory functions. Phosphatidylinositol

turnover is correlated with the rate of lens epithelial cell division, while phosphatidylethanolamine methylation seems to be related to the initiation of lens cell formation(47).

Increasing lens capsule permeability in cataract(48) could also affect AH composition. Some minor proteomic changes in AH have been associated with cataract maturity and lens condition(49), however they have been considered to be of minor clinical meaning.

Interestingly, the inconclusiveness of the changes in AH composition related to cataract maturity may subordinate to the limited permeability of the anterior lens capsule, restricted to small and mid-size proteins as albumin, with a cut off molecular weight of 166 ± 82 kDa, three to six folds smaller than the lipid species studied in this work(sphingomyelins (SM) around 350 kDa, phosphatidylcholines (PC) around 800 kDa) and clearly smaller than most organic surfactants.

With minor lens permeability to most organic surfactants and a characteristically decreased lens-AH metabolic interaction, cataract did not show to be an ideal model to show the potential clinical implications of AH ST in this condition.

In contrast, the physiopathological, anatomy related models(50) used to explain and study the pathological rise of intraocular pressure (IOP) postulates open angle glaucoma (OAG) as an ideal condition for our study, where metabolical and biophysical changes coexist and may contribute to the onset and progression of the disease.

In rodent model, the lysophospholipids/ phosphilipid ratio is significantly increased in AH of glaucoma subjects. L ysophospholipids stem from phospholipids under oxidative or

osmotic stress. Dovetailing with these findings, some phospholipid species have been shown to be uniquely present in AH of OAG in humans. Furthermore, the overall concentration of phospholipids was decreased. Dovetailing with these findings, some phospholipid species have been shown to be uniquely present in AH of OAG in humans(51),(52).

Meta-analyses based evidence links pathogenicity of OAG with inflammation(53),(54) and oxidative stress. A close relationship has been found between systemic oxidative stress markers such as cpRNFLT and 8-OHdG and angle glaucoma(55). These studies report that an oxidative-stress induced decrease in blood flow may hinder AH outflow through the Schlemm's canal and the collector channels. Furthermore, a significant increase in superoxide dismutase and glutathione peroxidase activities was found in AH of OAG patients when compared to cataracts, evolving up regulation of physiological response to oxidative stress in OAG(56). In addition, a higher concentration of free radicals like superoxide, target of superoxide dismutase mediated response, was found in AH of patients with OAG when compared to cataract(57). Those findings suggest a combined mechanism, where a misbalance between a decreased anti-oxidative capacity and an increased ROS-mediated oxidative stress may be responsible for AH reflected metabolic changes.

The lipidomic analysis to glaucoma patients shows a lipid alteration in AH concentration of certain lipid pathways. The increase in ChoE and the decrease of SMS activity and the resultant increase in SM and ceramides advocate for oxidative misbalance related changes in lipid synthesis pathways. Our study also found a significant increase in dyacil species of phosphocolines in OAG. The presence of high levels of dyacil phosphocolines in plasma has been linked with increased levels of oxidative stress, age and coronary

conditions(58). These findings dovetail with other reports highlighting a phosphocoline synthesis up regulation secondary to oxidative misbalance.

Furthermore, the characteristic anatomical features involved in glaucoma point to the ST of AH as a potential important parameter. ST defines, with viscosity, the flowability of the fluid through the outflow anatomical pathways(59). The trabecular meshwork constitutes a structured anatomical section that binds the anterior chamber with the lumen of the Schlemm's canal. Histologically, it entails a complex holey structure boarded up with septums of collagenous tissue(60). As it approaches the Schlemm's canal the space between septums narrows, the surface area between the AH and the trabecular septums increases and the trabecular meshwork takes a cavern-like histological appearance. In the closest section of the trabecular meshwork to the Schlemm's canal, so called juxtacanalicular portion, the morphology changes to narrow intercellular web of canals that lead to the lumen(61). The Schlemm's canal is paved with a monolayer of endothelial cells. AH is transported through the endothelial monolayer in pinocitic-like vacuoles that merge with the cell membrane in the luminal side(62),(63). As expected from anatomy, the AH outflow resistance mainly locates in the juxtacanalicular portion of the Schlemm's canal.

The AH outflow mechanism suggests the role of biophysical fluidic properties in the outflow resistance. As the AH approaches the Schlemm's canal, the area of trabecular meshwork-AH interphase spikes, hypotetically increasing the role of the fluid ST in the flowability of the AH. Moreover, reports have suggested a close metabolical interaction between the trabecular meshwork and the AH, mainly with the exchange of large molecules as gycosaminoglycans with amphiphilic properties(64),(65),(66). Trends suggesting variation of ST data between different types of glaucoma were observed in our study. These trends get more evident in types of glaucoma where major changes in AH composition have been

found, such as pigmentary and inflammatory (uveitic).

AH metabolomic analyses may be of special relevance in anterior segment disease where a metabolical cause have been found to be the cause, like Fuchs endothelial dystrophy (FED). The physiopathological origin of FED has been a subject of study during last decades. Driven by the deeper knowledge of corneal endothelial cell metabolism, the treatment and the diagnosis of the disease have crucially evolved. DMEK, the surgical transplantation technique which follows the AH extraction in the FED group of our study, has revolutionized the treatment of FED, shifting to a more disease specific transplantation with better visual outcomes and lower rates of postoperative complications(67),(68). Although representing some new challenging steps compared to prior techniques, such as a manual graft preparation(69) and graft unfolding(70), the technique entails an important step between the penetrating keratoplasty and others, minimally invasive procedures(71), that may become the gold standard for FED treatment in the years to come.

FED physiopathology is directly linked with histological changes in the Descemet membrane, resulting in collagenous excrescences called guttae, that compromise endothelial function as well as light transmission. Although it is known to be a multifactorial condition, experimental studies and reports coming from endothelial cell in-vitro culture, and surgical experience derived from endothelial keratoplasty, advocate for an endothelial origin of the disease(72). Postoperative findings after (Descemet membrane endothelial keratoplasty) DMEK postulate in favor of this idea. Follow up of large series of DMEK patients do not show recurrence of FED endothelial in the transplanted graft, even after late graft failure. Few reports about the presence of de novo guttae in the transplanted graft could be explained by the incidence of the disease, having used a sub clinically FED-affected graft(73).

The endothelial cell metabolism plays a key functional role by exchanging intracellular sodium and water with potassium from the AH through the activity of an ATPse transmembrane pump(74). The pump works against the negative swelling potential of the stromal layer, maintaining a thin, transparent cornea. The flat, hexagonal configuration of the endothelial monolayer assures for a maximal surface area. This can be easily observed when trauma denudes a stromal region, resulting in migration and possibly in division at different pace(75). The endothelial monolayer and the AH share over three square centimeters of surface where a strong metabolical exchange takes place(76). This morphological intimate disposition of the endothelial cell towards the AH evidences that changes in cell metabolism may directly reflect in AH composition.

We found significant changes in lipid profiling of AH in patients with FED when compared to controls. These changes have been proven to be independent from age, lens condition or cataract maturity. Lipidomic profiling unraveled an increase in phosphatidylcholines, ceramides as well as an increase in unsaturated ChoE. The findings express an up regulation of the SM synthase activity, the main enzyme that regulates SM and cholesterol biosynthesis, and its dysregulation has been linked with oxidative stress related diseases(77). The ChoE and cholesterol synthesis pathways have also been linked with oxidative stress(78) and SM synthase-related protein is a suppressor of ceramide induced mitochondrial apoptosis(79). Adding evidence presents the rise in SM as a potential part of the endothelial cell response to oxidative stress in FED and potentially as a result of the inadequate adaptive cell mechanisms to oxidations, led by unfolded protein response(80).

Consequently, observed changes of concentration of ampiphilic lipids may trigger the significant changes in fluid's ST that were observed in our study. Unsaturated lipids have a more complex and irregular spacial structure than saturated species. This decreases the

intermolecular electrostatic forces reducing the intermolecular adhesion and the viscosity and ST of the fluid(81). Furthermore an overall increase in lipid concentration, meaning an increase in the concentration of surface active molecules, explains the decrease in ST by the previously mentioned principle of micelle synthesis. Observed changes in ST may stem from changes in the lipidomic profile of AH in FED as compared to controls. Findings suggest a relation between those changes and oxidative stress induced alteration in the endothelial lipid metabolism.

Being a physiopathological cause of the disease, those changes may contribute to its progression by worsening the intracellular oxidative misbalance. Further studies should better assess the extent, severity and the time occurrence of those changes within the disease chronology. If proven to occur in preclinical stages, or to correlate with disease severity, they may play an important role as biomarker for endothelial cell disease metabolism and a tool for preclinical diagnosis.

Lipid and proteomic expression have undergone a significant evolution during the last decades, showing large potential as preclinical diagnosis tools, predisposition and susceptibility biomarkers and disease characterization and grading and will undoubtedly be of crucial use in the future practise of ophthalmology. Special interest is focused in early, preclinical diagnosis of multifactorial conditions where environment and genetical predisposition play a key role, like FED or OAG.

In an ideal future scenario, the metabolomic expression of AH may serve as a metabolic fingerprint, giving information and demarcating the patients future risk exposure for several anterior chamber related pathologies. This may optimize the screening methodology increasing its cost effectiveness and may entail a crucial shift to a deeper disease

categorization that will enable an earlier, more specific clinical approach. Finding disease biomarkers for anterior segment pathologies in AH may spare countless unnecessary screening consultations, providing the clinician and the patient with a sharper image of the disease chronology, giving the opportunity to determine and modulate environmental factors in a preclinical stage.

However, pre surgical AH extraction is not exempt of potential vision threatening complications, and its potential future utilities have to be complemented with a careful assessment of its risk benefit ratio under different circumstances as a natural way to advance into a more efficient, evidence based medicine.

6. CONCLUSIONS

1. Intraoperative extraction of 150 microliters of aqueous humor through a corneal paracentesis as the first step of an anterior segment surgery, represents a reproducible, technically feasible and relatively safe method to obtain aqueous humor samples in humans. The procedure requires a correct logistical framework including sample handling, transportation and storage and should always be preceded by an informed consent and an ethical committee approval.

2. The concentration of 32 and 37 out of 110 lipids changes significantly in Fuchs endothelial dystrophy and open angle glaucoma respectively, when compared to controls. These differences mainly stem from an increase in sphingomyelins and cholesteryl esters in Fuchs endothelial dystrophy and open angle glaucoma.

3. Sphingomyelins and cholesteryl esters are involved in the metabolical regulation of oxidative stress responses, and their changes in concentration may represent an indirect marker for increased oxidative stress levels linked with the pathogenesis of these conditions.

4. Resulting from changes in the metabolic profile, surface tension of aqueous humor in Fuchs endothelial dystrophy is lower than in controls. Those differences have been found to be statistically significant.

7. REFERENCES

1. Kiel JW, Hollingsworth M, Rao R, Chen M, Reitsamer HA. Ciliary blood flow and aqueous humor production. Prog Retin Eye Res. 2011 Jan;30(1):1–17.

2. Roy Chowdhury U, Hann CR, Stamer WD, Fautsch MP. Aqueous humor outflow: dynamics and disease. Invest Ophthalmol Vis Sci. 2015 May;56(5):2993–3003.

3. Selbach JM, Gottanka J, Wittmann M, Lütjen-Drecoll E. Efferent and afferent innervation of primate trabecular meshwork and scleral spur. Invest Ophthalmol Vis Sci. 2000 Jul;41(8):2184–91.

4. Lütjen-Drecoll E, Tamm E, Kaufman PL. Age changes in rhesus monkey ciliary muscle: light and electron microscopy. Exp Eye Res. 1988 Dec;47(6):885–99.

5. Holmberg □keS. Schlemm's canal and the trabecular meshwork. An electron microscopic study of the normal structure in man and monkey (Cercopithecus ethiops). Doc Ophthalmol [Internet]. 1965 [cited 2015 Nov 22];19(1). Available from: http://link.springer.com/10.1007/BF00180763

6. Speakman JS. DRAINAGE CHANNELS IN THE TRABECULAR WALL OF SCHLEMM'S CANAL. Br J Ophthalmol. 1960 Sep 1;44(9):513–23.

7. Harrison R. Glaucoma. Arch Ophthalmol. 1963 Dec 1;70(6):842–69.

8. Mizokami K, Sugiura T, San Juan RG. The development of human trabecular meshwork. Med Electron Microsc. 1994 Dec;27(3-4):275–81.

9. Grierson I, Lee WR. The fine structure of the trabecular meshwork at graded levels of intraocular pressure. (1) Pressure effects within the near-physiological range (8-30

mmHg). Exp Eye Res. 1975 Jun;20(6):505–21.

10. Lütjen-Drecoll E. Functional morphology of the trabecular meshwork in primate eyes. Prog Retin Eye Res. 1999 Jan;18(1):91–119.

11. Kayes J. Pressure gradient changes on the trabecular meshwork of monkeys. Am J Ophthalmol. 1975 Apr;79(4):549–56.

12. Grierson I, Lee WR. The fine structure of the trabecular meshwork at graded levels of intraocular pressure. (1) Pressure effects within the near-physiological range (8-30 mmHg). Exp Eye Res. 1975 Jun;20(6):505–21.

13. Johnson M, Chan D, Read AT, Christensen C, Sit A, Ethier CR. The pore density in the inner wall endothelium of Schlemm's canal of glaucomatous eyes. Invest Ophthalmol Vis Sci. 2002 Sep;43(9):2950–5.

14. Nelson DL, Cox MM, Lehninger AL. Lehninger principles of biochemistry. 6., internat. ed. New York: Freeman; 2013.

15. Edwards G, Aribindi K, Guerra Y, Lee RK, Bhattacharya SK. Phospholipid profiles of control and glaucomatous human aqueous humor. Biochimie. 2014 Jun;101:232–47.

16. Wang H, Edwards G, Garzon C, Piqueras C, Bhattacharya SK. Aqueous humor phospholipids of DBA/2J and DBA/2J-Gpnmb(+)/SjJ mice. Biochimie. 2015 Jun;113:59–68.

17. Mohanty BP, Bhattacharjee S, Paria P, Mahanty A, Sharma AP. Lipid biomarkers of lens aging. Appl Biochem Biotechnol. 2013 Jan;169(1):192–200.

18. Lim A, Wenk MR, Tong L. Lipid-Based Therapy for Ocular Surface Inflammation and

Disease. Trends Mol Med. 2015 Dec;21(12):736–48.

19. Kunchithapautham K, Atkinson C, Rohrer B. Smoke exposure causes endoplasmic reticulum stress and lipid accumulation in retinal pigment epithelium through oxidative stress and complement activation. J Biol Chem. 2014 May 23;289(21):14534–46.

20. Turkdogan KA, Akpinar O, Karabacak M, Akpinar H, Turkdogan FT, Karahan O. Association between oxidative stress index and serum lipid levels in healthy young adults. JPMA J Pak Med Assoc. 2014 Apr;64(4):379–81.

21. Mukhopadhyay R. Mouse models of atherosclerosis: explaining critical roles of lipid metabolism and inflammation. J Appl Genet. 2013 May;54(2):185–92.

22. van Diepen JA, Berbée JFP, Havekes LM, Rensen PCN. Interactions between inflammation and lipid metabolism: relevance for efficacy of anti-inflammatory drugs in the treatment of atherosclerosis. Atherosclerosis. 2013 Jun;228(2):306–15.

23. Niki E. Lipid peroxidation products as oxidative stress biomarkers. BioFactors Oxf Engl. 2008;34(2):171–80.

24. Wojcik K, Kaminska A, Blasiak J, Szaflik J, Szaflik J. Oxidative Stress in the Pathogenesis of Keratoconus and Fuchs Endothelial Corneal Dystrophy. Int J Mol Sci. 2013 Sep 23;14(9):19294–308. 25. Kim EC, Meng H, Jun AS. N-Acetylcysteine increases corneal endothelial cell survival in a mouse model of Fuchs endothelial corneal dystrophy. Exp Eye Res. 2014 Oct;127:20–5.

26. Malijevský A, Jackson G. A perspective on the interfacial properties of nanoscopic liquid drops. J Phys Condens Matter Inst Phys J. 2012 Nov 21;24(46):464121.

27. Faria R, Santana MM, Aveleira CA, Simões C, Maciel E, Melo T, et al. Alterations in phospholipidomic profile in the brain of mouse model of depression induced by chronic unpredictable stress. Neuroscience. 2014 Jul 25;273:1–11.

28. Kawai M, Kirkness JP, Yamamura S, Imaizumi K, Yoshimine H, Oi K, et al. Increased phosphatidylcholine concentration in saliva reduces surface tension and improves airway patency in obstructive sleep apnoea. J Oral Rehabil. 2013 Aug;n/a – n/a.

29. Kazakov VN. Dynamic surface tensiometry in medicine [Internet]. Amsterdam; New York: Elsevier; 2000 [cited 2015 Jul 27]. Available from: http://site.ebrary.com/id/10190301

30. Chapter 3 Dynamic interfacial tensiometry of biological liquids obtained from healthy persons. In: Studies in Interface Science [Internet]. Elsevier; 2000 [cited 2015 Nov 23]. p. 68–98. Available from: http://linkinghub.elsevier.com/retrieve/pii/S1383730300800277

31. Koster T, Rosendaal FR, Reitsma PH, van der Velden PA, Briët E, Vandenbroucke JP. Factor VII and fibrinogen levels as risk factors for venous thrombosis. A case-control study of plasma levels and DNA polymorphisms--the Leiden Thrombophilia Study (LETS). Thromb Haemost. 1994 Jun;71(6):719–22.

32. Chapter 3 Dynamic interfacial tensiometry of biological liquids obtained from healthy persons. In: Studies in Interface Science [Internet]. Elsevier; 2000 [cited 2015 Nov 23]. p. 68–98. Available from: http://linkinghub.elsevier.com/retrieve/pii/S1383730300800277

33. Rey AD. Generalized Young-Laplace Equation for Nematic Liquid Crystal Interfaces and its Application to Free-Surface Defects. Mol Cryst Liq Cryst Sci Technol Sect Mol

Cryst Liq Cryst. 2001 Oct;369(1):63–74.

34. Griffiths W, Karu K, Hornshaw M, Woffendin G, Wang Y. Metabolomics and metabolite profiling: past heroes and future developments. Eur J Mass Spectrom. 2007;13(1):45.

35. Alonso A, Marsal S, JuliÃ A. Analytical Methods in Untargeted Metabolomics: State of the Art in 2015. Front Bioeng Biotechnol [Internet]. 2015 Mar 5 [cited 2015 Nov 23];3. Available from: http://www.frontiersin.org/Bioinformatics_and_Computational_Biology/10.3389/fbioe.2015.00023/abstract

36. Barr J, Vázquez-Chantada M, Alonso C, Pérez-Cormenzana M, Mayo R, Galán A, et al. Liquid Chromatography−Mass Spectrometry-Based Parallel Metabolic Profiling of Human and Mouse Model Serum Reveals Putative Biomarkers Associated with the Progression of Nonalcoholic Fatty Liver Disease. J Proteome Res. 2010 Sep 3;9(9):4501–12.

37. van der Kloet FM, Bobeldijk I, Verheij ER, Jellema RH. Analytical error reduction using single point calibration for accurate and precise metabolomic phenotyping. J Proteome Res. 2009 Nov;8(11):5132–41.

38. Czirok A, Little CD. Pattern formation during vasculogenesis. Birth Defects Res Part C Embryo Today Rev. 2012 Jun;96(2):153–62.

39. White HE. Modern college physics. London; New York: Van Nostrand; 1972.

40. Ikegami M, Weaver TE, Grant SN, Whitsett JA. Pulmonary surfactant surface tension influences alveolar capillary shape and oxygenation. Am J Respir Cell Mol Biol. 2009 Oct;41(4):433–9.

41. Ribeiro W, Mata JL, Saramago B. Effect of concentration and temperature on surface tension of sodium hyaluronate saline solutions. Langmuir ACS J Surf Colloids. 2007 Jun 19;23(13):7014–7.

42. Fagone P, Jackowski S. Membrane phospholipid synthesis and endoplasmic reticulum function. J Lipid Res. 2008 Dec 19;50(Supplement):S311–6.

43. Suetsugu S, Kurisu S, Takenawa T. Dynamic Shaping of Cellular Membranes by Phospholipids and Membrane-Deforming Proteins. Physiol Rev. 2014 Oct 1;94(4):1219–48.

44. Bergmanson JP, Sheldon TM, Goosey JD. Fuchs' endothelial dystrophy: a fresh look at an aging disease. Ophthalmic Physiol Opt J Br Coll Ophthalmic Opt Optom. 1999 May;19(3):210–22.

45. Kato Y, Igarashi H, Kanno H, Tanaka K, Yoshida A. Metabolic changes during cataract formation by ultraviolet radiation in the incubated rabbit lens. Hokkaido Igaku Zasshi. 2009 Nov;84(6):423–30.

46. Michael R, Bron AJ. The ageing lens and cataract: a model of normal and pathological ageing. Philos Trans R Soc B Biol Sci. 2011 Apr 27;366(1568):1278–92.

47. Zelenka PS. Lens lipids. Curr Eye Res. 1984 Nov;3(11):1337–59.

48. Kastner C, Löbler M, Reske T, Sternberg K, Guthoff R, Schmitz K-P. Determination

of human anterior lens capsule permeability for fluorescent model substances and after-cataract preventive drugs. Biomed Eng Biomed Tech [Internet]. 2012 Jan 27 [cited 2015 Aug 3];57(SI-1 Track-D). Available from: http://www.degruyter.com/view/j/bmte.2012.57.issue-s1-D/bmt-2012-4340/bmt-2012-4340.xml

49. Bennett KL, Funk M, Tschernutter M, Breitwieser FP, Planyavsky M, Ubaida Mohien C, et al. Proteomic analysis of human cataract aqueous humour: Comparison of one-dimensional gel LCMS with two-dimensional LCMS of unlabelled and iTRAQ®-labelled specimens. J Proteomics. 2011 Feb 1;74(2):151–66.

50. Gupta S, Agarwal P, Saxena R, Agrawal S, Agarwal R. Current concepts in the pathophysiology of glaucoma. Indian J Ophthalmol. 2009;57(4):257.

51. Edwards G, Aribindi K, Guerra Y, Lee RK, Bhattacharya SK. Phospholipid profiles of control and glaucomatous human aqueous humor. Biochimie. 2014 Jun;101:232–47.

52. Wang H, Edwards G, Garzon C, Piqueras C, Bhattacharya SK. Aqueous humor phospholipids of DBA/2J and DBA/2J-Gpnmb(+)/SjJ mice. Biochimie. 2015 Jun;113:59–68.

53. Nga ADC, Yap S-L, Samsudin A, Abdul-Rahman PS, Hashim OH, Mimiwati Z. Matrix metalloproteinases and tissue inhibitors of metalloproteinases in the aqueous humour of patients with primary angle closure glaucoma - a quantitative study. BMC Ophthalmol. 2014;14:33.

54. Agarwal P, Daher AM, Agarwal R. Aqueous humor TGF-β2 levels in patients with open-angle glaucoma: A meta-analysis. Mol Vis. 2015;21:612–20.

55. Himori N, Kunikata H, Shiga Y, Omodaka K, Maruyama K, Takahashi H, et al. The association between systemic oxidative stress and ocular blood flow in patients with normal-tension glaucoma. Graefes Arch Clin Exp Ophthalmol Albrecht Von Graefes Arch Klin Exp Ophthalmol. 2015 Oct 30;

56. Goyal A, Srivastava A, Sihota R, Kaur J. Evaluation of oxidative stress markers in aqueous humor of primary open angle glaucoma and primary angle closure glaucoma patients. Curr Eye Res. 2014 Aug;39(8):823–9.

57. Oshida E, Arai K, Sakai M, Chikuda M. [Study of free radicals in aqueous humor in glaucoma and cataracts: differences in presence or absence of diabetes mellitus and neovascular glaucoma]. Nippon Ganka Gakkai Zasshi. 2014 Sep;118(9):759–67.

58. Frey B, Haupt R, Alms S, Holzmann G, König T, Kern H, et al. Increase in fragmented phosphatidylcholine in blood plasma by oxidative stress. J Lipid Res. 2000 Jul;41(7):1145–53.

59. Berthier E, Beebe DJ. Flow rate analysis of a surface tension driven passive micropump. Lab Chip. 2007;7(11):1475.

60. Lütjen-Drecoll E. Functional morphology of the trabecular meshwork in primate eyes. Prog Retin Eye Res. 1999 Jan;18(1):91–119.

61. Llobet A, Gasull X, Gual A. Understanding Trabecular Meshwork Physiology: A Key to the Control of Intraocular Pressure? Physiology. 2003 Oct 1;18(5):205–9.

62. Parc CE, Johnson DH, Brilakis HS. Giant vacuoles are found preferentially near collector channels. Invest Ophthalmol Vis Sci. 2000 Sep;41(10):2984–90.

63. Johnson M. “What controls aqueous humour outflow resistance?” Exp Eye Res. 2006 Apr;82(4):545–57.

64. Knepper PA, Goossens W, Hvizd M, Palmberg PF. Glycosaminoglycans of the human trabecular meshwork in primary open-angle glaucoma. Invest Ophthalmol Vis Sci. 1996 Jun;37(7):1360–7.

65. Kuleshova ON, Zaidman AM, Korel’ AV. Glycosaminoglycans of the trabecular meshwork of the eye in primary juvenile glaucoma. Bull Exp Biol Med. 2007 Mar;143(3):381–4.

66. Baba H. Probability of the presence of glycosaminoglycans in aqueous humor. Graefes Arch Clin Exp Ophthalmol Albrecht Von Graefes Arch Für Klin Exp Ophthalmol. 1983;220(3):117–21.

67. Rodríguez-Calvo-de-Mora M, Quilendrino R, Ham L, Liarakos VS, van Dijk K, Baydoun L, et al. Clinical Outcome of 500 Consecutive Cases Undergoing Descemet’s Membrane Endothelial Keratoplasty. Ophthalmology. 2014 Oct 22;

68. Anshu A, Price MO, Price FW. Risk of corneal transplant rejection significantly reduced with Descemet’s membrane endothelial keratoplasty. Ophthalmology. 2012 Mar;119(3):536–40.

69. Groeneveld-van Beek EA, Lie JT, van der Wees J, Bruinsma M, Melles GRJ. Standardized “no-touch” donor tissue preparation for DALK and DMEK: harvesting undamaged anterior and posterior transplants from the same donor cornea. Acta Ophthalmol (Copenh). 2013 Mar;91(2):145–50.

70. Dapena I, Moutsouris K, Droutsas K, Ham L, van Dijk K, Melles GRJ. Standardized

"no-touch" technique for descemet membrane endothelial keratoplasty. Arch Ophthalmol. 2011 Jan;129(1):88–94.

71. Okumura N, Koizumi N, Ueno M, Sakamoto Y, Takahashi H, Tsuchiya H, et al. ROCK Inhibitor Converts Corneal Endothelial Cells into a Phenotype Capable of Regenerating In Vivo Endothelial Tissue. Am J Pathol. 2012 Jul;181(1):268–77.

72. Matthaei M, Hu J, Kallay L, Eberhart CG, Cursiefen C, Qian J, et al. Endothelial cell microRNA expression in human late-onset Fuchs' dystrophy. Invest Ophthalmol Vis Sci. 2014 Jan;55(1):216–25.

73. Christopoulos V, Garner A. Emergence of cornea guttata in donor tissue: a cause of late graft failure. Eye Lond Engl. 1993;7 (Pt 6):772–4.

74. Bourne WM. Biology of the corneal endothelium in health and disease. Eye. 2003 Nov;17(8):912–8.

75. Choi SO, Jeon HS, Hyon JY, Oh Y-J, Wee WR, Chung T, et al. Recovery of Corneal Endothelial Cells from Periphery after Injury. Ljubimov AV, editor. PLOS ONE. 2015 Sep 17;10(9):e0138076.

76. Garner LF, Owens H, Yap MK, Frith MJ, Kinnear RF. Radius of curvature of the posterior surface of the cornea. Optom Vis Sci Off Publ Am Acad Optom. 1997 Jul;74(7):496–8.

77. Grimm MOW, Grimm HS, Pätzold AJ, Zinser EG, Halonen R, Duering M, et al. Regulation of cholesterol and sphingomyelin metabolism by amyloid-β and presenilin. Nat Cell Biol. 2005 Nov;7(11):1118–23.

78. Kim J-H, Ee S-M, Jittiwat J, Ong E-S, Farooqui AA, Jenner AM, et al. Increased expression of acyl-coenzyme A: cholesterol acyltransferase-1 and elevated cholesteryl esters in the hippocampus after excitotoxic injury. Neuroscience. 2011 Jun 30;185:125–34.

79. Tafesse FG, Vacaru AM, Bosma EF, Hermansson M, Jain A, Hilderink A, et al. Sphingomyelin synthase-related protein SMSr is a suppressor of ceramide-induced mitochondrial apoptosis. J Cell Sci. 2014 Jan 15;127(Pt 2):445–54.

80. Gregersen N, Bross P. Protein misfolding and cellular stress: an overview. Methods Mol Biol Clifton NJ. 2010;648:3–23.

81. Alberts B, editor. Molecular biology of the cell. 4th ed. New York: Garland Science; 2002. 1548 p.

8. ACKNOWLEDGEMENTS

The authors would like to express their gratitude to the following persons for their contribution to this work.

Gonzalo Saracibar, PhD. University of the Basque Country, (UPV/EHU).

Jaime Aramberri, MD. Begitek Clínica Oftalmológica.

Lisanne Ham, PhD and Marieke Bruisma, PhD. Netherlands Institute for Innovative Ocular Surgery (NIIOS).

Marina Rodriguez Calvo de Mora, MD. Hospital Universitario Carlos Haya.

RESUMEN DE TESIS DOCTORAL

IDIOMA ORIGINAL: INGLÉS

IDIOMA DE LA TRADUCCIÓN: CASTELLANO

Título original: Biophysical properties of aqueous humour in ocular pathologies.

Título traducido: Propiedades biofísicas del humor acuoso en diferentes patologias oculares.

Autor: Javier Cabrerizo[1,2,4]

Directores: Elena Vecino[3,4], Aritz Urcola[1,2,4]

1 Department of Ophthalmology, University Hospital of Alava, Spain

2 Green Eye Project, Research, Spain

3 Department of Cell Biology and Histology, University of the Basque Country, UPV/EHU, Spain

4 Experimental Ophthalmo-Biology Group, (GOBE), University of the Basque Country, (UPV/EHU), Spain

LISTA DE ABREVIATURAS

Humor acuoso	**AH**
Distrofia endotelial de Fuchs	**DEF**
Esclerotoma profunda no perforante	**EPNP**
Glaucoma de ángulo abierto	**GAA**
Tensión superficial	**TS**
Queratolpalstia endotelial de membrana de Descemet	**DMEK**

1. INTRODUCCIÓN

El limbo corneoescleral contiene estructuras diseñadas para evacuar el humor acuso desde la cámara anterior del ojo hacia la circulación general. Estos elementos se encuentran entre el espolón escleral y la línea de Schwalbe que finalmente se continua con a membrana de Descemet del endotelio corneal. Su composición consta de tejido corneal, escleral, iridiano y del cuerpo ciliar; constituyendo elementos estructurales claves en el drenaje del humor acuoso como son: el canal de Schlemm, los canales colectores y la malla trabecular, y en ella sus tres regiones: uveal, corneoescleral y yuxtacanalicular.

El canal Schlemm es un canal venoso circular de 36 µm de circunferencia y 350-500 µm de diámetro en su luz interna. La superficie de la luz está tapizada por células endoteliales que están unidas entre sí por uniones zonula occludens. En la pared interna del canal, a lo largo de su trayecto sinuoso, encontramos vesículas citoplasmáticas o vacuolas de grandes dimensiones de origen pinocítico que pueden llegar a medir 14 µm con aperturas puntuales hacia la luz del canal de 0.3 – 2.0 µm postulandose que pueda ser un drenaje directo desde los espacios trabeculares hacia el canal de Schlemm.

Existe controversia con respecto al hallazgo de poros inter y transcelulares en la pared interna del canal de Shlemm; puesto que algunos autores que analizan mediante microscopia electrónica de barrido la monocapa endotelial sostienen que su número aumenta con la elevación de la presión; otros, concluyen que su número se reduce en los ojos glaucomatosos.

Donde sí parecen estar de acuerdo las últimas publicaciones es en destacar el dinamismo de este sistema de drenaje, y postulan que los cambios encontrados en su ultraestructura pudieran hablarnos a favor de un sistema sensible y cambiante con los cambios de presión intraocular.

En física se denomina tensión superficial de un líquido a la cantidad de energía necesaria para aumentar su superficie por unidad de área. Las fuerzas intermoleculares en los líquidos, junto con las fuerzas existentes entre distintas superficies dan lugar a esta resistencia y condicionan la capacidad de capilaridad del líquido al contactar con una superficie sólida. Las fuerzas que afectan a cada molécula son diferentes en el interior del líquido y en la superficie. Así en el seno de un líquido cada molécula esta sometida a fuerzas de

atracción que en promedio se anulan, permitiendo tener una energía bastante baja pero en la superficie existe una fuerza neta hacia el interior.

Los agentes surfactantes al colocarse en la interfase entre dos sistemas actúan disminuyendo la tensión superficial y facilitando así la continuidad entre los mismos. Las moléculas más conocidas en este campo son los fosfolípidos y actúan como agentes anfipáticos al constar de una parte hidrófila y otra hidrófoba. Su acción es clave en la superficie alveolar evitando la atelectasia alveolar en la fase final de la espiración, y por el contrario su deficiencia precipita en Síndrome de Distress respiratorio del lactante.

La malla trabecular y el tejido conectivo yuxtacanalicular contiene matriz extracelular y es conocido que la composición de glucosaminoglicanos y ácido hialurónico en esta estructura está alterada en el glaucoma. La disminución del contenido en ácido hialurónico tanto en la malla trabecular como en tejido yuxtacanalicular puede dificultar la capacidad de drenaje del humor acuso al elevarse su tensión superficial, incrementándose así las uniones intercelulares en la capa endotelial y finalmente colapsar los espacios trabeculares existentes en condiciones normales. Esto conlleva irremediablemente a la elevación de la presión intraocular; pero paradójicamente, puede elevarse también de forma mecánica tal y como se observa típicamente en la cirugía de la catarata tras la introducción de sustancias viscoelásticas compuestas de ácido hialurónico en cámara anterior que bloquean los espacios trabeculares. El desequilibrio en la proporción de glucosaminoglicanos mediante la inyección exógena sustancias viscoelásticas o de condritin sulfato en cámara anterior puede elevar significativamente la presión intraocular y permite desarrollar así un modelo de glaucoma experimental. El análisis proteómico de humor acuoso de pacientes con glaucoma mediante electroforésis ha demostrado diferencias cualitativas en su composición respecto a controles jugando un papel relevante en el glaucoma pseudoexfoliativo.

En el único estudio hasta la fecha que analizan la tensión superficial del humor acuso se ha observado una disminución de la misma en los ojos afectos de glaucoma primario de ángulo abierto respecto a los ojos seleccionados como controles, siendo estos últimos os pacientes sometidos a cirugía de catarata. En este estudio la tensión superficial se analizó mediante la observación del tamaño y ángulo de contacto de una gota en suspensión siguiendo la técnica de Bashford-Adams. Desafortunadamente, al seleccionar un grupo de pacientes afectos de glaucoma excesivamente heterogéneo (tipos distintos de glaucoma y sometidos

previamente a diversos fármacos antiglaucomatosos) y errores en la metodología en el diseño del estudio (recogida de material, condiciones biofísicas durante la conservación y posterior análisis) los resultados son contradictorios y no concluyentes. De todos modos, se postula que el humor acuoso de los ojos afectos de glaucoma al tener una menor tensión superficial, esto pueda interferir negativamente en la formación de vacuolas en su vía de drenaje hacia el canal de Schlemm. Estos mismos autores animan a proseguir futuros trabajos en esta misma línea de investigación y enfocarse a su vez en el análisis y la composición lipídica del humor acuoso en el glaucoma, al ser otro de los puntos clave para la formación de vesículas pinocítocas y su posterior drenaje.

3. HIPÓTESIS

Cataratas, glaucoma y distrofia endotelial de Fuchs representan patologías muy comunes del segmento anterior del ojo. La necesidad potencial de un procedimiento quirúrgico las convierte en patologías adecuadas para la toma de muestras de humor acuoso sin comorbilidad añadida. La extracción intraoperatoria de 150 microlitros de humor acuoso a través de una paracentesis corneal durante el primer paso de una cirugía del segmento anterior representa un método reproducible, técnicamente factible y relativamente seguro para obtener muestras de humor acuoso en humanos.

Debido a la estrecha relación anatómica y fisiológica entre el humor acuoso y las estructuras de la cámara anterior, se espera encontrar diferencias en el perfil metabólico del humor acuoso. Las características metabólicas de estos cambios deben correlacionarse con las fisiopatología de las patologías subyacentes.

Variaciones cuantitativas y cualitativas en los metabolitos del humor acuoso pueden desencadenar cambios en las propiedades biofísicas, tales como la tensión superficial, con potencial relevancia clínica.

La hipótesis de esta Tesis Doctoral es la presencia de cambios en el perfil lipidómico del humor acuoso que se correlacionan con cambios en la tensión superficial del fluido.

4. OBJETIVOS

Determinar las diferencias en la tensión superficial del humor acuoso relacionadas con diferentes patologías del segmento anterior .

Determinar las posibles diferencias en el perfil lipidomico del humor acuoso relacionadas con diferentes patologías del segmento anterior .

Ofrecer una idea de la posible relación entre los cambios en la composición del humor acuoso y sus propiedades biofísicas y los procesos fisiopatológicos implicados en esas enfermedades .

5. MATERIAL Y MÉTODOS

202 muestras de HA fueron analizadas en el estudio. Pacientes con antecedentes de cirugía ocular u otra patología aguda del segmento anterior fueron excluidos del estudio. Cualquier medicación ocular tópica en los últimos seis meses anteriores al estudio fue monitorizada. Las muestras fueron tomadas en el primer gesto quirurgico durante lensectomia electiva o implante de lente fáquica, cirugía de cataratas por facoemulsificación, EPNP y DMEK en controles (n=22), cataratas (n=56), glaucoma (n=81) y DEF (n=43), respectivamente. 150 microlitros fueron aspirados por una paracentesis al comienzo de cada acto quirúrgico. Las muestras fueron almacenadas en un banco de tehidos a -80 grados.

En 44 casos se realizo una gradación de la madurez de la catarata utilizando diferentes parámetros durante la facoemulsificación: tiempo total de faco, tiempo de faco longitudinal, tiempo de faco torsional y energia acmulada. Diferentes tipos de glaucoma fueron categorizados: ángulo abierto (n=55), ángulo estrecho (n=7), pseudoexfoliativo (n=8), pigmentario (n=2), neovascular (n=1), corticoideo (n=1), uveítico (n=6) y miópico (n=1).

El diagnóstico de la DEF se realizó mediante exploración en lámpara de hendidura, análisis por microscopía endotelial y paquimetría corneal. El grado de afectación fue determinado por la confluencia y area de las gutas y la presencia de edema total o estromal posterior.

El análisis de tensión superficial se realizo con un tensiómetro óptico mediante la técnica de gota oscilante. Una cámara de alta resolución realiza una foto de una gota de HA en el momento de equilibrio energético. Aplicando un análisis matemático sobre el contorno de la gota el sistema es capaz de inferir la TS del fluido.

Complementariamente, se realizo un análisis del perfil lipidómico de 30 muestras, 10 controles, 10 GAA y 10 DEF. Tras la extracción de los metabolitos, se utilizó espectrometría de masas la c caracterización y cuantificación de cada metabolito.

6. RESULTADOS

No se encontraron diferencias estadísticamente significativas en la tensión superficial entre cataratas y controles y entre glaucomas y controles. La madurez de la catarata, medida por parámetros de facoemulsificación intraquirúrgicos, no demostro correlación con la tensión superficial. Se observo una tendencia entre ciertos tipos de glaucoma y variaciones de la TS.

Se encontró una disminución de la TS en DEF respecto a los controles. Están diferencias demostraron significación estadística. No se encontraron cambios en relación a la edad y el género de la TS.

De manera complementaria, el estudio lipidómico reveló diferencias de concentración estadísticamente significativas en 37 y 32 especies de lípidos en GAA y DEF respectivamente. Estas diferencias residente en determinadas especies, ceramidas, phosphatidylcolinas y esteres de colesterol.

7. DISCUSIÓN

Los cambios en el perfil lipidómico del humor acuoso reflejan alteraciones metabólicos relacionados con relación fisiopatológica con determinadas enfermedades del segmento anterior del ojo. Determinar, cuantificar y establecer hipótesis de los mecanismos que desempeñan estos cambios, constituye el propósito de este trabajo.

Mínimos cambios en concentración de moléculas con poder surfactante, mayormente proteínas y compuesto lipídicos, pueden provocar cambios significativos en la TS. Esto establece la alta sensibilidad de

la TS como marcador de cambios de concentración de un fluido orgánico.

Asimismo, los cambios en el perfil lipidómico observados en GAA y DEF corresponden con alteraciones derivadas del disbalance redox intracelular. El aumento de ceramidas y de la concentración de diferentes tipos de fosfocolinas y de ésteres de colesterol puede evidenciar un aumento del plegamiento durante la síntesis proteica, como respuesta a cambios oxidativos.

El estrés oxidativo parece estar implicado en la patogénesis de ambas patologías y además parece contribuir a su continuación una vez los cambios fisiopatológicos han sido instaurados. La implicación del estrés oxidativo en patologías de segmento anterior consta cada vez con mayor evidencia científica como respaldo.

En un contexto ideal, el análisis metabólico del HA podría dar información respecto a la susceptibilidad de sufrir determinadas patologías oculares, permitiendo cambios conductuales para modular su aparición.

8. CONLCUSIONES

1. La extracción intraoperatoria de 150 microlitros de humor acuoso a través de una paracentesis corneal es un aforma técnicamente factible y relativamente segura de obtener muestras de humor acuoso en humanos. El procedimiento requiere un marco logístico correcto, incluida la manipulación de muestras, transporte y almacenamiento, y siempre debe ir precedido de un consentimiento informado y de la aprobación de un comité de ética.

2. La concentración de 32 y 37 de los 110 lípidos cambia significativamente en la distrofia endotelial de Fuchs y en el glaucoma de ángulo abierto, respectivamente, en comparación con los controles. Estas diferencias se derivan principalmente de un aumento en esfingomielinas y ésteres de colesterol.

3. Las esfingomielinas y ésteres de colesterol están involucrados en la regulación metabólica de las respuestas de estrés oxidativo, y los cambios en su concentración pueden representar un marcador indirecto para el aumento de los niveles de estrés oxidativo relacionados con la patogénesis de estas

enfermedades.

4. Como resultado de los cambios en el perfil metabólico, la tensión superficial del humor acuoso en la distrofia endotelial de Fuchs es más bajo que en los controles.